

Atmospheric Oxidation of Vinyl Ethers



Thesis submitted to the Faculty of Chemistry
The Bergische Universität Wuppertal
For the Degree of Doctor of Science
(Dr. rerum naturalium)

by
Shouming Zhou

April, 2007

Diese Dissertation kann wie folgt zitiert werden:

urn:nbn:de:hbz:468-20070799

[<http://nbn-resolving.de/urn/resolver.pl?urn=urn%3Anbn%3Ade%3Ahbz%3A468-20070799>]

The work described in this thesis was carried out in the Department of Physical Chemistry, the Bergische Universität Wuppertal, under the scientific supervision of Prof. Dr. Th. Benter, during the period of December, 2002 to April, 2007.

Referee: Prof. Dr. Th. Benter

Co-referee: Prof. Dr. P. Wiesen

To my parents, Haiyan and Rolynn

给我的父母、海燕和若苓

Acknowledgements

I would like to express my appreciation to Prof. Dr. Th. Benter for the opportunity to do this Ph.D. in his research group and for the supervision of this work.

My sincere thanks also go to Prof. Dr. P. Wiesen for agreeing to co-referee the thesis.

I wish to express my sincere gratitude to Dr. I. Barnes who not only helped me to understand at least a part of the vast domain of Atmospheric Chemistry but also gave his inspiring guidance and encouragement throughout my research. His suggestions and support were invaluable in my work.

My thanks also to Prof. Dr. T. Zhu for trusting me and giving me the opportunity to pursue my scientific research in Wuppertal.

I would also like to thank Dr. J. Kleffmann and Dr. R. Kurtenbach for helpful discussions on aerosol studies.

My gratitude is also extended to Dr. I. Bejan, M. Albu and Dr. M. Spittler for their suggestions and comments on laboratory work and data analysis.

The help given by W. Nelsen and R. Giese, the technical staff of this group, is much appreciated.

I greatly acknowledge the European Commission for funding.

Finally, I would like to extend my heart-felt thanks to my family. My parents' blessing, and especially, my wife's understanding and support made this work possible.

Abstract

Recent field campaign and modeling studies have highlighted significant discrepancies between expected levels of pollutants from solvent use using current emission inventories and observed levels. This indicates either inadequate emission inventory calculations and/or knowledge of the atmospheric fate of emitted compounds, of which mostly significant fraction is composed of oxygenated organic compounds such as ethers.

Vinyl ethers are widely applied in industry as oxygenated solvents, additives and in different types of coatings. They are released to the atmosphere entirely from anthropogenic sources. Consequently, a better understanding of the atmospheric fate of vinyl ethers is highly desirable.

This work presents investigations on the gas-phase chemistry of vinyl ethers performed in a 405 l borosilicate glass chamber and a 1080 l quartz glass reactor in the Bergische University Wuppertal, Germany.

Relative rate coefficients were determined for the OH radical, ozone and NO₃ radical initiated oxidation of selected vinyl ethers. Using *in situ* Fourier transform infrared (FTIR) absorption spectroscopy the following rate coefficients were obtained at room temperature and atmospheric pressure in synthetic air (in cm³ molecule⁻¹ s⁻¹):

| Vinyl ether | $k_{\text{OH}} \times 10^{11}$ | $k_{\text{O}_3} \times 10^{16}$ | $k_{\text{NO}_3} \times 10^{12}$ |
|--|--------------------------------|---------------------------------|----------------------------------|
| Propyl vinyl ether, n-C ₃ H ₇ OCH=CH ₂ | 9.73±1.94 | 2.34±0.48 | 1.85±0.53 |
| Butyl vinyl ether n-C ₄ H ₉ OCH=CH ₂ | 11.3±3.1 | 2.59±0.52 | 2.10±0.54 |

Abstract

| | | | |
|--|-----------|-----------|-----------|
| Ethyleneglycol monovinyl ether HOCH ₂ CH ₂ OCH=CH ₂ | 10.4±2.15 | 2.02±0.41 | 1.95±0.50 |
| Ethyleneglycol divinyl ether H ₂ C=CHOCH ₂ CH ₂ OCH=CH ₂ | 12.3±3.25 | 1.69±0.41 | 2.23±0.46 |
| Diethyleneglycol divinyl ether H ₂ C=CHOCH ₂ CH ₂ OCH ₂ CH ₂ OCH=CH ₂ | 14.2±3.00 | 2.70±0.56 | 6.14±1.38 |

Product investigations on the gas-phase reactions of the OH radical, ozone and NO₃ radical with propyl vinyl ether (PVE) and butyl vinyl ether (BVE) were performed in the 405 l borosilicate glass chamber by *in situ* FTIR spectroscopy. At room temperature and atmospheric pressure of synthetic air the products observed and their molar formation yields were as follows:

| Reactants \ Products | | Formate (%) | HCHO (%) | HPMF ^a (%) | CO (%) | FA ^b (%) |
|----------------------|--|---|---|------------------------------|------------------------------|-------------------------------|
| OH | Propyl vinyl ether, n-C ₃ H ₇ OCH=CH ₂ | 78.6±8.8 ⁱ⁾ 63.0±9.0 ⁱⁱ⁾ | 75.9±8.4 ⁱ⁾ 61.3±6.3 ⁱⁱ⁾ | - | - | - |
| | Butyl vinyl ether n-C ₄ H ₉ OCH=CH ₂ | 64.7±7.1 ⁱ⁾ 52.2±6.3 ⁱⁱ⁾ | 64.3±6.9 ⁱ⁾ 52.9±6.3 ⁱⁱ⁾ | - | - | - |
| O ₃ | Propyl vinyl ether, n-C ₃ H ₇ OCH=CH ₂ | 88.3±9.3 ⁱⁱⁱ⁾ 89.7±9.9 ^{iv)} | - 12.9±4.0 ^{iv)} | - 13.0±3.4 ^{iv)} | - 10.9±2.6 ^{iv)} | - 1.94±0.59 ^{iv)} |
| | Butyl vinyl ether n-C ₄ H ₉ OCH=CH ₂ | 78.5±8.8 ⁱⁱⁱ⁾ 76.7±8.9 ^{iv)} | - 10.5±1.8 ^{iv)} | - 12.0±2.9 ^{iv)} | - 8.2±1.3 ^{iv)} | - 2.6±0.54 ^{iv)} |
| NO ₃ | Propyl vinyl ether, n-C ₃ H ₇ OCH=CH ₂ | 52.7±5.9 | 55.0±6.3 | - | - | - |
| | Butyl vinyl ether n-C ₄ H ₉ OCH=CH ₂ | 43.6±4.5 | 48.0±5.6 | - | - | - |

i) with NO_x present; ii) without NO_x present; iii) with cyclohexane as OH radical scavenger;

iv) with 1,3,5-trimethylbenzene as OH radical tracer

a) HPMF---hydroperoxy methyl formate; b) FA---formic anhydride

Hydroxyl radical yields of $(17\pm 9)\%$ and $(18\pm 9)\%$ have been estimated for the reactions of PVE and BVE with ozone, respectively. Total nitrate formation yields of $(56.0\pm 12.3)\%$ and $(57.1\pm 12.3)\%$ have been estimated for the NO_3 radical initiated oxidation of PVE and BVE, respectively.

Simplified reaction mechanisms for the reactions of the OH radical, ozone and NO_3 radical with the investigated vinyl ethers are proposed.

Secondary organic aerosol (SOA) formation was observed in the reactions of ozone with PVE and BVE. The observed aerosol profiles showed typical behavior associated with homogeneous nucleation. In the presence of an excess of cyclohexane to scavenge OH, SOA yields of 0.4% were obtained for PVE and 0.3-1.1% for BVE. The role that the OH radical scavenger might play in the SOA formation is unclear.

This work has augmented the atmospheric chemistry database for vinyl ethers; it has substantially improved the knowledge on the distribution of oxidation products formed in the atmospheric degradation of vinyl ethers. All the information will allow a better assessment of the potential environmental impacts of vinyl ethers.

Content

| | |
|--|----|
| <u>Chapter 1</u> Introduction | 1 |
| 1.1 Oxygenated volatile organic compounds..... | 2 |
| 1.2 Atmospheric chemistry of vinyl ethers..... | 3 |
| 1.2.1 Kinetic studies of vinyl ethers..... | 4 |
| 1.2.2 Product and mechanistic studies of vinyl ethers..... | 6 |
| 1.2.3 Secondary organic aerosol (SOA) formation from vinyl ethers..... | 9 |
| 1.3 Aims of the work..... | 10 |
| | |
| <u>Chapter 2</u> Experimental Section | 12 |
| 2.1 Reaction chambers..... | 12 |
| 2.1.1 Description of the 405 l reactor..... | 12 |
| 2.1.2 Description of the 1080 l reactor and scanning mobility particle sizer (SMPS) system..... | 13 |
| 2.1.2.1 Description of the 1080 l reactor..... | 14 |
| 2.1.2.2 Description of the scanning mobility particle sizer (SMPS) system..... | 15 |
| 2.2 Experimental procedure and data evaluation..... | 17 |
| 2.2.1 General..... | 17 |
| 2.2.2 Kinetic studies..... | 18 |
| 2.2.2.1 Relative rate method..... | 18 |
| 2.2.2.2 OH radical reaction..... | 19 |
| 2.2.2.3 O ₃ and NO ₃ radical reactions..... | 20 |
| 2.2.3 Product studies..... | 21 |
| 2.2.3.1 Correction of product formation yields..... | 21 |
| 2.2.3.2 OH radical reaction..... | 22 |
| 2.2.3.3 O ₃ reaction..... | 23 |
| 2.2.3.4 NO ₃ radical reaction..... | 24 |

| | |
|---|------------|
| 2.2.4 Secondary organic aerosol (SOA) formation..... | 24 |
| 2.2.4.1 Aerosol yield..... | 24 |
| 2.2.4.2 Experimental procedure..... | 26 |
| 2.3 The dark reaction of the vinyl ethers..... | 26 |
| | |
| <u>Chapter 3</u> Kinetic Studies on the OH Radical, O₃ and NO₃ Radical Initiated | |
| Oxidation of Selected Vinyl Ethers..... | 29 |
| 3.1 Results and discussions..... | 29 |
| 3.1.1 OH radical reactions..... | 29 |
| 3.1.2 O ₃ reactions..... | 43 |
| 3.1.3 NO ₃ radical reactions..... | 52 |
| 3.2 Atmospheric implications..... | 65 |
| | |
| <u>Chapter 4</u> Mechanisms of the Atmospheric Oxidation of Vinyl Ethers..... | 67 |
| 4.1 Product studies of the OH radical initiated oxidation of vinyl ethers..... | 67 |
| 4.1.1 Experimental results..... | 68 |
| 4.1.1.1 Results for the OH radical reaction with PVE..... | 68 |
| 4.1.1.2 Results for the OH radical reaction with BVE..... | 71 |
| 4.1.2 Discussion of the OH radical reactions..... | 74 |
| 4.2 Product studies of the ozone initiated oxidation of vinyl ethers..... | 84 |
| 4.2.1 Experimental results..... | 84 |
| 4.2.1.1 Results for the reaction of ozone with PVE..... | 84 |
| 4.2.1.2 Results for the reaction of ozone with BVE..... | 88 |
| 4.2.2 Discussion on the ozone reactions..... | 92 |
| 4.3 Product studies on the NO ₃ radical initiated oxidation of vinyl ethers..... | 100 |
| 4.3.1 Experimental results..... | 100 |
| 4.3.1.1 Results for the reaction of the NO ₃ with PVE..... | 100 |
| 4.3.1.2 Results for the reaction of the NO ₃ with BVE..... | 102 |
| 4.3.2 Discussion on the reactions of the NO ₃ radical with vinyl ethers..... | 104 |
| 4.4 Atmospheric implications..... | 110 |
| | |
| <u>Chapter 5</u> Exploratory Studies on Secondary Organic Aerosol Formation | |
| in Ozonolysis of Alkyl Vinyl Ethers..... | 112 |

Content

| | |
|--|------------|
| 5.1 SOA formation from the ozonolysis of PVE and BVE..... | 113 |
| 5.1.1 Size distribution of SOA..... | 113 |
| 5.1.2 Aerosol yields and partition coefficients for SOA in the ozonolysis of PVE and BVE..... | 115 |
| 5.2 Discussion on SOA formation in the ozonolysis of PVE and BVE..... | 118 |
| | |
| <u>Chapter 6</u> Summary..... | 122 |
| | |
| <u>Appendix I</u> Syntheses..... | 127 |
| <u>Appendix II</u> Gases and Chemicals Used..... | 130 |
| <u>Appendix III</u> Gas-phase Infrared Absorption Cross Sections | 132 |
| | |
| <u>References</u> | 134 |

Chapter 1

Introduction

The troposphere is the region of the Earth's atmosphere in which we live and into which volatile organic compounds (VOCs) are emitted from biogenic (e.g. wetlands, vegetation, termites, naturally occurring natural gas vent and biomass fires) and anthropogenic sources (e.g. motor vehicle exhaust, solvent usage, industrial operation, oil refining, petrol storage and distribution, natural gas pipe leakage, food manufacture and biomass burning) [1,2]. It is estimated that the yearly worldwide emission of methane is 150 and 350 million tons from biogenic and anthropogenic sources, respectively. Large uncertainties are associated with the emissions of non-methane organic compounds (NMOCs) and around 100 and 1000 million tons yr⁻¹ is estimated for the emissions from anthropogenic and biogenic sources, respectively [3].

In addition to emissions of VOCs, oxides of nitrogen ($\text{NO}_x = \text{NO} + \text{NO}_2$) and sulfur-containing compounds are released into the troposphere, leading to a complex series of chemical and physical transformations, which result in the formation of ozone in urban and regional areas as well as in the global troposphere [4], acid deposition [5], and the formation of secondary particulate matter through gas/particle partitioning of both emitted chemicals and the atmospheric reaction products of VOCs, NO_x , SO_2 , and organosulfur compounds [6-9].

During a typical "summer smog" episode, high levels of ozone are observed as a result of the atmospheric degradation of VOCs in the presence of NO_x . Increasing ozone levels in industrialized regions, e.g. Europe, where the O_3 levels have doubled over the last century [10], is now of major concern since ozone is not only a greenhouse gas but also a harmful secondary pollutant having adverse effects on

human health, vegetation, and building materials. In order to reduce the level of oxidants the European Union (EU) has adopted several emission directives to regulate the emissions of NO_x and VOCs from traffic and organic solvent usage. It is predicted that these measures will result in a reduction of around 10% in VOCs emissions within the European region [11,12] in the near future.

1.1 Oxygenated volatile organic compounds

There is evidence for a large global source of oxygenated volatile organic compounds (OVOCs) in the atmosphere [13,14 and references therein]. These compounds are emitted directly into the atmosphere from biogenic and anthropogenic sources and are also formed *in situ* in the atmosphere from the oxidation of all hydrocarbons present within the atmosphere [15,16 and references therein]. OVOCs are heavily involved in key atmospheric processes and play a central role in the chemical processes that determine the oxidizing capacity of the atmosphere [13,14]. It is thought that oxygenated organics also make a significant contribution to the organic fraction of atmospheric aerosols [17].

Since a number of organic solvents, e.g. aromatics and halocarbons have shown not only to have adverse health effects, but also to undergo complex chemical reactions in the atmosphere, which lead to the formation of environmentally damaging compounds, it is now well accepted that the switch from aromatic and halocarbon solvents to oxygenated compounds is inevitable both in terms of toxicity problems and reducing the level of oxidant formation in the troposphere. From available experimental data, it has been suggested that the ozone forming potential of oxygenates is likely to be less than aromatic and unsubstituted hydrocarbons but considerably greater than that of the chlorocarbons [14,18-27]. Table 1.1 summarizes the development in solvent consumption during the last 20 years in West Europe [28].

The increasing use of organic oxygenates as solvents has led to the need for knowledge on their contribution to the oxidizing capacity of the atmosphere, their possible contribution to toxic contaminant formation, indoor pollution and their contribution to secondary organic aerosol (SOA) formation [15-17]. Therefore, a large number of gas-phase reactions of small-chain oxygenated organic compounds has

been investigated and reviewed over the last decade [1,16,17,28-36].

The initial step in the oxidation of simple OVOCs such as alcohols, ethers, carbonyls and esters in the atmosphere is mainly reaction with the OH radical. The kinetics and mechanisms for such OVOCs have been reasonably established for compounds with carbon skeletons with up to six carbon atoms [18-21,28,37-42]. However, the oxidation of higher molecular weight and polyfunctional OVOCs is much less clear and knowledge is rather sparse. In addition, current structure-activity relationships can not predict the reactivity of these more complex species with any degree of accuracy.

Table 1.1 Development in the consumption of solvents in Western Europe (as percentage of total) [28].

| Category | 1980 | 1986 | 1990 | 1995 | 2000 |
|---------------------------------------|------|------|------|------|------|
| Oxygen-containing solvent | 36.5 | 45 | 51 | 58 | 65 |
| Aliphatic | 28.5 | 22 | 20.5 | 19 | 15 |
| Aromatics | 20.5 | 20 | 19 | 17 | 15.5 |
| Chlorinated hydrocarbons | 14.5 | 13 | 9.5 | 6 | 1.5 |
| Total consumption (10 ⁶ t) | 5.1 | 4.75 | 4.7 | 4.15 | 3.3 |

1.2 Atmospheric chemistry of vinyl ethers

Field measurements indicate that OVOCs constitute a major component of the trace gases found in the troposphere [13]. However, recent field campaign and modeling studies [43,44] have highlighted significant discrepancies between the expected levels of pollutants from solvent use using current emission inventories and the observed levels. This indicates either inadequacy in the emission inventory calculations and/or knowledge of the atmospheric fate of the emitted solvents, a large proportion of which are oxygenated organic compounds such as ethers.

Vinyl ethers (ROCH=CH₂) are widely applied in industry as oxygenated solvents, additives and in different types of coatings [45,46]. They are a class of ethers that is

released to the atmosphere entirely from anthropogenic sources. Due to the presence of the alkene moiety in vinyl ethers it is to be expected that they will show moderate to high reactivity towards the major atmospheric oxidants, i.e. OH radical, ozone and NO₃ radical, and under certain circumstances possibly Cl atoms. To date only limited kinetic and product data are available in the literature on the gas-phase reactions of a few vinyl ethers with the OH radical [16,47-56], O₃ [29,48-55,58,59] and the NO₃ radical [16,48,49,51-54,57,60].

1.2.1 Kinetic studies of vinyl ethers

Like other carbon-carbon double bond containing compounds the principle degradation processes of vinyl ethers are controlled mainly by chemical reaction with OH radicals, ozone and NO₃ radicals. Perry *et al.* [47] reported an absolute rate coefficient for the reaction of the OH radical with methyl vinyl ether (MVE). As can be seen in Table 1.2, the value obtained by Perry *et al.* [47] was in fair agreement with that reported by Mellouki [51] who used a relative kinetic technique. However, both determinations are substantially lower than the value estimated by Grosjean and Williams [49] from structure-activity-relationships (SAR) and linear free-energy relationships (LFER).

In last few years, several research groups have conducted kinetic studies on alkyl vinyl ethers. As shown in Table 1.2, using pulsed laser photolysis-laser induced fluorescence (PLP-LIF) and a relative kinetic technique, Mellouki *et al.* [51,56] have measured rate coefficients for the reaction of OH radicals with a series of alkyl vinyl ethers. Among them, only the result for propyl vinyl ether (PVE) is in agreement with that obtained by Al Mulla [55] who used a relative kinetic method. The result from Al Mulla for the reaction of OH with ethyl vinyl ether (EVE) is lower than Mellouki's determinations; for reactions of OH with butyl vinyl ether (BVE) and iso-butyl vinyl ether (iBVE) the values are higher than the other determinations although they agree, in part, within the combined quoted errors. The rate coefficient for the OH reaction with tert-butyl vinyl ether (tBVE) obtained by Al Mulla is higher than Mellouki's measurements by a factor of more than two.

Table 1.2 Rate coefficients (in $\text{cm}^3 \text{molecule}^{-1} \text{s}^{-1}$) measured at 298 K for the reactions of the OH radical, O_3 and the NO_3 radical with vinyl ethers reported in the literature

| Vinyl ether | OH reaction ($k_{\text{OH}} \times 10^{11}$) | Technique / Ref | O_3 reaction ($k_{\text{O}_3} \times 10^{16}$) | Technique / Ref | NO_3 reaction ($k_{\text{NO}_3} \times 10^{12}$) | Technique / Ref |
|---|---|------------------------------------|--|--------------------------------------|--|------------------------------------|
| MVE, $\text{CH}_3\text{OCH}=\text{CH}_2$ | 3.35±0.34 | FP-RF [47] ⁱ⁾ | - | - | 0.47 | SAR-estimation [49] ⁱⁱ⁾ |
| | 4.5±0.7 | relative rate [51] | | | 0.72±0.15 | relative rate [57] |
| | 6.4 | SAR-estimation [49] ⁱⁱ⁾ | | | | |
| EVE, $\text{C}_2\text{H}_5\text{OCH}=\text{CH}_2$ | 6.8±0.7 | PLP-LIF [50,51] ⁱⁱⁱ⁾ | 2.0±0.2 | concentration fit [50] | 1.7±1.3 | relative rate [60] |
| | 7.3±0.9 | relative rate [50,51] | 1.54±0.3 | p-f-o kinetics [59] ^{iv)} | 1.31±0.27 | relative rate [57] |
| | 5.51±0.13 | relative rate [55] | 1.3 | relative and S-CL [55] ^{v)} | | |
| PVE, $\text{C}_3\text{H}_7\text{OCH}=\text{CH}_2$ | 10±1 | PLP-LIF [51,56] ⁱⁱⁱ⁾ | 2.4±0.4 | concentration fit [51] | 1.33±0.30 | relative rate [57] |
| | 11±1 | relative rate [51] | 2.4 | relative and S-CL [55] ^{v)} | | |
| | 11.5±0.4 | relative rate [55] | | | | |
| BVE, $n\text{-C}_4\text{H}_9\text{OCH}=\text{CH}_2$ | 10±1 | PLP-LIF [51,56] ⁱⁱⁱ⁾ | 2.9±0.2 | concentration fit [51] | 1.70±0.37 | relative rate [57] |
| | 11±1 | relative rate [51] | 2.3 | relative and S-CL [55] ^{v)} | | |
| | 16.3±2.8 | relative rate [55] | | | | |
| iBVE, $i\text{-C}_4\text{H}_9\text{OCH}=\text{CH}_2$ | 11±1 | PLP-LIF [51,56] ⁱⁱⁱ⁾ | 3.1±0.2 | concentration fit [51] | - | - |
| | 11±1 | relative rate [51] | 2.3 | relative and S-CL [55] ^{v)} | | |
| | 15.9±5.9 | relative rate [55] | | | | |
| tBVE, $t\text{-C}_4\text{H}_9\text{OCH}=\text{CH}_2$ | 11±1 | PLP-LIF [51,56] ⁱⁱⁱ⁾ | 5.0±0.5 | concentration fit [51] | - | - |
| | 11±1 | relative rate [51] | 2.4 | relative and S-CL [55] ^{v)} | | |
| | 25.2±1.8 | relative rate [55] | | | | |

- i) Flash Photolysis - Resonance Fluorescence (FP-RF), Arrhenius expressions for the temperature range 299-427 K are reported;
ii) Structure-activity relationship (SAR); iii) Pulsed Laser Photolysis - Laser Induced Fluorescence (PLP-LIF), Arrhenius expressions for the temperature range 230-373 K are reported; iv) pseudo-first-order kinetics; v) Static system - Chemiluminescence analysis (S-CL).

Mellouki [51] and Al Mulla [55] also measured rate coefficients for the ozonolysis of alkyl vinyl ethers. As can be seen in Table 1.2, only the results for PVE + O₃ and BVE + O₃ from Al Mulla [55] are consistent with those reported by Mellouki [51]. The rate coefficients for the ozonolysis of EVE, iBVE and tBVE determined by Al Mulla [55] are significantly lower than the values determined by Mellouki [51].

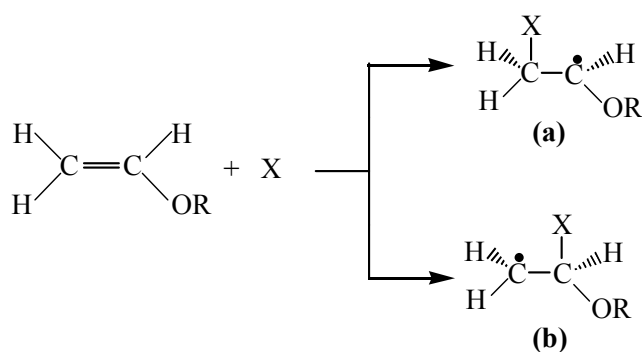
Kinetic studies on the NO₃ radical initiated oxidation of vinyl ethers are much sparser than those for the OH radical and ozone reactions. Only data from Scarfogliero *et al.* [57] and Pfrang *et al.* [60] for reactions of the NO₃ radical with MVE, EVE, PVE and BVE are available in the literature. Though the rate coefficient for the reaction of NO₃ with EVE from Scarfogliero *et al.* [57] is in agreement with that determined by Pfrang *et al.* [60], the data reported by Pfrang *et al.* [60] has large error limits. They had considerable difficulties with the measurements and concluded that the data would benefit from refinement.

Accurate kinetic data is essential for a reliable estimation of the tropospheric lifetimes of the vinyl ethers with respect to photooxidation by atmospheric reactive species since this will determine the scale of their geographical impact, i.e. local, regional or global. Therefore, an extended database for the reaction of vinyl ethers with atmospheric reactive species i.e. OH radical, ozone and NO₃ radical is necessary.

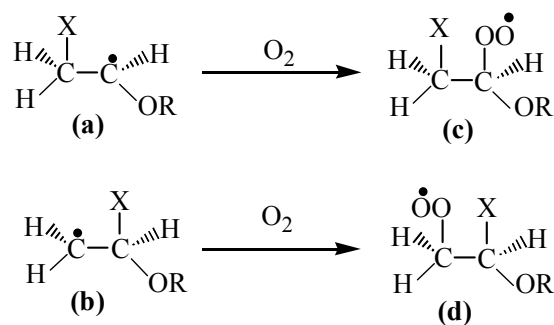
1.2.2 Product and mechanistic studies of vinyl ethers

Investigations of the products and mechanisms for the gas-phase reactions of alkyl vinyl ethers have only appeared during the last few years: MVE reaction with OH, O₃ and NO₃ by Klotz *et al.* [52], EVE and ethyl propenyl ether (EPE) reaction with O₃ by Grosjean *et al.* [29], EVE reaction with OH radical and O₃ by Thiault *et al.* [50], EVE and EPE reaction with OH and NO₃ radicals and O₃ by Barnes *et al.* [48], MVE, EVE, PVE and BVE reaction with OH and O₃ by Al Mulla [55] and MVE, EVE, PVE and BVE reaction with NO₃ radicals by Scarfogliero *et al.* [57].

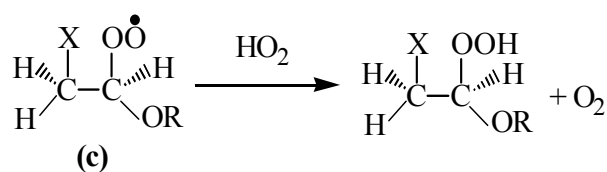
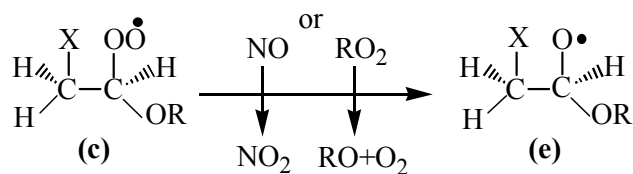
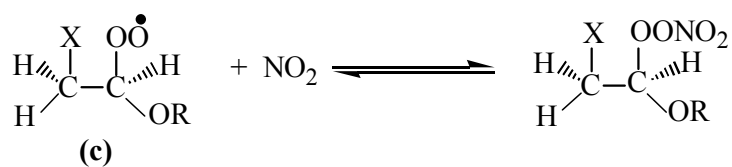
It is established that the OH and NO₃ radical initiated oxidation of vinyl ethers proceeds essentially by the radicals addition to the carbon-carbon double bond. The addition of OH and NO₃ radicals results in the formation of β-hydroxyalkyl (X = OH) and β-nitrooxyalkyl (X = NO₃) radicals, respectively.



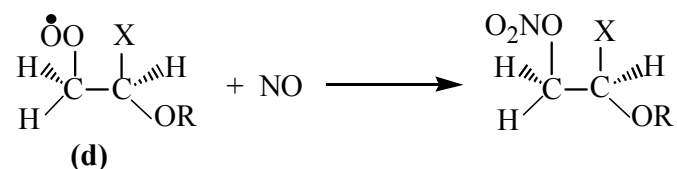
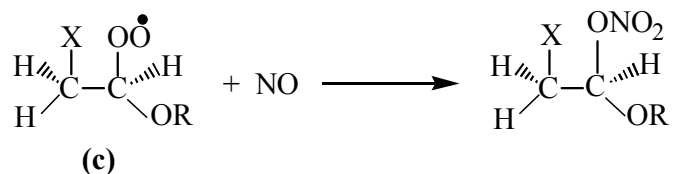
The β -hydroxy/ β -nitrooxy alkyl radicals (a) and (b) react with O_2 to give the corresponding peroxy radicals (c) and (d), respectively:



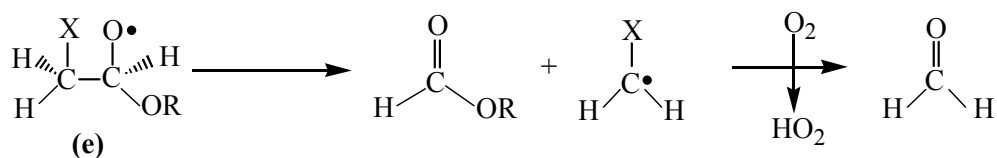
As alkyl peroxy radicals the β -hydroxy/ β -nitrooxy alkyl peroxy radicals react with NO_2 , NO , peroxy radicals and HO_2 radicals. Take radical (c) as an example:



The reaction of β -hydroxy/ β -nitrooxy alkyl peroxy radicals (c) and (d) with NO will also lead to the formation of nitrates.



The possible reactions of β -hydroxy/ β -nitrooxy alkoxy radical are isomerization, decomposition or reaction with O_2 . The product studies on the OH and NO_3 radical initiated oxidation of MVE [52] and EVE [48,50,55,57] indicate that the β -hydroxy/ β -nitrooxy alkoxy radicals formed after OH and NO_3 addition to the terminal carbon-carbon double bond in the alkyl vinyl ether mainly decompose to produce formaldehyde and the corresponding alkyl formates. Take radical (e) as an example:

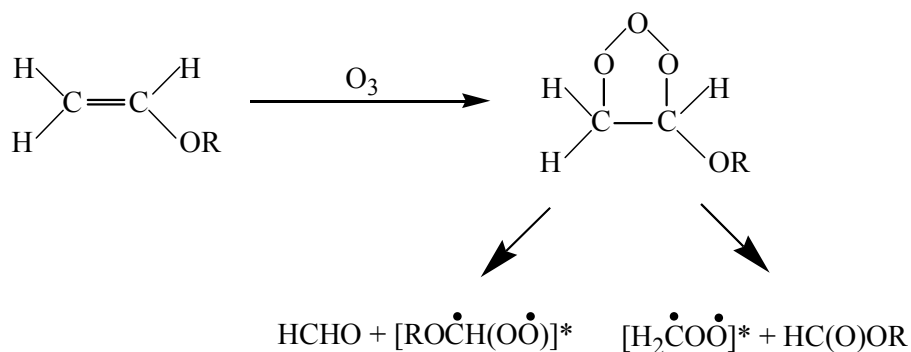


For the OH radical reactions, the molar yields of the alkyl formates for the different vinyl ethers investigated by Klotz *et al.* (OH + MVE) [52] and Al Mulla (alkyl vinyl ethers + OH) [55] fall within the range of (60-80) molar % for NO_x -containing systems and (50-70) molar % for NO_x -free systems. However, Thiault *et al.* [50] have reported a very high formate yield for the reaction of OH with EVE.

The observations of formates and HCHO formation for the reactions of NO_3 radicals with MVE, EVE, PVE and BVE reported by Scarfogliero *et al.* [57] largely agree with those made by Klotz *et al.* [52] for the reaction of NO_3 with MVE. No other product studies on the reactions of NO_3 with vinyl ethers currently exist.

As discussed by Barnes *et al.* [48], Klotz *et al.* [52], Thiault *et al.* [50] and Al Mulla [55], the general mechanism for the ozonolysis of vinyl ethers is initial addition of O_3 to the terminal carbon-carbon double bond in the vinyl ethers to form an energy-rich

primary ozonide, which rapidly decomposes, as shown below, to form carbonyls and so-called Criegee biradicals. The decomposition of Criegee biradicals gives formates and HCHO.



The formation yields of formates and HCHO for the ozonolysis of vinyl ethers determined by Klotz *et al.* [52] for MVE, Thiault *et al.* [50] and Al Mulla [55] for EVE and Barnes *et al.* [48] for EVE, iBVE, tBVE and EPE fall within the ranges (75±15) and (20±10) molar %, respectively. However, the formate yield reported by Grosjean and Grosjean [29,58] for EVE + O₃ is much lower (factor of 2) and the HCHO yields much higher (factor of 2 or more) than those reported by the other aforementioned authors. Higher yields of HCHO are also obtained by Al Mulla [55] for the reactions of ozone with iBVE and tBVE. The reason for this large discrepancy is presently not known.

1.2.3 Secondary organic aerosol (SOA) formation from vinyl ethers

It is commonly accepted that seven or more C-atoms are required for aerosol formation from non-cyclic hydrocarbons and six for cyclic species [61-63]. MVE, with only 3 carbon atoms, is the smallest compound studied until now that has been shown to produce aerosol during its atmospheric degradation. Klotz *et al.* [52] have postulated that oxalic acid and/or condensation reactions, possibly involving the Criegee intermediates are responsible for the SOA formation in the ozonolysis of MVE. Recently Sadezky *et al.* [64] reported SOA formation in the gas-phase reactions

of ozone with other alkyl vinyl ethers (EVE, PVE, BVE, iBVE and tBVE). The formation yields of SOA were reduced in the presence of an excess amount of cyclohexane (used as OH radical scavenger), water and formic acid (Criegee biradical scavengers). Using mass spectrometry the authors identified the formation of oligomers having the basic structure $-[\text{CH}(\text{R})-\text{O}-\text{O}]_n-$, where $\text{R}=\text{H}$ for alkyl vinyl ethers and $\text{R}=\text{CH}_3$ for EPE, as major constituents of the SOA. The mechanism of the formation of the oligomer is unclear but is assumed by the authors to involve reaction of the Criegee biradicals with the double bond of the vinyl ethers.

The aerosol profiles observed in the ozonolysis of alkyl vinyl ethers [52,64] showed typical behavior associated with homogeneous nucleation. According to Odum *et al.* [8] if condensation plays a significant role in the aerosol formation, the evaluation should give higher aerosol yields when the initial reactant concentrations are raised.

1.3 Aim of the work

As discussed previously, the atmospheric chemistry of vinyl ethers has only been studied to date for a few alkyl vinyl ethers. Among these studies there are quite a number of discrepancies between the results reported by the different research groups. Ideally a complete understanding of the atmospheric behavior and environmental impact of a chemical is highly desirable before its widespread deployment, especially in the case of high volume chemicals such as oxygenated solvents. For many chemicals, such as vinyl ether solvents, the pre-use environmental impact analysis is often very rudimentary.

The purpose of this work was to provide a scientific evaluation of the atmospheric fate of alkyl vinyl ethers and ethyleneglycol vinyl ethers, which are either presently being used in industry or are being considered as replacements for other atmospherically detrimental solvents.

The research work involved measuring rate coefficients for the reactions of PVE, BVE, ethyleneglycol monovinyl ether (EGMVE), ethyleneglycol divinyl ether (EGDVE) and diethyleneglycol divinyl ether (DEGDVE) with the OH radical, O_3 and the NO_3 radical at atmospheric pressure and room temperature using a relative kinetic technique.

Laboratory chamber studies were performed to identify and quantify the oxidation products from the reactions of PVE and BVE with the OH radical, O₃ and the NO₃ radical. This information was used to formulate atmospheric degradation mechanisms for the reactions of the alkyl vinyl ethers with the atmospheric oxidants.

Using scanning mobility particle sizer (SMPS) exploratory SOA studies were performed on the ozonolysis of PVE and BVE in the presence of an excess of cyclohexane.

Chapter 2

Experimental Section

2.1 Reaction chambers

2.1.1 Description of the 405 l reactor

All the kinetic and product studies performed in this work were carried out in a 405 liter evacuable chamber. A detailed description of the reactor can be found in the literature [65,66]. Only a brief description is given below. Figure 2.1 shows a schematic representation of the reactor.

The chamber is comprised of a cylindrical borosilicate glass vessel, having a length of 1.5 m and an inner diameter of 60 cm, and is closed at both ends by Teflon coated aluminum flanges. One of the metal flanges contains inlet ports for reactants and bath gases, vacuum connections and a capacitance manometer (Membranovac MV 110 S2). Additional inlet and outlet ports and a magnetically coupled Teflon mixing fan to ensure homogeneous mixing of the reactants are located on the other flange. The reactor can be evacuated to 10^{-3} Torr by a pumping system consisting of a Balzer turbo/molecular pump, model WZ 500, backed by a Leybold double stage rotary fore pump, model D 40 B. Two types of photolysis sources are available for the experiments: 18 fluorescent lamps (Philips TLA 40 W/05; $300 \leq \lambda \leq 450$ nm, $\lambda_{\max} = 360$ nm) spaced evenly around the outside of the reactor and 3 low-pressure mercury vapor lamps (Philips TUV40W; $\lambda_{\max} = 254$ nm) placed inside a quartz glass tube which

is mounted centrally inside the main reactor vessel and supported by the end flanges. In order to maintain the reactor at room temperature during the photolysis of the reactants, the lamps are cooled by flowing ambient air through the lamp housing units. A White-type mirror system (base path length 1.4m) mounted internally within the chamber, and coupled to an FTIR spectrometer (Fourier Transform-Infrared Spectrometer; Nicolet Magna 550) equipped with a globar as IR source and a liquid nitrogen cooled MCT-detector (mercury-cadmium-tellurium detector), enables *in situ* infrared monitoring of both reactants and products. The White system was operated with a total optical absorption path of 50.4 m and infrared spectra were recorded with a spectral resolution of 1 cm^{-1} . The spectrometer and the external transfer optics are permanently purged with dry air to maintain atmospheric water vapor at a minimum. The spectrometer is directly controlled by the software OMNIC, installed on a personal computer.

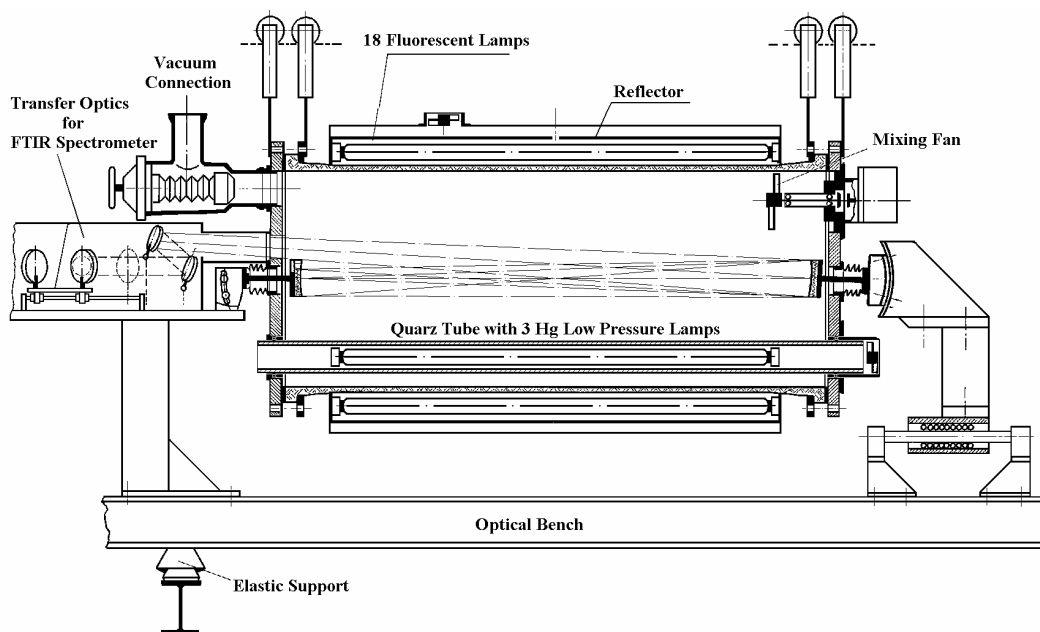


Figure 2.1 Schematic representation of the 405 l borosilicate glass chamber

2.1.2 Description of the 1080 l reactor and scanning mobility particle sizer (SMPS) system

2.1.2.1 Description of the 1080 l reactor

All the studies on the SOA formation performed in this work were carried out in a 1080 l reaction chamber equipped with a Scanning Mobility Particle Sizer (SMPS) system. There are some constructive similarities between the 1080 l reactor and the 405 l reaction chamber and a detailed description can be found in the literature [67]. Only a brief description is given here.

The reactor, which has a total length of 6.2 m and an inner diameter of 0.47 m, consists of two quartz glass cylinders connected by a central enamel flange ring and silicon rubber seals and is closed at both ends by aluminum flanges. Figure 2.2 shows a schematic representation of the reaction chamber experimental setup.

The reactor can be evacuated by a turbo molecular pump (Leybold-Heraeus PT 450) backed by a Leybold D65B double stage rotary vacuum pump to a pressure of less than 10^{-3} mbar. To ensure homogeneous mixing of the reactants three fans with Teflon blades are mounted inside the chamber. Both end flanges contain inlet systems for

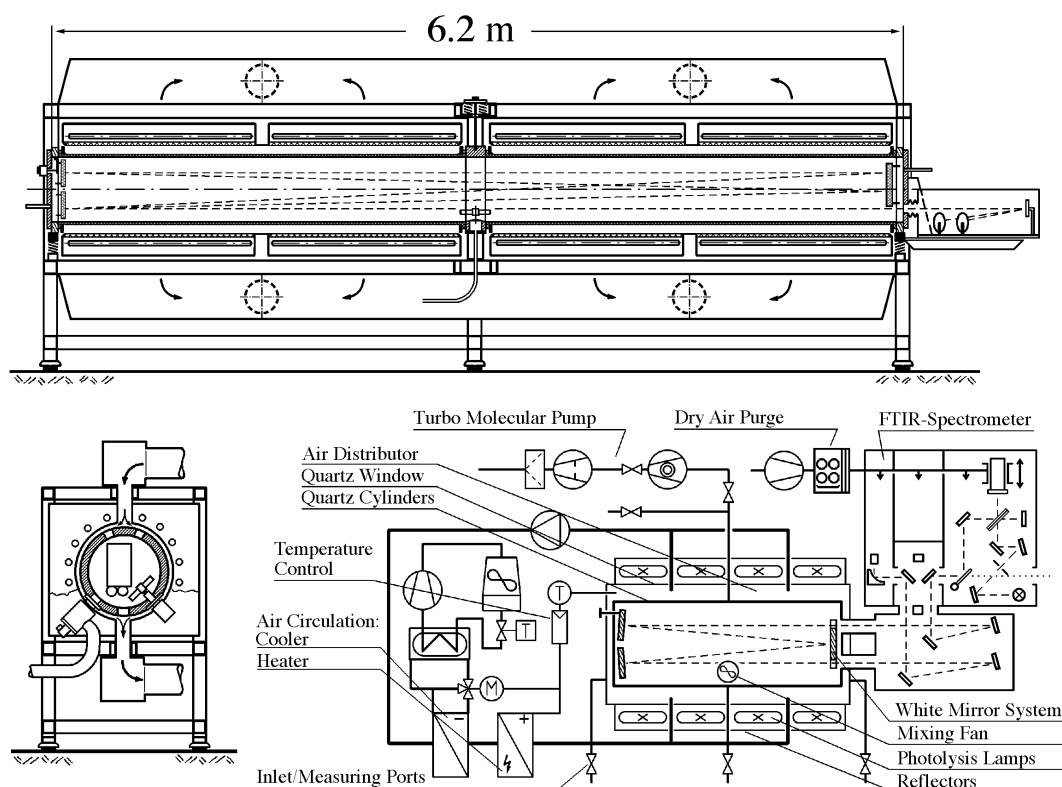


Figure 2.2 Schematic representation of the 1080 l quartz glass reactor

reactants and bath gases and ports for mounting pressure and temperature measurement instruments. The chamber is equipped with 32 super actinic fluorescent lamps (Philips TL 05/40 W: $320 \leq \lambda \leq 480$ nm, $\lambda_{\max} = 360$ nm) and 32 low-pressure mercury lamps (Philips TUV40W, $\lambda_{\max} = 254$ nm). A White type multi-reflection mirror system with a base length of (5.91 ± 0.01) m for sensitive *in situ* long path absorption monitoring of both reactants and products in the IR spectral range is mounted on the flanges. The White system was operated at 82 traverses, giving a total optical path length of (484.7 ± 0.8) m. The IR spectra were recorded with a spectral resolution of 1 cm^{-1} using a Bruker IFS 88 FTIR spectrometer equipped with an MCT detector. An outlet port for particle sampling is located in the central flange of the reactor.

2.1.2.2 Description of the scanning mobility particle sizer (SMPS) system

The Model 3934 SMPS system consists of an electrostatic classifier and two independent condensation particle counters (CPC) (TSI 3022 A connected to the classifier and a standalone TSI 3025 ultra-fine condensation particle counter UCPC). The TSI 3022 A CPC was mainly used in the present work.

The SMPS uses a bipolar charger in the electrostatic classifier to charge the particle to a known charge distribution. The particles are then classified according to their ability to traverse an electrical field and counted with the CPC. Figure 2.3 shows a schematic diagram of the electrostatic classifier with the TSI 3022 A CPC.

The electrostatic classifier used in the present work is a model 3071 A manufactured by the TSI company. The aerosol sample enters through an inertial impactor which removes larger particles that may carry more than a single charge and lie outside the measurement range. The aerosol then passes through the Kr-85 charger. The charger consists of 2 mCi (7.4×10^7 Bq) of Kr-85 radioactive gas contained in a capillary tube. This creates a high level of positive and negative ions and brings the aerosol charge level to a Fuchs' equilibrium charge distribution [68]. The center rod inside the electrostatic classifier is connected to a variable high voltage source and the outer cylinder is kept at ground potential and this creates an electric field. Some of the particles are attracted to the center rod when the particles pass through the classifier.

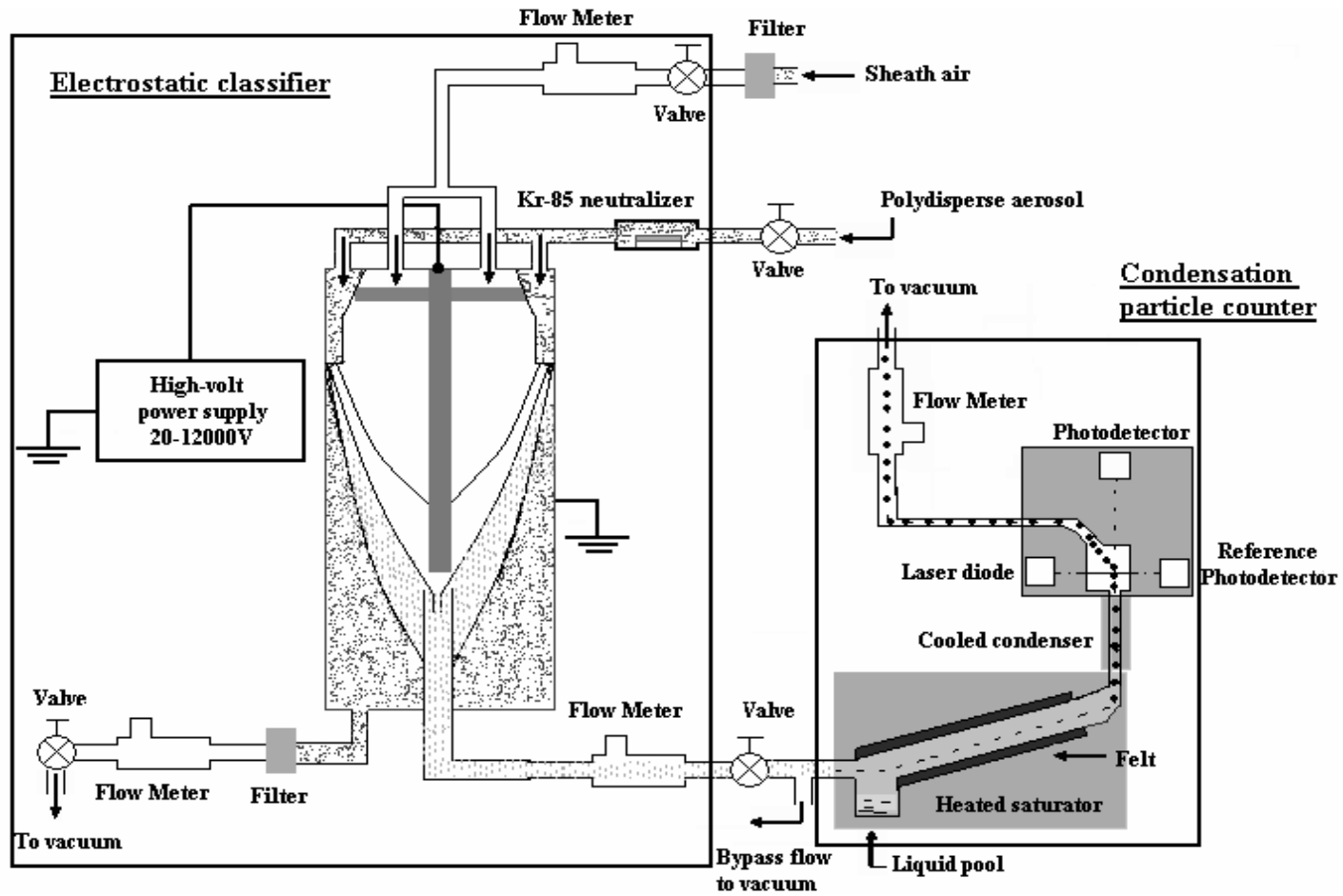


Figure 2.3 Schematic representation of the SMPS system

The electrical mobility of a particle is inversely proportional to the size of the particle. Particles with a higher mobility will be captured near the top of the rod and others will go on through the exhaust. Some of the particles will have the correct mobility to go through the opening at the bottom. The classifier separates aerosols based on their electrical mobility, which is dependent on their charge state and particle size, allowing for a flow of monosize particles to exit the classifier. This mono-dispersed aerosol can then be counted by the CPC.

The CPC employed in the present work is the model 3022 A. An internal pump draws the aerosol into the CPC with low-flow operation (0.3 liter per minute). A volumetric flowmeter controls the flow rate. Upon entering the instrument, the sample passes through a heated saturator (37 °C), where n-butanol evaporates into the air stream and saturates the flow. The aerosol sample then passes into a cooled condenser tube (10 °C), where vapor supersaturates and condenses onto the airborne particles. This produces larger, easily detectable aerosol droplets. These droplets pass through a heated optical detector (36 °C) immediately after leaving the condenser.

For concentrations below 10^4 particles cm^{-3} the detector counts individual pulses produced as each particle (droplet) passes through the sensing zone (single-count mode). Higher concentrations up to 10^7 particles cm^{-3} are measured by detecting light scattered by all particles in the sensing zone at any one time and comparing the intensity of the scattered light with calibration levels (photometric mode).

2.2 Experimental procedure and data evaluation

2.2.1 General

All the experiments performed in this work were carried out at (298±3) K in synthetic air. The compounds under investigations were introduced into the evacuated reactor by methods which depended on their states, i.e. solid, liquid or gaseous, and on their vapor pressure: gas and liquid compounds were injected by means of syringes (gas-tight syringes and microliter syringes), either directly into the chamber or in a stream of bath gas. For the liquid compounds with high boiling-point the inlet port

was also heated. Solid compounds were introduced into the reactor using a special inlet system. This inlet system consists of a long glass tube having a small glass container attached in the middle where weighed amounts of the substances can be added. One port of this inlet system is connected to the bath gas by a Teflon tube and the other port is connected to the reaction chamber through a steel tube and a special valve. The solid compounds are then heated in the small glass container until a certain pressure is reached. The content of the glass container is then added to the evacuated reactor by opening the valve and flushing the heated glass container with a slow flow of the bath gas. In order to avoid condensation of the semi-volatile compounds onto the inlet system, the system was heated with an electrical heating band. The concentrations of the reactants and products were determined by computer-aided subtraction of calibrated reference spectra. The source of the chemicals used and their stated purity are listed in Appendix II. The values of the FT-IR integral cross sections that have been used in the quantification procedure are given in Appendix III.

2.2.2 Kinetic studies

A relative kinetic technique was used to determine the rate coefficients for the reactions of OH radical, O₃ and NO₃ radical with selected vinyl ethers.

2.2.2.1 Relative rate method

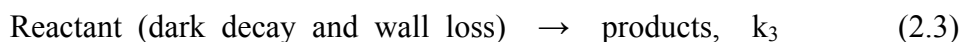
In the relative rate method the disappearance of reactants, i.e. vinyl ethers, due to reaction with the reactive species (OH, O₃ and NO₃) is measured relative to that of a reference compound(s), whose rate coefficient(s) with the reactive species is(are) reliably known, e.g. for the OH radical reaction:



Additionally, vinyl ethers and the reference hydrocarbon(s) could be lost by deposition on the reactor walls or photolysis. However, when the vinyl ethers were

admitted into the chamber, as discussed later, in addition to wall loss, dark decays of the compounds were observed accompanied by the formation of new bands in the IR spectrum.

The combined dark decay and wall loss was found to obey first order kinetics and can be represented by,



The following equation has been used to evaluate the kinetic data:

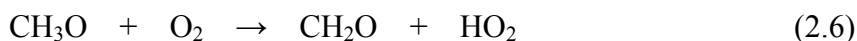
$$\ln \left\{ \frac{[\text{Reactant}]_{t_0}}{[\text{Reactant}]_t} \right\} - k_3(t - t_0) = \frac{k_1}{k_2} \times \left(\ln \left\{ \frac{[\text{Reference}]_{t_0}}{[\text{Reference}]_t} \right\} - k_4(t - t_0) \right) \quad (I)$$

where $[\text{Reactant}]_{t_0}$ and $[\text{Reference}]_{t_0}$ are the concentrations of the reactants and reference compound(s), respectively, at time t_0 ; $[\text{Reactant}]_t$ and $[\text{Reference}]_t$ are the corresponding concentrations at time t ; k_1 and k_2 are the rate coefficients for the reaction of reactants and reference(s) with OH radical, respectively; k_3 and k_4 are the dark loss rates of reactants and reference(s), respectively. Plots of $\ln([\text{Reactant}]_{t_0}/[\text{Reactant}]_t) - k_3(t - t_0)$ versus $\ln([\text{Reference}]_{t_0}/[\text{Reference}]_t) - k_4(t - t_0)$ should give straight lines with slopes k_1/k_2 . The rate coefficient k_1 can be derived from the known rate coefficient k_2 . Since the dark losses of the vinyl ethers and reference(s) are first order reactions, the rate k_3 and k_4 can be derived from the slope of plots of $\ln([\text{Reactant}]_{t_0}/[\text{Reactant}]_t)$ and $\ln([\text{Reference}]_{t_0}/[\text{Reference}]_t)$ versus time before reactions (2.1) and (2.2) are initiated. Frequent checks were made to verify that the dark losses of both the vinyl ethers and reference(s) did not change during the course of the reactions by measuring their rates in the pre- and post-reaction periods.

The rate coefficients for the ozone and NO_3 radical reactions with the vinyl ethers have been determined using the relative kinetic technique in a manner analogous to that described above for the OH radical reactions.

2.2.2.2 OH radical reaction

Kinetic experiments for the reactions of OH radical with selected vinyl ethers were performed at (750±10) Torr total pressure of synthetic air using two hydrocarbons as reference compounds. The photolysis of either CH₃ONO-NO-air mixtures in the visible light ($\lambda_{\text{max}} = 360$ nm) or H₂O₂ under UV light ($\lambda_{\text{max}} = 254$ nm) was used for the production of OH radicals,



The addition of nitric oxide, NO, to the CH₃ONO-air mixtures is generally used to enhance OH production and to suppress the formation of O₃ and, hence of NO₃ radicals. Using the photolysis of methyl nitrite or hydrogen peroxide, OH radical concentrations of about 1×10^8 molecules cm⁻³ can be readily obtained for time scales of 10 minutes or more. The synthesis and storage of CH₃ONO is given in Appendix I. H₂O₂ was supplied as an 85% solution and was used without further pre-concentration.

2.2.2.3 O₃ and NO₃ radical reaction

All the experiments on the reactions of O₃ and NO₃ radicals with vinyl ethers were carried out at (740±10) Torr total pressure of synthetic air. Ozone was added step-wise to pre-mixed mixtures containing the vinyl ether, reference compound(s) and cyclohexane. Cyclohexane was present in excess to scavenge more than 95% of OH radicals produced in the reaction system. Ozone was generated as a mixture in O₂ by passing O₂ through an ozone generator.

NO₃ radicals were produced by the thermal dissociation of N₂O₅ prepared in solid form according to a literature method [69] given in Appendix I:



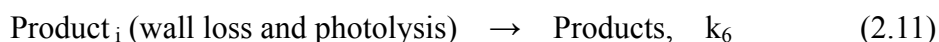
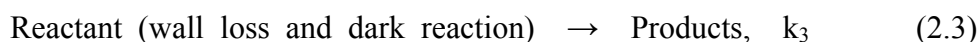
As for the investigations on the ozonolysis of the vinyl ethers the experiments on the NO₃ radical reactions were performed using multiple additions of N₂O₅ to a mixture of the vinyl ether and reference compound(s) (isoprene or 2,3-dimethyl-1,3-butadiene). N₂O₅ was added to the chamber by passing air over the surface of solid N₂O₅, which was placed in a dry ice-ethanol cooling trap at -50°C.

2.2.3 Product studies

2.2.3.1 Correction of product formation yields

In some cases the concentrations of the products can not be evaluated directly due to dark wall loss of the product and/or reaction of the product with the reactive species, e.g. OH radicals. In such cases the yields were corrected with the method outlined by Tuazon *et al.* [70].

In order to correct the formation yields of the products in the OH radical initiated oxidation of vinyl ethers the following reaction sequence needs to be considered:



If the reasonable assumption is made that the OH radical concentration remains essentially constant over the small irradiation periods, then from the rate law,

$$\frac{d[\text{Reactant}]}{dt} = -k_3[\text{Reactant}] - k_1[\text{Reactant}] \times [\text{OH}] \quad (\text{II})$$

one obtains

$$\frac{d[\text{Reactant}]}{[\text{Reactant}]} = -(k_3 + k_1 \times [\text{OH}])dt \quad (\text{III})$$

By making the reasonable assumption that the OH radical concentrations were

essentially constant over the small irradiation period t_1 - t_2 , integration of the above equation and rearrangement leads to the following expression for the OH concentration:

$$[\text{OH}]_{t_1-t_2} = \frac{\ln \frac{[\text{Reactant}]_{t_1}}{[\text{Reactant}]_{t_2}} - k_2}{k_1} \quad (\text{IV})$$

where $[\text{OH}]_{t_1-t_2}$ is the OH radical concentration between time t_1 and t_2 ; $[\text{Reactant}]_{t_1}$ and $[\text{Reactant}]_{t_2}$ are the concentrations of reactants, i.e. vinyl ethers at time t_1 and t_2 , respectively; k_1 is the rate coefficient for the reaction of OH radicals with the reactants and k_3 is the dark loss rate of the reactants.

The product concentration is given by:

$$\begin{aligned} [\text{Product}_i]_{t_2} = & [\text{Product}_i]_{t_1} \times \exp(-(k_5 \times [\text{OH}] + k_6) \times (t_2 - t_1)) + \\ & \frac{Y_{t_1-t_2} \times [\text{Reactant}]_{t_1} \times k_5 [\text{OH}]}{(k_5 - k_1) \times [\text{OH}] + k_6} \times (\exp(-(k_1 \times [\text{OH}] + k_3) \times (t_2 - t_1)) \\ & - \exp(-(k_5 \times [\text{OH}] + k_6) \times (t_2 - t_1))) \end{aligned} \quad (\text{V})$$

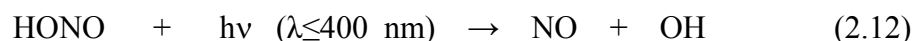
where $[\text{Product}_i]_{t_1}$ and $[\text{Product}_i]_{t_2}$ are the concentrations of Product_i observed at time t_1 and t_2 , respectively; k_5 is rate coefficient of Product_i with OH radical; k_6 is the dark wall loss rate of Product_i ; $Y_{t_1-t_2}$ is the formation yield of individual product over time period of t_1 - t_2 . Use of eq. (IV) and (V) allows the formation yield of the product $Y_{t_1-t_2}$ to be calculated. The corrected concentrations of Product_i are then given by,

$$[\text{Product}_i]_{t_2}^{\text{corr.}} = [\text{Product}_i]_{t_1}^{\text{corr.}} + Y_{t_1-t_2} \times ([\text{Reactant}]_{t_2} - [\text{Reactant}]_{t_1}) \quad (\text{VI})$$

where $[\text{Product}_i]_{t_1}^{\text{corr.}}$ and $[\text{Product}_i]_{t_2}^{\text{corr.}}$ are the corrected product concentrations at time t_1 and t_2 , respectively.

2.2.3.2 OH radical reaction

In order to understand the reaction mechanism in the presence and absence of NO_x the photolysis of both nitrous acid (HONO) and hydrogen peroxide (H₂O₂) were used as the OH radical source for the product investigations. According to the method given in Appendix I, HONO, a NO_x-containing OH radical source, was synthesized by adding a 1% NaNO₂ aqueous solution dropwise into a flask containing 30% sulfuric acid [71]. The photolysis of HONO produces OH radicals and NO:

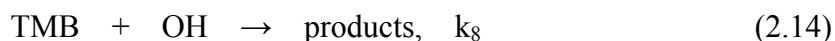
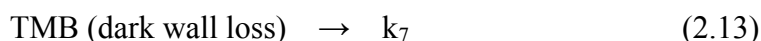
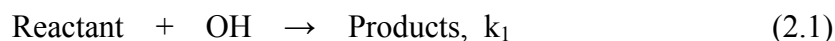


The photolysis of H₂O₂ was shown in reaction 2.6.

2.2.3.3 O₃ reaction

Two types of experiments were performed for product investigations on the ozonolysis of vinyl ethers: i) experiments in which an excess of cyclohexane was added to scavenge more than 95% of the OH radicals produced in the reaction and ii) experiments in which 1,3,5-trimethylbenzene (TMB) was added as a tracer for the OH radicals. Ozone was added step-wise to pre-mixed vinyl ether and cyclohexane or TMB in synthetic air.

In the OH radical “tracer type” of experiment the product concentrations measured cannot be evaluated directly since the vinyl ether also reacts with the OH radicals and produces products which are also formed in the ozonolysis of the vinyl ether. Use of TMB as an OH tracer allows the OH radical concentration to be evaluated:



The method of correction of the concentrations of the reactant and products due to OH radical reaction is the same as that used in the OH initiated oxidation of vinyl ether which is described above in detail. The amount of vinyl ether which reacts with OH radicals is given by:

$$\Delta[\text{Reactant}]_{t_{n+1}-t_n}^{\text{OH}} = [\text{Reactant}]_{t_n} \left(1 - \exp \left(- \frac{k_1}{k_8} \left(\ln \frac{[\text{TMB}]_{t_n}}{[\text{TMB}]_{t_{n+1}}} - k_7(t_{n+1} - t_n) \right) \right) \right) \quad (\text{VII})$$

where $\Delta[\text{Reactant}]_{t_{n+1}-t_n}^{\text{OH}}$ is the concentration of vinyl ether which consumed by OH radicals over time period of t_n-t_{n+1} ; $[\text{Reactant}]_{t_n}$ is the concentration of vinyl ether at time t_n , k_1 is the rate coefficient for the reaction of vinyl ether with OH radicals taken from kinetic studies; k_7 is the dark loss rate of TMB and k_8 is the rate coefficient for the reaction of OH with TMB ($k_8 = 5.67 \times 10^{-11} \text{ cm}^3 \text{ molecule}^{-1} \text{ s}^{-1}$) [15], $[\text{TMB}]_{t_n}$ and $[\text{TMB}]_{t_{n+1}}$ are the concentrations of TMB at time t_n and t_{n+1} , respectively.

The total amount of OH radicals formed in the ozonolysis of vinyl ether between times t_n and t_{n+1} is given by [52]:

$$[\text{OH}]_{t_{n+1}-t_n}^{\text{total}} = [\text{OH}]_{t_{n+1}-t_n} + \sum_i \Delta[\text{Reactant}_i]_{t_{n+1}-t_n}^{\text{OH}} \quad (\text{VIII})$$

where $[\text{OH}]_{t_{n+1}-t_n}^{\text{total}}$ is the total amount of OH radicals formed in the reaction of ozone with vinyl ether in the time interval $t_{n+1}-t_n$; $[\text{OH}]_{t_{n+1}-t_n}$ is the OH radical concentration over time interval $t_{n+1}-t_n$; $\Delta[\text{Reactant}_i]_{t_{n+1}-t_n}^{\text{OH}}$ represents the concentration of each species that consumes OH radicals including the vinyl ether; t_n and t_{n+1} are the reaction times. The concentrations calculated for each time interval $t_{n+1}-t_n$ can then be added to give the total amount over the reaction time range.

2.2.3.4 NO₃ radical reaction

The product studies on the reactions of the NO₃ radical with the vinyl ethers were performed in a manner analogous to the NO₃ kinetic studies, however, without addition of the reference compounds.

2.2.4 Secondary organic aerosol (SOA) formation

The SOA formation from the ozonolysis of PVE and BVE was measured in the presence of an excess of cyclohexane.

2.2.4.1 Aerosol yield

In the present work the SOA formation yield, Y , is defined as the fraction of the reactant, i.e. vinyl ether, which is converted into aerosol:

$$Y = \frac{\Delta M_0 (\mu\text{g}/\text{m}^3)}{\Delta[\text{Reactant}] (\mu\text{g}/\text{m}^3)} \quad (\text{IX})$$

where, ΔM_0 is the total organic aerosol mass concentration resulting from the oxidation of a given reacted amount of reactant, $\Delta[\text{Reactant}]$.

The oxidation of the vinyl ethers gives rise to many different products and the total concentration of any given product, C_i in both the gas and aerosol phases is given as:

$$C_i = G_i + A_i \quad (\text{X})$$

where, G_i is the concentration of species i in the gas-phase and A_i is that in the aerosol phase. So the total organic aerosol mass concentration ΔM_0 can be expressed by:

$$\Delta M_0 = \sum_{i=1}^n A_i \quad (\text{XI})$$

If α_i is a mass-based stoichiometric coefficient of species i , the total concentration of species i is also given by

$$C_i = \alpha_i \times \Delta[\text{Reactant}] \quad (\text{XII})$$

According to the gas/aerosol partition model proposed by Odum *et al.* [8] a semi-volatile compound can partition between the gas and aerosol phase, i.e. the compound resides in both the gas and aerosol phase. The partitioning between these two phases is described by the partitioning coefficient K_i :

$$K_i = \frac{A_i/M_0}{G_i} \quad (\text{XIII})$$

where the M_0 is the absorbing organic mass concentration.

Combining equations (IX)-(XIII) leads to the following expression for the total aerosol yield from the vinyl ether:

$$Y = \sum_{i=1}^n Y_i = M_0 \sum_{i=1}^n \left(\frac{\alpha_i \times K_i}{1 + M_0 \times K_i} \right) \quad (\text{XIV})$$

From a fit of the SOA yield Y to the absorbing organic mass concentration M_0 , the parameters α_i and K_i can be determined.

2.2.4.2 Experimental procedure

All the experiments on the SOA formation from the ozonolysis of alkyl vinyl ethers were carried out in the 1080 l quartz chamber in synthetic air. Excess amounts of cyclohexane were introduced to trap the OH radical produced in the system. The vinyl ether and cyclohexane were first injected into the heated inlet and flushed into the evacuated reactor in a stream of synthetic air. The chamber was then pressurized to around 1000 mbar and infrared spectra were then recorded and the gas mixture was sampled using the SMPS system. The loss in pressure in the chamber due to sampling with the SMPS was compensated by an air flow. The reaction was initiated by introduction of a continuous flow of ozone to the pre-mixed vinyl ether/cyclohexane/air mixtures.

In all the experiments the FTIR was operated with 1 cm⁻¹ resolution and a total of 30 to 40 spectra were recorded. The SMPS instrument scan times were adjusted to match those of the FTIR.

2.3 The dark reaction of vinyl ethers

In the present studies when PVE, BVE, EGDVE and DEGDVE were admitted into the chamber, in addition to wall loss, dark decays of the compounds were observed accompanied by the formation of new bands in the IR spectra which could be assigned to acetaldehyde (CH₃CHO) and an alcohol. Taking PVE as an example, the dark decay of PVE resulted in the formation of CH₃CHO and propanol (C₃H₇OH). The dark product spectrum and reference spectra are shown in Figure 2.4.

This process was not enhanced in the presence of light showing that photolytic losses of vinyl ethers are not important. The enhanced loss of the vinyl ethers at the walls is attributed to acid catalyzed hydrolysis, e.g.



The combined dark decay and wall loss was found to obey first order kinetics.

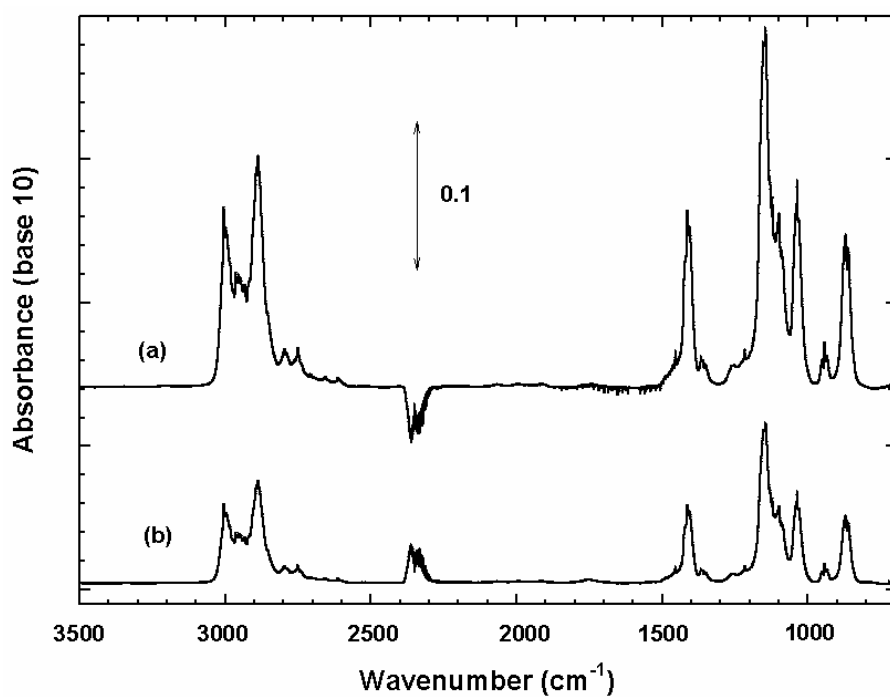


Figure 2.5 Dark reaction of ethyleneglycol monovinyl ether (EGMVE) in the chamber: (a) product spectrum obtained after introducing EGMVE into the chamber and leaving to stand in the dark for 15 min; (b) reference spectrum of 2-methyl-1,3-dioxolane

Chapter 3

Kinetic Studies on the OH Radical, O₃ and NO₃ Radical Initiated Oxidation of Selected Vinyl Ethers

In order to assess the potential environmental impacts of vinyl ethers, a series of kinetic studies on the OH, O₃ and NO₃ initiated oxidation of PVE, BVE, EGMVE, EGDVE and DEGDVE have been conducted. All the kinetic measurements were carried out in the 405 l borosilicate glass chamber at the University of Wuppertal, Germany.

3.1 Results and discussions

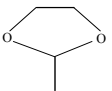
3.1.1 OH radical reactions

Kinetic experiments for the reactions of OH radical with selected vinyl ethers were performed at (298±3) K and (750±10) Torr total pressure of synthetic air. Typically, at least three experimental runs were performed for each reaction to test the reproducibility of the results. The OH radical source and the reference compounds used in the OH kinetic studies are listed in Table 3.1.

The initial concentrations of the vinyl ethers and the reference compound(s) were

approximately 5.0 ppm (1 ppm = 2.46×10^{13} molecule cm^{-3} at 298 K) and 4.9-5.5 ppm, respectively; those of CH_3ONO , NO and H_2O_2 were 1.5-4.0 ppm, 9.8-19.8 ppm, and ~ 20 ppm, respectively. The reactants were monitored in the infrared at the following wavenumbers (in cm^{-1}): PVE at 965, 1211.2 and 3129; BVE at 3128.9 and 1614; EGMVE at 3131; EGDVE at 3127; isobutene at 890; isoprene at 893.4 and 905.9 and TMB at 836.

Table 3.1 Measured rate coefficient ratios, k_1/k_2 , and values of the rate coefficients k_1 (in $\text{cm}^3 \text{molecule}^{-1} \text{s}^{-1}$) for the reactions of OH radical with selected vinyl ethers obtained at 298 K in 750 Torr of synthetic air using the relative kinetic technique.

| Vinyl ether | OH source | Reference | k_1/k_2 | $k_1 \times 10^{11}$ | Average $k_1 \times 10^{11}$ |
|---|-----------------------------------|------------------------|-----------------|----------------------|------------------------------|
| PVE, $\text{n-C}_3\text{H}_7\text{OCH}=\text{CH}_2$ | $\text{CH}_3\text{ONO}+\text{NO}$ | Isobutene | 1.89 ± 0.03 | 9.71 ± 1.96 | 9.73 ± 1.94 |
| | | Isoprene | 0.95 ± 0.02 | 9.75 ± 1.00 | |
| BVE, $\text{n-C}_4\text{H}_9\text{OCH}=\text{CH}_2$ | $\text{CH}_3\text{ONO}+\text{NO}$ | Isobutene | 2.13 ± 0.06 | 10.9 ± 2.2 | 11.3 ± 3.10 |
| | | Isoprene | 1.14 ± 0.04 | 11.5 ± 2.4 | |
| EGMVE $\text{HOCH}_2\text{CH}_2\text{OCH}=\text{CH}_2$ | H_2O_2 | TMB | 1.83 ± 0.05 | 10.4 ± 2.15 | 10.4 ± 2.15 |
| EGDVE $\text{H}_2\text{C}=\text{CHOCH}_2\text{CH}_2\text{O}-$ $\text{CH}=\text{CH}_2$ | $\text{CH}_3\text{ONO}+\text{NO}$ | TMB | 2.04 ± 0.07 | 11.6 ± 2.45 | 12.3 ± 3.25 |
| | | H_2O_2 | TMB | 2.28 ± 0.05 | |
| | H_2O_2 | Isoprene | 1.24 ± 0.05 | 12.5 ± 2.56 | |
| DEGDVE $\text{H}_2\text{C}=\text{CHOCH}_2\text{CH}_2\text{O}-$ $\text{CH}_2\text{CH}_2\text{OCH}=\text{CH}_2$ | $\text{CH}_3\text{ONO}+\text{NO}$ | Isobutene | 2.78 ± 0.10 | 14.3 ± 2.90 | 14.2 ± 3.00 |
| | | Isoprene | 1.41 ± 0.04 | 14.2 ± 2.88 | |
| 2-methyl-1,3-dioxolane  | H_2O_2 | Ethene | 1.26 ± 0.04 | 1.07 ± 0.23 | 1.05 ± 0.25 |
| | | Propene | 0.39 ± 0.01 | 1.03 ± 0.21 | |

Apart from EGMVE all the rate coefficients for the OH radical reactions with the vinyl ethers were determined using two reference compounds. In the kinetic study of

OH + EGDVE, both CH₃ONO and H₂O₂ were used as radical sources to check for possible influences of the OH radical source on the kinetics.

In addition to the vinyl ethers, a kinetic study on the reaction of OH with 2-methyl-1,3-dioxolane was also performed. This compound is a product formed in the dark wall decay of EGMVE (see Section 2.3). The measurements were made relative to ethene and propene using H₂O₂ as the OH radical source (see Table 3.1).

Examples of the kinetic data, plotted according to eq. (I), for all the vinyl ethers investigated and 2-methyl-1,3-dioxolane are shown in Figures 3.1 to 3.6.

Good linear relationships were generally found for all the vinyl ethers and 2-methyl-1,3-dioxolane with the different reference compounds and OH radical sources. The data plots for EGMVE showed more scatter than those for the other compounds. This arises from the relatively fast dark reaction of EGMVE, which makes a large contribution to the overall decay of EGMVE and thus the uncertainty in the decay.

The rate coefficient ratios k_1/k_2 , obtained from the experiments at 298 K are listed in Table 3.1. The rate coefficients, k_1 , determined for the reaction of OH with PVE, BVE, EGMVE, EGDVE and DEGDVE, were put on an absolute basis using the following values of k_2 : $k_2(\text{isobutene, 298 K}) = 5.14 \times 10^{-11}$, $k_2(\text{isoprene, 298 K}) = 1.01 \times 10^{-10}$ and $k_2(\text{TMB, 298 K}) = 5.67 \times 10^{-11} \text{ cm}^3 \text{ molecule}^{-1} \text{ s}^{-1}$ [72].

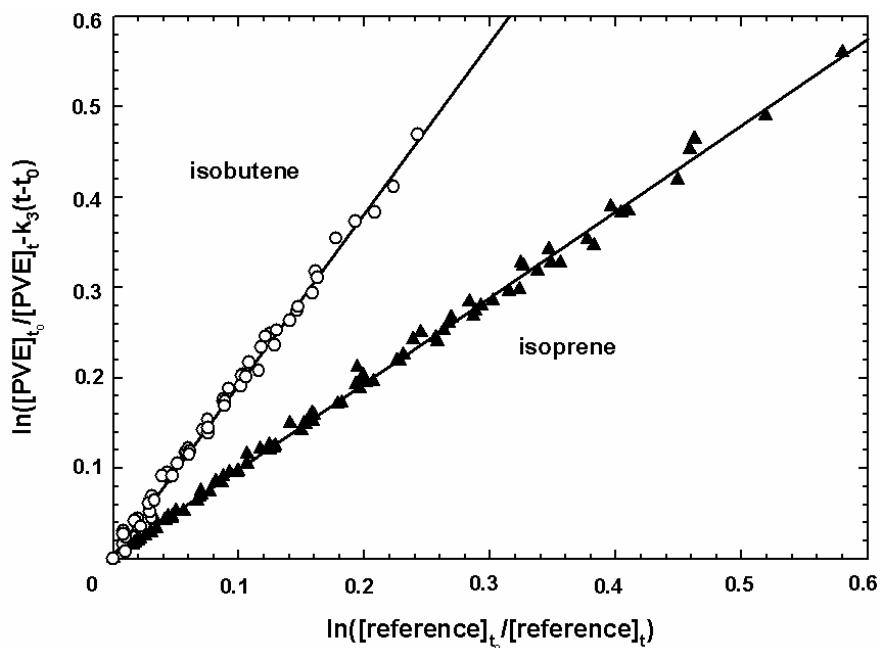


Figure 3.1 Plots of the kinetic data according to eq. (I) for the gas-phase reaction of OH radical with propyl vinyl ether (PVE).

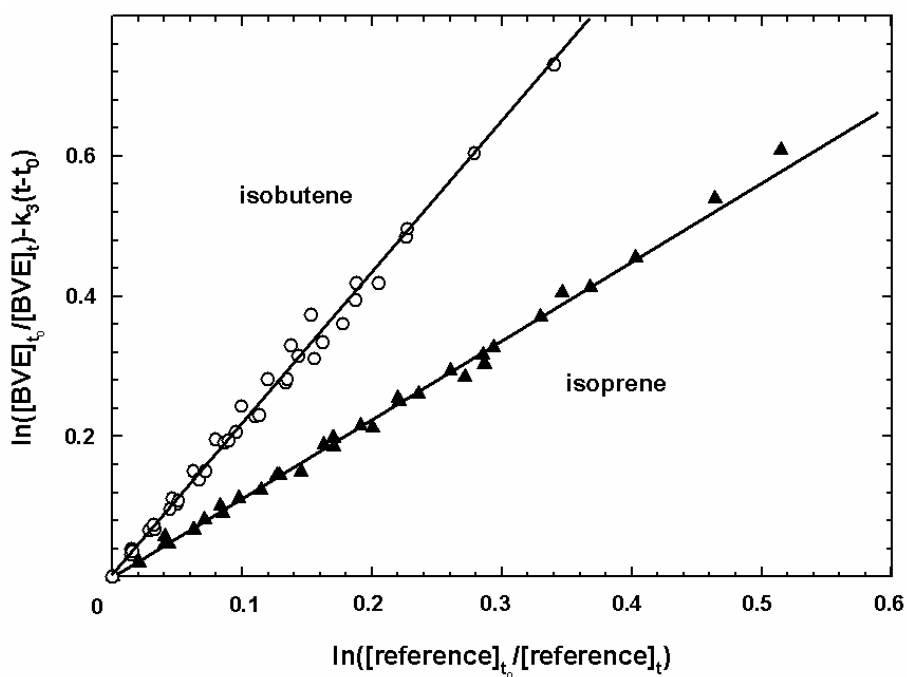


Figure 3.2 Plots of the kinetic data according to eq. (I) for the gas-phase reaction of OH radical with butyl vinyl ether (BVE).

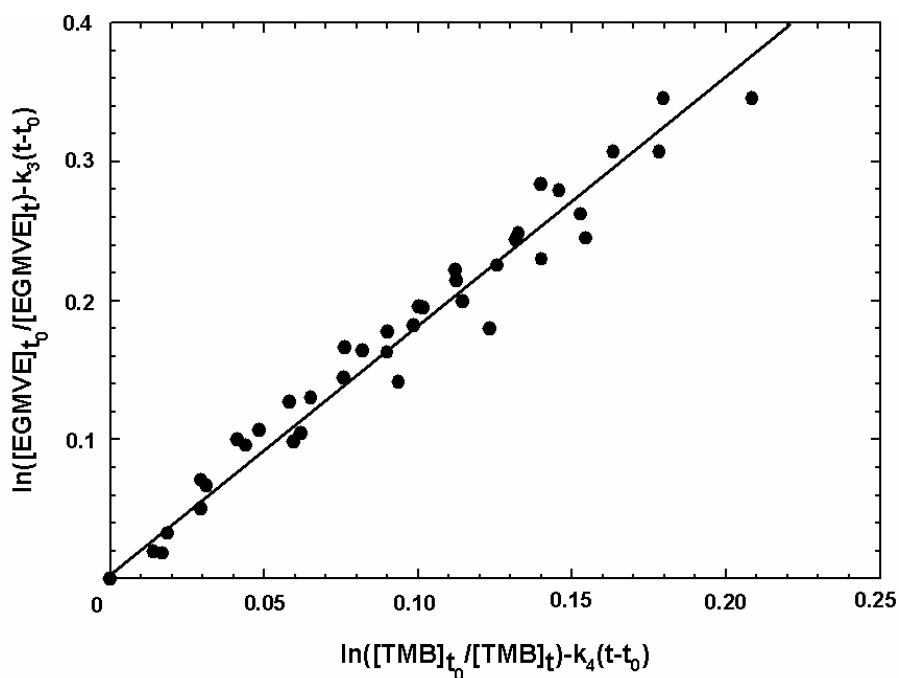


Figure 3.3 Plots of the kinetic data according to eq. (I) for the gas-phase reaction of OH radical with ethyleneglycol monovinyl ether (EGMVE).

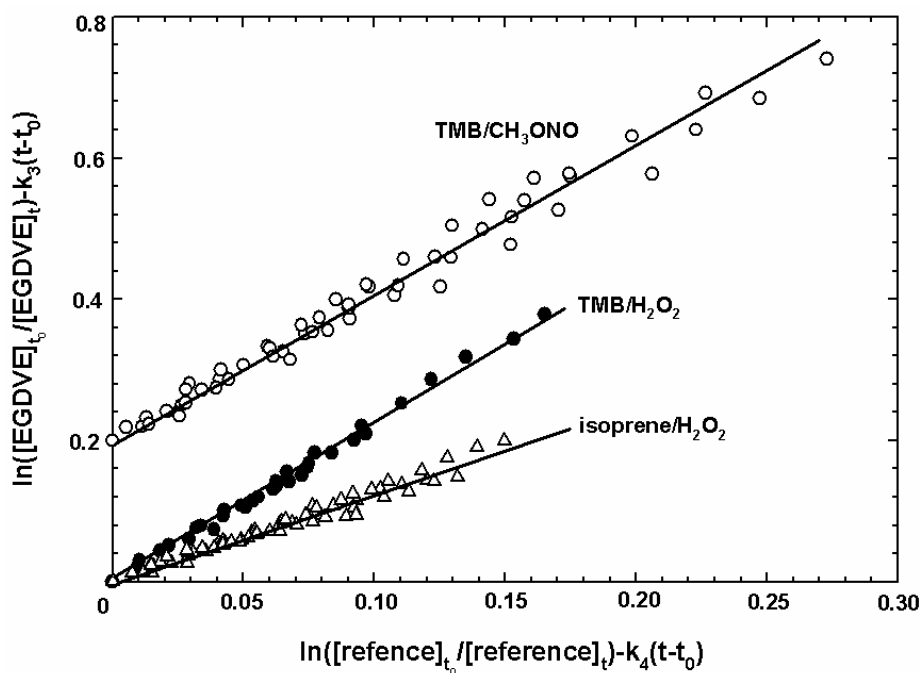


Figure 3.4 Plots of the kinetic data according to eq. (I) for the gas-phase reaction of OH radical with ethyleneglycol divinyl ether (EGDVE). The data for TMB/CH₃ONO has been offset by 0.2 on the y-axis for clarity.

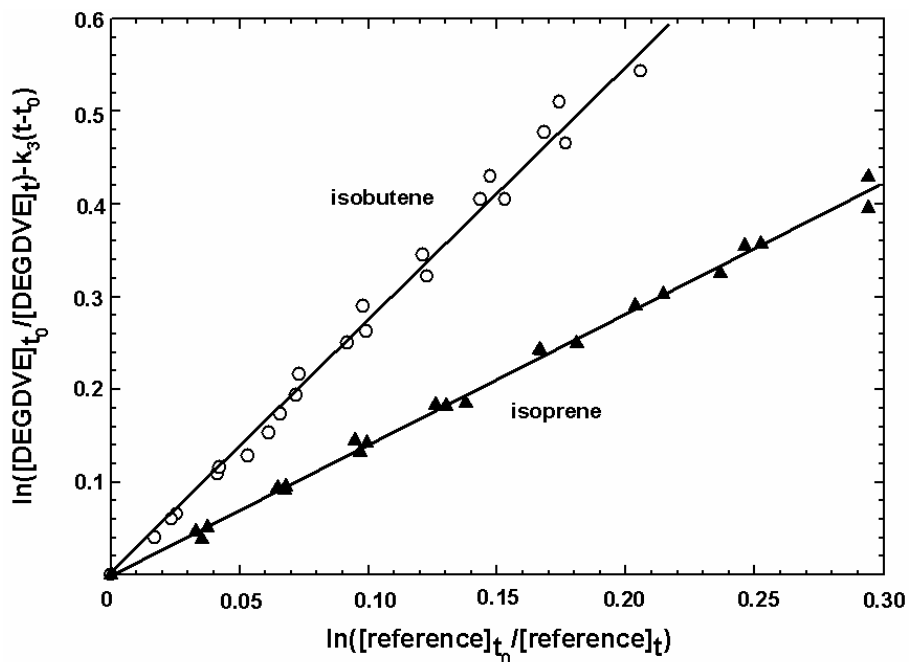


Figure 3.5 Plots of the kinetic data according to eq. (I) for the gas-phase reaction of OH radical with diethyleneglycol divinyl ether (DEGDVE).

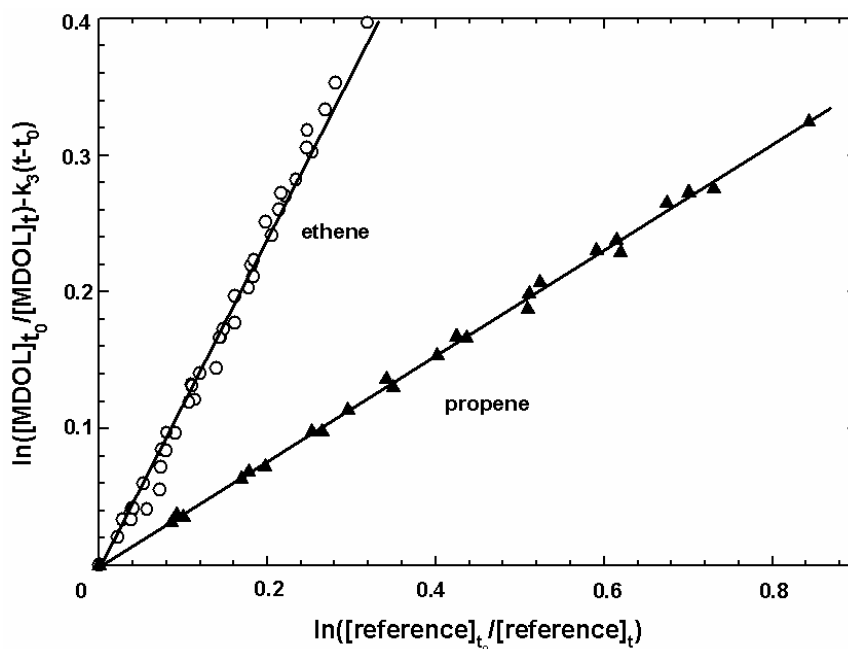


Figure 3.6 Plots of the kinetic data according to eq. (I) for the gas-phase reaction of OH radical with 2-methyl-1,3-dioxolane.

The corrections to the data for dark losses of the vinyl ethers were approximately: 10% for PVE and BVE, 40% for EGMVE and 15% for EGDVE and DEGDVE. No evidence for photolysis of the vinyl ethers was found with either the visible fluorescence lamps or the UV lamps. The quoted errors are a combination of the least squares standard 2σ deviations plus an additional 20% to cover uncertainties in the values of the rate coefficients of the reference compounds.

As can be seen in Table 3.1, there is excellent agreement between the values obtained using the different reference compounds and also the different OH radical sources. We, therefore, prefer to quote rate coefficients for the reactions of OH with the vinyl ethers that are averages of the determinations obtained using either the different reference compounds or different OH radical sources. Averaging the values of the rate coefficients and taking errors that encompass the extremes of the determinations for each reaction gives rate coefficients (in $\text{cm}^3 \text{ molecule}^{-1} \text{ s}^{-1}$ units) at 298K of:

$$\begin{aligned} k_1(\text{OH}+\text{PVE}) &= (9.73 \pm 1.94) \times 10^{-11}, \\ k_1(\text{OH}+\text{BVE}) &= (11.3 \pm 3.1) \times 10^{-11}, \\ k_1(\text{OH}+\text{EGMVE}) &= (10.4 \pm 2.15) \times 10^{-11}, \end{aligned}$$

$$k_1(\text{OH}+\text{EGDVE}) = (12.3 \pm 3.25) \times 10^{-11},$$

$$\text{and } k_1(\text{OH}+\text{DEGDVE}) = (14.2 \pm 3.00) \times 10^{-11}$$

These values are listed in Table 3.2 where they are compared with the available literature kinetic data on vinyl ethers.

From Table 3.2 it is obvious that the rate coefficients for the reaction of OH with PVE and BVE measured in this study are in excellent agreement with the values reported by Mellouki and coworkers [51,56], which were obtained using pulsed laser photolysis-laser induced fluorescence (PLP-LIF) and also a relative kinetic technique.

Table 3.2 Comparison of the rate coefficients (in cm³ molecule⁻¹ s⁻¹) measured in the present work at 298 K for the reactions of OH with selected vinyl ethers with values reported in the literature at the same temperature.

| Vinyl ether | k × 10 ¹¹ | Technique | References |
|--|--|---|--|
| MVE, CH ₃ OCH=CH ₂ | 3.35 ± 0.34 4.5 ± 0.7 6.4 | FP-RF ⁱ⁾ Relative Rate SAR-estimation | Perry <i>et al.</i> [47] Mellouki [51] Grosjean and Williams [49] |
| EVE, C ₂ H ₅ OCH=CH ₂ | 6.8 ± 0.7 7.3 ± 0.9 7.79 ± 1.71 5.51 ± 0.13 | PLP-LIF ⁱⁱ⁾ Relative Rate Relative Rate Relative Rate | Mellouki <i>et al.</i> [50,51] Mellouki <i>et al.</i> [50,51] Zhou <i>et al.</i> [53] Al Mulla [55] |
| PVE, C ₃ H ₇ OCH=CH ₂ | 10 ± 1 11 ± 1 9.73 ± 1.94 11.5 ± 0.4 | PLP-LIF ⁱⁱ⁾ Relative Rate Relative Rate Relative Rate | Mellouki <i>et al.</i> [51,56] Mellouki [51] This work Al Mulla [55] |
| BVE, n-C ₄ H ₉ OCH=CH ₂ | 10 ± 1 11 ± 1 11.3 ± 3.1 16.3 ± 2.8 | PLP-LIF ⁱⁱ⁾ Relative Rate Relative Rate Relative Rate | Mellouki <i>et al.</i> [51,56] Mellouki [51] This work Al Mulla [55] |
| iBVE, i-C ₄ H ₉ OCH=CH ₂ | 11 ± 1 11 ± 1 10.8 ± 2.3 15.9 ± 5.3 | PLP-LIF ⁱⁱ⁾ Relative Rate Relative Rate Relative Rate | Mellouki <i>et al.</i> [51,56] Mellouki [51] Barnes <i>et al.</i> [48] Al Mulla [55] |

| | | | |
|---|-----------|---|--------------------------------|
| tBVE, t-C ₄ H ₉ OCH=CH ₂ | 11±1 | PLP-LIF ⁱⁱ⁾ Relative Rate Relative Rate Relative Rate | Mellouki <i>et al.</i> [51,56] |
| | 11±1 | | Mellouki [51] |
| | 12.5±3.2 | | Barnes <i>et al.</i> [48] |
| | 25.2±1.8 | | Al Mulla [55] |
| EGMVE HOCH ₂ CH ₂ OCH=CH ₂ | 10.4±2.15 | Relative Rate | This work |
| EGDVE H ₂ C=CHOCH ₂ CH ₂ O- CH=CH ₂ | 12.3±3.25 | Relative Rate | This work |
| DEGDVE H ₂ C=CHOCH ₂ CH ₂ O- CH ₂ CH ₂ OCH=CH ₂ | 14.2±3.00 | Relative Rate | This work |

i) flash photolysis – resonance fluorescence (FP-RF), Arrhenius expressions for the temperature range 299-427 K are reported; ii) pulsed laser photolysis – laser induced fluorescence (PLP- LIF); Arrhenius expressions for the temperature range 230-373 K are reported.

Recently, Al Mulla [55] has reported rate coefficients for the OH radical reaction with a series of alkyl vinyl ethers determined with the relative kinetic technique, where only the result for OH with PVE is in good agreement with those of Mellouki [51,56] and the present study. The result from Al Mulla [55] for OH with EVE is lower than the determinations reported by Zhou *et al.* [53] and Mellouki *et al.* [50,51]; for OH with BVE and iBVE the values are higher than other determinations although they agree, in part, within the combined quoted errors. The rate coefficient for the reaction of OH with tBVE obtained by Al Mulla is higher than other measurements by a factor of two. The reason for such a large discrepancy is presently not known.

The value of $6.4 \times 10^{-11} \text{ cm}^3 \text{ molecule}^{-1} \text{ s}^{-1}$ estimated by Grosjean and Williams [49] from structure-activity-relationships (SAR) and linear free-energy relationships (LFER) for the reaction of OH with MVE, is substantially higher than the two experimentally determined values [47,51]. The rate coefficients for the reaction of OH with MVE obtained by Perry *et al.* [47] and Mellouki [51] are in fair agreement when account is taken of the errors quoted by the authors.

Table 3.3 compares the rate coefficients for reactions the OH radical with alkyl vinyl

ethers and those for OH reactions with simple ethers, alkenes and unsaturated carbonyls.

In Table 3.3 it can be seen that there is an increase in the rate coefficients for the reaction of OH with vinyl ethers on progressing from MVE through EVE, PVE to BVE, and thereafter the rate coefficients for iBVE and tBVE are indistinguishable from that of BVE.

The rate coefficients for the OH radical initiated oxidation of simple ethers (ROR, R = alkyl group) and alkenes show similar reaction trends with the exception of the compounds containing the tert-butyl group (see Table 3.3). The rates for the reactions of OH radicals with alkyl vinyl ethers are higher than those of OH with simple ethers and significantly higher than those of OH with the corresponding alkenes. As discussed by Mellouki and coworkers [50,51] the kinetic evidence supports that the alkoxy groups, -OR, in the alkyl vinyl ethers activate the double bond towards electrophilic addition by OH more than alkyl groups, -R. Whereas the rate coefficients for the reaction of OH with alkenes do not seem to be influenced very much by the nature of the R group ($k_{(\text{OH}+\text{alkene})} \approx 3 \times 10^{-11} \text{ cm}^3 \text{ molecule}^{-1} \text{ s}^{-1}$ for R = CH₃ to C₄H₉), those of OH with alkyl vinyl ethers increase from approximately 4×10^{-11} for R = CH₃O- to $1.1 \times 10^{-10} \text{ cm}^3 \text{ molecule}^{-1} \text{ s}^{-1}$ for R = CH₃CH₂CH₂CH₂O-. However, based on the values reported by Barnes *et al.* [48], Zhou *et al.* [53] and Mellouki *et al.* [50,51], it would appear that for alkoxy chains longer than C₄ the electron donating influence of the -OR group on the double bond towards electrophilic addition of OH radicals has reached a limiting value.

The effect of the -OR group entity on the reactivity of the double bond toward OH addition can also be compared with that of other oxygenated entities, i.e. a vinyl carbonyl (CH₂=CH-CO-R), a vinyl ester grouping (CH₂=CH-OC(O)R), and an alkyl acrylate grouping (CH₂=CH-C(O)OR), where R is an H atom or alkyl group.

There is not presently a large database for these types of oxygenated compounds, but from the data that are available in the literatures [15,72-77], which are also listed in Table 3.3, it can be seen that the rate coefficients for acrolein (CH₂=CHC(O)H), methacrolein (CH₂=C(CH₃)C(O)H), methyl vinyl ketone (CH₂=CHC(O)CH₃), vinyl acetate (CH₂=CHO(O)CCH₃) and methyl acrylate (CH₂=CH-C(O)OCH₃) with OH radicals are somewhat lower than those of the corresponding alkenes, propene, 1-butene and hence lower than those of the corresponding alkyl vinyl ethers.

Table 3.3 Comparison of the rate coefficients (in $\text{cm}^3 \text{ molecule}^{-1} \text{ s}^{-1}$) for the reactions of OH with alkyl vinyl ethers with values reported in the literature for ethers, alkenes and unsaturated carboxylic compounds at the same temperature.

| Vinyl ether ($\text{k} \times 10^{11}$) | | Ether ($\text{k} \times 10^{11}$) | | Alkene ($\text{k} \times 10^{11}$) | | Unsaturated carbonyl ($\text{k} \times 10^{11}$) | |
|--|--------------------|---|--|--|--------------------|---|--------------------|
| MVE $\text{CH}_3\text{OCH}=\text{CH}_2$ | 3.9 ^{a)} | Methylethylether $\text{CH}_3\text{OCH}_2\text{CH}_3$ | 0.69 ^{d)} 0.82 ^{k)} | Propene $\text{CH}_3\text{CH}=\text{CH}_2$ | 2.63 ^{f)} | Acrolein $\text{H}(\text{O})\text{CCH}=\text{CH}_2$ | 1.96 ^{h)} |
| EVE $\text{C}_2\text{H}_5\text{OCH}=\text{CH}_2$ | 7.3 ^{a)} | Diethylether $\text{CH}_3\text{CH}_2\text{OCH}_2\text{CH}_3$ | 1.31 ^{e)} 1.36 ^{k)} | 1-Butene $\text{C}_2\text{H}_5\text{CH}=\text{CH}_2$ | 3.14 ^{f)} | Methacrolein $\text{H}(\text{O})\text{CC}(\text{CH}_3)=\text{CH}_2$ | 2.85 ^{h)} |
| PVE $\text{n-C}_3\text{H}_7\text{OCH}=\text{CH}_2$ | 10.2 ^{b)} | Ethyl-n-propyl ether $\text{n-C}_3\text{H}_7\text{OCH}_2\text{CH}_3$ | 1.77 ^{k)} | 1-Pentene $\text{n-C}_3\text{H}_7\text{CH}=\text{CH}_2$ | 3.14 ^{f)} | Methyl vinyl ketone $\text{CH}_3\text{C}(\text{O})\text{CH}=\text{CH}_2$ | 1.88 ⁱ⁾ |
| BVE $\text{n-C}_4\text{H}_9\text{OCH}=\text{CH}_2$ | 11.5 ^{b)} | Ethyl-n-butyl ether $\text{n-C}_4\text{H}_9\text{OCH}_2\text{CH}_3$ | 2.13 ^{e)} 2.03 ^{k)} | 1-Hexene $\text{n-C}_4\text{H}_9\text{CH}=\text{CH}_2$ | 3.7 ^{f)} | Vinyl acetate $\text{CH}_3\text{C}(\text{O})\text{OCH}=\text{CH}_2$ | 2.04 ^{j)} |
| iBVE $\text{i-C}_4\text{H}_9\text{OCH}=\text{CH}_2$ | 10.9 ^{c)} | Ethyl-i-butyl ether $\text{i-C}_4\text{H}_9\text{OCH}_2\text{CH}_3$ | 2.03 ^{k)} | 4-Methyl-1-pentene $\text{i-C}_4\text{H}_9\text{CH}=\text{CH}_2$ | 3.8 ^{g)} | Methyl acrylate $\text{CH}_3\text{O}(\text{O})\text{CCH}=\text{CH}_2$ | 2.5 ^{l)} |
| tBVE $\text{t-C}_4\text{H}_9\text{OCH}=\text{CH}_2$ | 11.5 ^{c)} | Ethyl-t-butylether $\text{t-C}_4\text{H}_9\text{OCH}_2\text{CH}_3$ | 0.88 ^{e)} 0.86 ^{k)} | 3,3-Dimethyl-1-butene $\text{t-C}_4\text{H}_9\text{CH}=\text{CH}_2$ | 2.8 ^{f)} | | |

a) Data taken as an average of the experimental determinations of Perry *et al.* [47] and Mellouki [51]; b) Data taken as an average of the values determined in the present work and that reported by Mellouki [51]; c) Data taken as an average of the values determined by Barnes *et al.* [48] and that reported by Mellouki [51]; d) Data taken from Starkey *et al.* [76]; e) Data taken from Atkinson [1]; f) Data taken from Atkinson and Arey [15]; g) Data taken from Kwok *et al.* [77]; h) Data taken from Atkinson [78]; i) Data taken from Atkinson *et al.* [79]; j) Data taken from Al Mulla [55]; k) Estimated values from Structure-Activity-Relationships using the group rate constants assumed by Mellouki *et al.* [16]. l) Data taken from Saunders *et al.* [73].

A deactivating effect on the rate of electrophilic OH addition to the double bond from the -C(O)R, -OC(O)R and -C(O)OR constellations is to be expected because of the negative inductive effect introduced by the carbonyl functionality. In the case of vinyl aldehyde the decrease in the reactivity of the double bond is offset to some extent by H-atom abstraction of the aldehydic hydrogen. The meager kinetic dataset presently available on these types of oxygenates does not warrant a more detailed comparison at this time.

In the OH radical reaction, apart from OH addition to the double bond, H-atom abstraction by the OH radical may occur. In Table 3.4 the rate coefficients for the overall reactions of OH with alkyl vinyl ethers and the corresponding alkenes are compared with the partial rate coefficients for H-atom abstraction from the alkyl groups.

Though there is no similar trend in the H-abstraction from vinyl ethers and alkenes it is obvious that for MVE, tBVE, propene and 1-butene that the OH radical reactions proceed essentially by OH addition to the carbon-carbon double bond under atmospheric conditions, with H-atom abstraction from the alkyl groups accounting for less than 5% of the overall reaction at room temperature. For the other alkyl vinyl ethers from EVE to iBVE and the alkenes from 1-pentene to 3,3-dimethyl-1-butene the rate data show that H-atom abstraction accounts for between 10-17% of the total reaction at room temperature. However, as presented in Chapter 4, in the product study of the OH radical reaction with PVE and BVE no evidence was found for products resulting from the H-atom abstraction channel.

To the best of my knowledge there are no other experimentally determined rate coefficients for the reactions of OH with ethyleneglycol vinyl ethers presently available in the literature with which the values determined in this work can be compared.

A number of rate coefficients have been reported for the reactions of OH with unsaturated alcohols [81-83]. Papagni *et al.* [81] have established that the rate coefficients for the reactions of OH with the unsaturated alcohols are larger than those of OH with the corresponding alkenes by factors of between 1.6 to 2.1, which is somewhat larger than the constituent group factor of 1.6 for -CH₂OH recommended by Kwok and Atkinson [77]. Recently Imamura *et al.* [82] have reported constituent factors for -CH₂OH and -CH₂CH₂OH which are consistent with those of Papagni *et al.* [81].

Table 3.4 Comparison of the overall rate coefficients (at 298 K, in units of $\text{cm}^3 \text{molecule}^{-1} \text{s}^{-1}$) for the reactions of OH with vinyl ethers and analogous alkenes with the rate coefficients estimated for H-atom abstraction from the alkyl groups in the compounds.

| Vinyl ether ($\text{k} \times 10^{11}$) | | | Alkene ($\text{k} \times 10^{11}$) | | |
|--|----------------------------|--------------------------------|--|--------------------|--------------------------------|
| | Overall rate ^{a)} | Abstraction rate ^{b)} | | Overall rate | Abstraction rate ^{c)} |
| MVE $\text{CH}_3\text{OCH}=\text{CH}_2$ | 3.9 | 0.14 | Propene $\text{CH}_3\text{CH}=\text{CH}_2$ | 2.63 ^{d)} | 0.014 |
| EVE $\text{C}_2\text{H}_5\text{OCH}=\text{CH}_2$ | 7.3 | 0.68 | 1-Butene $\text{C}_2\text{H}_5\text{CH}=\text{CH}_2$ | 3.14 ^{d)} | 0.11 |
| PVE $\text{n-C}_3\text{H}_7\text{OCH}=\text{CH}_2$ | 10.2 | 1.1 | 1-Pentene $\text{n-C}_3\text{H}_7\text{CH}=\text{CH}_2$ | 3.14 ^{d)} | 0.25 |
| BVE $\text{n-C}_4\text{H}_9\text{OCH}=\text{CH}_2$ | 11.5 | 1.4 | 1-Hexene $\text{n-C}_4\text{H}_9\text{CH}=\text{CH}_2$ | 3.7 ^{d)} | 0.39 |
| iBVE $\text{i-C}_4\text{H}_9\text{OCH}=\text{CH}_2$ | 10.9 | 1.3 | 4-Methyl-1-pentene $\text{i-C}_4\text{H}_9\text{CH}=\text{CH}_2$ | 3.8 ^{c)} | 0.39 |
| tBVE $\text{t-C}_4\text{H}_9\text{OCH}=\text{CH}_2$ | 11.5 | 0.2 | 3,3-Dimethyl-1-butene $\text{t-C}_4\text{H}_9\text{CH}=\text{CH}_2$ | 2.8 ^{d)} | 0.50 |

a) Data from Table 3.3; b) Data taken from Mellouki *et al.* [16] assuming that the $-\text{OCH}=\text{CH}_2$ group has the same substituted factor as a simple ether $-\text{OR}$ ($\text{R}=\text{alkyl}$); c) Estimated from structure-activity-relationships given in Kwok *et al.* [77]; d) Data taken from Atkinson and Arey [15].

EGMVE ($\text{CH}_2=\text{CHOCH}_2\text{CH}_2\text{OH}$) is structurally very similar to EVE ($\text{CH}_2=\text{CHOCH}_2\text{CH}_3$); the only difference being substitution of one of the methyl H-atoms in the $-\text{CH}_2\text{CH}_3$ group of EVE by an $-\text{OH}$ group. The rate coefficient for the reaction of OH with EGMVE (see Table 3.2) is about a factor of 1.4 higher than that of OH with EVE.

This enhancement, although somewhat lower than the enhancement factors of 1.6-2.1

observed for the unsaturated alcohols compared to the structurally analogous alkenes, indicates that substitution of the OH group on the alkyl group of EVE has enhanced the rate coefficient of the OH reaction.

Unfortunately there are no other rate coefficients for -OH group substituted alkyl vinyl ethers available to validate this single observation. However, since EGMVE, alkyl vinyl ethers, unsaturated alcohols and alkenes all react with OH by a similar reaction mechanism, i.e. OH radical addition to the carbon-carbon double bond in the compounds, it seems reasonable to assume that the rate coefficients for the reactions of OH radical with -OH group substituted alkyl vinyl ethers will be enhanced compared to those of the structurally analogous alkyl vinyl ethers.

Table 3.5 lists the rate coefficients for the OH radical reactions with ethyleneglycol vinyl ethers, diethers, some structurally similar unsaturated oxygenates and the estimated rate coefficients for H-atom abstraction from the -OCH₂CH₂O-R (R = H or alkyl) groups in the ethyleneglycol vinyl ethers obtained using the structure-activity-relationship recommended by Mellouki *et al.* [16].

As was observed for the alkyl vinyl ethers the rate coefficients for the reactions of OH with EGMVE, EGDVE and DEGDVE are significantly higher than those of diethers and higher than those of 3-buten-1-ol, 1,4-pentadiene and 1,5-hexadiene, respectively. This demonstrates that the ether group neighboring the double bond activates the reactivity towards OH radical reaction. The rate coefficient for the reactions of OH with EGDVE is higher than that of OH with EGMVE, which is to be expected since EGDVE contains two carbon-carbon double bonds. However, the rate coefficient for the reaction of OH with EGDVE is higher than that of OH with EGMVE by only $1.9 \times 10^{-11} \text{ cm}^3 \text{ molecule}^{-1} \text{ s}^{-1}$; this difference is much less than what one would predict for the addition of a second double bond entity using SAR and is seen in the trends for mono-alkenes and dialkenes where the rate coefficients of the OH radical reactions with 1,4-pentadiene and 1,5-hexadiene are almost twice those of propene and 1-butene (see Tables 3.4 and 3.5), respectively.

Interestingly, the rate coefficient for DEGDVE is higher than that of EGDVE by $1.9 \times 10^{-11} \text{ cm}^3 \text{ molecule}^{-1} \text{ s}^{-1}$, which is almost the calculated difference in the H-atom abstraction contributions for DEGDVE and EGDVE caused by the additional -CH₂CH₂- group. Until more information for kinetic and product studies on this type of compounds becomes available further speculation is unwarranted.

Table 3.5 Comparison of the rate coefficients (in $\text{cm}^3 \text{molecule}^{-1} \text{s}^{-1}$) for the reactions of OH with ethyleneglycol vinyl ethers with values reported in the literature for diethers, unsaturated organic compounds and that for OH abstraction from alkyl group in vinyl ethers at the same temperature.

| Vinyl ether ($\text{k} \times 10^{11}$) ^{a)} | | Diether ($\text{k} \times 10^{11}$) ^{b)} | | Unsaturated organics ($\text{k} \times 10^{11}$) | | Estimated H-atom abstraction rate ($\text{k} \times 10^{11}$) ^{e)} | |
|---|------|--|-----|---|-------------------|---|-----|
| EGMVE $\text{HOCH}_2\text{CH}_2\text{OCH}=\text{CH}_2$ | 10.4 | 1,2-Dimethoxyethane $\text{CH}_3\text{O}(\text{CH}_2)_2\text{OCH}_3$ | 2.7 | 3-Buten-1-ol $\text{HOCH}_2\text{CH}_2\text{CH}=\text{CH}_2$ | 5.5 ^{c)} | EGMVE $\text{HOCH}_2\text{CH}_2\text{OCH}=\text{CH}_2$ | 1.4 |
| EGDVE $\text{H}_2\text{C}=\text{CHOCH}_2\text{CH}_2\text{O}-$ $\text{CH}=\text{CH}_2$ | 12.3 | 1,3-Dimethoxypropane $\text{CH}_3\text{O}(\text{CH}_2)_3\text{OCH}_3$ | 5.1 | 1,4-Pentadiene $\text{CH}_2=\text{CHCH}_2\text{CH}=\text{CH}_2$ | 5.3 ^{d)} | EGDVE $\text{H}_2\text{C}=\text{CHOCH}_2\text{CH}_2\text{O}-$ $\text{CH}=\text{CH}_2$ | 1.9 |
| DEGDVE $\text{H}_2\text{C}=\text{CHOCH}_2\text{CH}_2\text{O}-$ $\text{CH}_2\text{CH}_2\text{OCH}=\text{CH}_2$ | 14.2 | 1,4-Dimethoxybutane $\text{CH}_3\text{O}(\text{CH}_2)_4\text{OCH}_3$ | 3.0 | 1,5-Hexadiene $\text{CH}_2=\text{CHCH}_2\text{CH}_2-$ $\text{CH}=\text{CH}_2$ | 6.2 ^{d)} | DEGDVE $\text{H}_2\text{C}=\text{CHOCH}_2\text{CH}_2\text{O}-$ $\text{CH}_2\text{CH}_2\text{OCH}=\text{CH}_2$ | 3.9 |

- a) This work; b) Data taken from Moriarty *et al.* [80]; c) Data taken from Imamura *et al.* [82]; d) Data taken from Al Mulla [55];
e) Estimated from structure-activity-relationships given in Mellouki *et al.* [16]

Compared to alkyl vinyl ethers, H-atom abstraction from ethyleneglycol vinyl ethers will occur to a significant extent (see Table 3.4 and 3.5), with this process accounting for between 14-27% of the overall OH radical reactions with the ethyleneglycol vinyl ethers.

Using 1-hexanol as a reference compound Stemmler *et al.* [84] have determined the rate coefficient for the reaction of the OH radical with 2-methyl-1,3-dioxolane. Their result of $9.4 \times 10^{-12} \text{ cm}^3 \text{ molecule}^{-1} \text{ s}^{-1}$ is in good agreement with the value of $(1.05 \pm 0.25) \times 10^{-11} \text{ cm}^3 \text{ molecule}^{-1} \text{ s}^{-1}$ (see Table 3.1) determined in the present work.

3.1.2 O₃ reactions

All the experiments on the reactions of O₃ with the selected vinyl ethers were carried out at $(298 \pm 3) \text{ K}$ and $(740 \pm 10) \text{ Torr}$ total pressure of synthetic air. For each reaction at least three experimental runs were performed. The reference compound(s) employed in the experiments are listed in Table 3.6.

Rate coefficients for the ozonolysis of PVE, BVE, EGMVE, EGDVE and DEGDVE were determined relative to cyclohexene and/or trans-2-butene in the presence of an excess of cyclohexane to scavenge more than 95% of OH radicals produced in the reaction systems.

The initial concentrations used in the ozonolysis experiments were: vinyl ethers 2.7-5.5 ppm; reference compound(s) 3.8-7.3 ppm; O₃ 1.0-1.8 ppm; cyclohexane 290 ppm.

The reactants were monitored at the following wavenumbers (in cm^{-1}): PVE at 965, 1211.2 and 3129; BVE at 3128.9 and 1614; EGMVE at 1622.2; EGDVE at 1619.7; DEGDVE at 1617.2; cyclohexene at 1139.7; trans-2-butene at 962.7 and 973.8.

Figures 3.7 to 3.11 show examples of the kinetic data plotted according to eq. (I) for all the vinyl ethers investigated.

The rate coefficient ratios, k_1/k_2 , obtained from these plots are listed in Table 3.6 and have been used in combination with $k_2(\text{cyclohexene}) = 8.1 \times 10^{-17}$ and $k_2(\text{trans-2-butene}) = 1.9 \times 10^{-16} \text{ cm}^3 \text{ molecule}^{-1} \text{ s}^{-1}$ [72] to put the rate coefficients for the reactions of O₃ with the vinyl ethers on an absolute basis. This results in rate coefficients for the ozonolysis of PVE, BVE, EGMVE, EGDVE and DEGDVE (in

units of $\text{cm}^3 \text{ molecule}^{-1} \text{ s}^{-1}$) of:

$$\begin{aligned}
 k_1 (\text{O}_3 + \text{PVE}) &= (2.34 \pm 0.48) \times 10^{-16}, \\
 k_1 (\text{O}_3 + \text{BVE}) &= (2.59 \pm 0.52) \times 10^{-16}, \\
 k_1 (\text{O}_3 + \text{EGMVE}) &= (2.02 \pm 0.41) \times 10^{-16}, \\
 k_1 (\text{O}_3 + \text{EGDVE}) &= (1.69 \pm 0.41) \times 10^{-16}, \\
 \text{and } k_1 (\text{O}_3 + \text{DEGDVE}) &= (2.70 \pm 0.56) \times 10^{-16}
 \end{aligned}$$

Table 3.6 Measured rate coefficient ratios, k_1/k_2 , and rate coefficients k_1 (in $\text{cm}^3 \text{ molecule}^{-1} \text{ s}^{-1}$) for the reactions of O_3 with PVE, BVE, EGMVE, EGDVE and DEGDVE obtained in present work at 298 K using the relative kinetic technique.

| Vinyl ether | Reference | k_1/k_2 | $k_1 \times 10^{16}$ | Average $k_1 \times 10^{16}$ |
|---|----------------|-----------------|----------------------|---------------------------------|
| PVE, $\text{n-C}_3\text{H}_7\text{OCH}=\text{CH}_2$ | Cyclohexene | 2.89 ± 0.15 | 2.34 ± 0.48 | 2.34 ± 0.48 |
| BVE, $\text{n-C}_4\text{H}_9\text{OCH}=\text{CH}_2$ | Cyclohexene | 3.20 ± 0.10 | 2.59 ± 0.52 | 2.59 ± 0.52 |
| EGMVE $\text{HOCH}_2\text{CH}_2\text{OCH}=\text{CH}_2$ | Cyclohexene | 2.49 ± 0.10 | 2.02 ± 0.41 | 2.02 ± 0.41 |
| EGDVE $\text{H}_2\text{C}=\text{CHOCH}_2\text{CH}_2\text{OCH}=\text{CH}_2$ | Cyclohexene | 2.01 ± 0.06 | 1.63 ± 0.33 | 1.69 ± 0.41 |
| | Trans-2-butene | 0.92 ± 0.02 | 1.75 ± 0.35 | |
| DEGDVE $\text{H}_2\text{C}=\text{CHOCH}_2\text{CH}_2\text{O}-$ $\text{CH}_2\text{CH}_2\text{OCH}=\text{CH}_2$ | Trans-2-butene | 1.42 ± 0.07 | 2.70 ± 0.56 | 2.70 ± 0.56 |

Corrections to the kinetic data for dark wall loss and dark reaction of the vinyl ethers were of the order of approximately 5% for PVE and BVE, 30-40% for EGMVE and 10-15% for EGDVE and DEGDVE. The quoted errors are again the combination of the least squares standard 2σ deviations plus an additional 20% for uncertainties in the value of the rate coefficient for the reference(s).

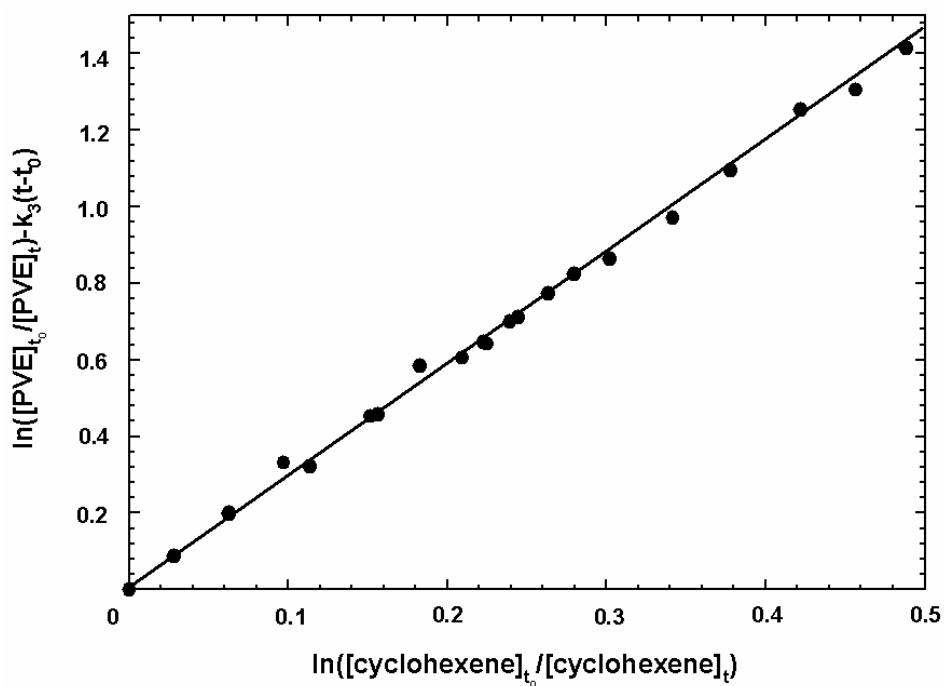


Figure 3.7 Plot of the kinetic data according to eq. (I) for the gas-phase reaction of O₃ with propyl vinyl ether (PVE).

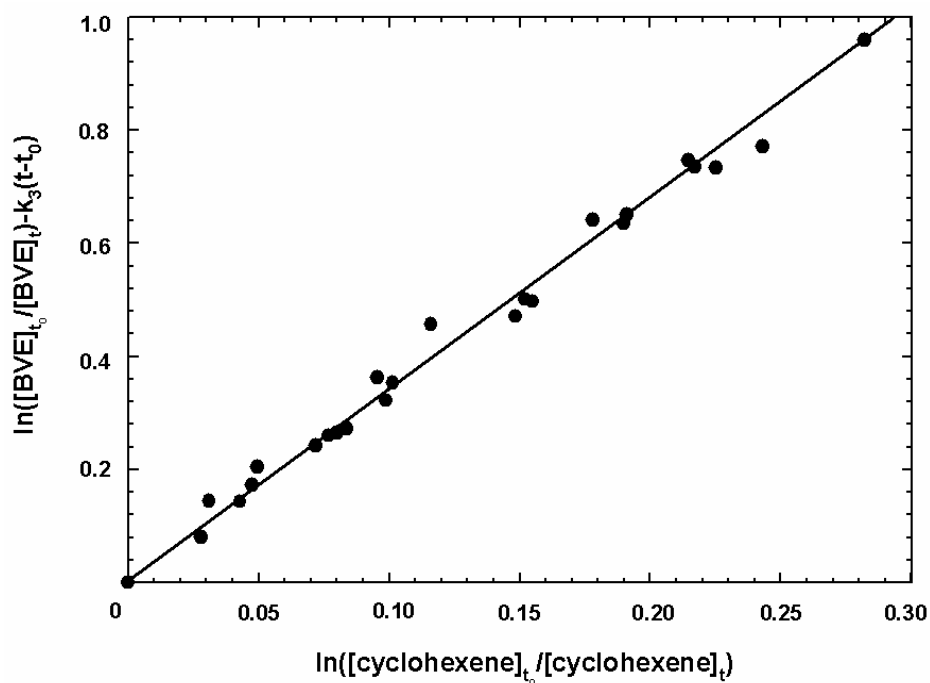


Figure 3.8 Plot of the kinetic data according to eq. (I) for the gas-phase reaction of O₃ with butyl vinyl ether (BVE).

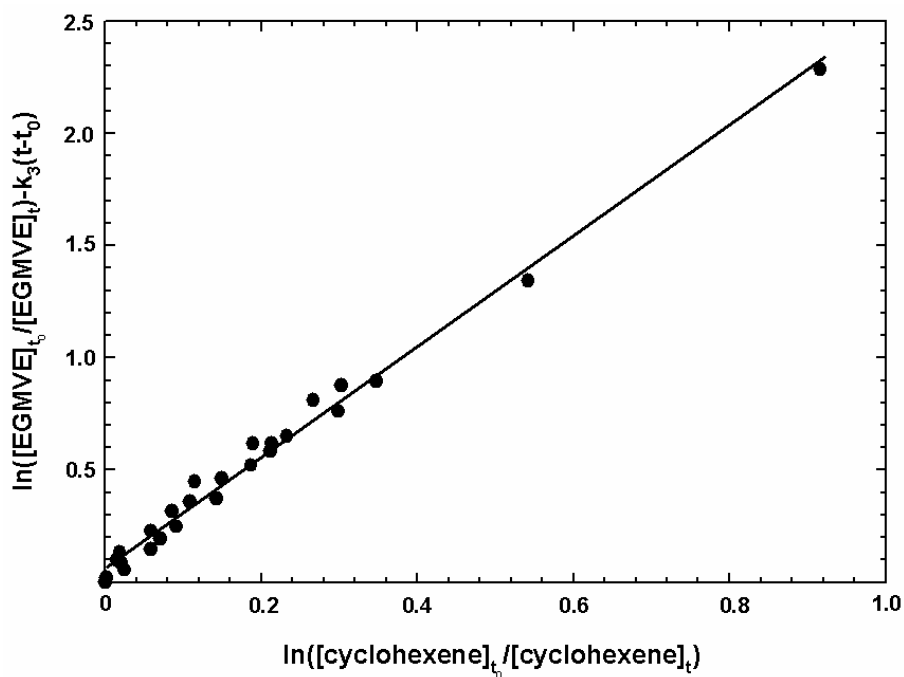


Figure 3.9 Plot of the kinetic data according to eq. (I) for the gas-phase reaction of O_3 with ethyleneglycol monovinyl ether (EGMVE).

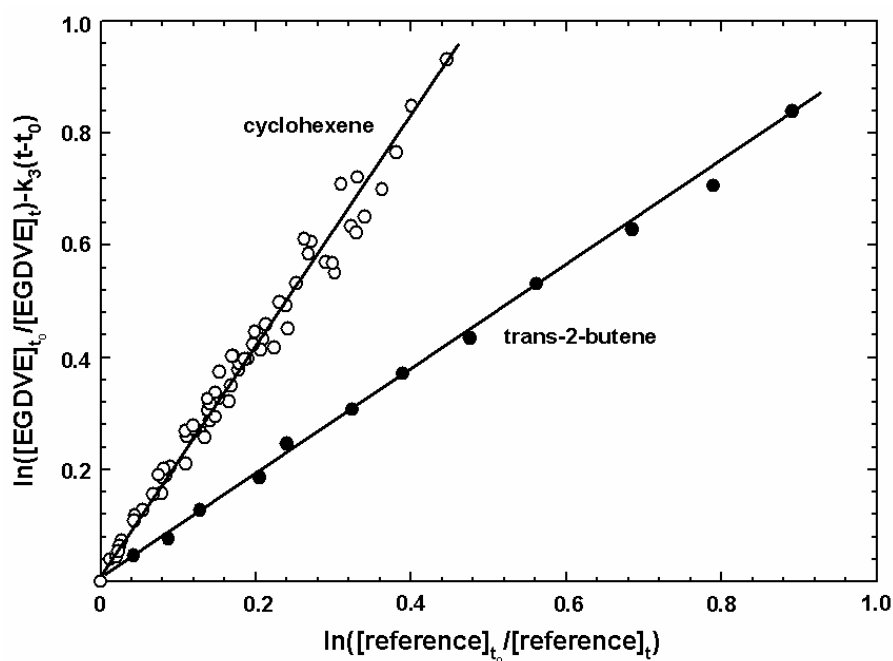


Figure 3.10 Plots of the kinetic data according to eq. (I) for the gas-phase reaction of O_3 with ethyleneglycol divinyl ether (EGDVE).

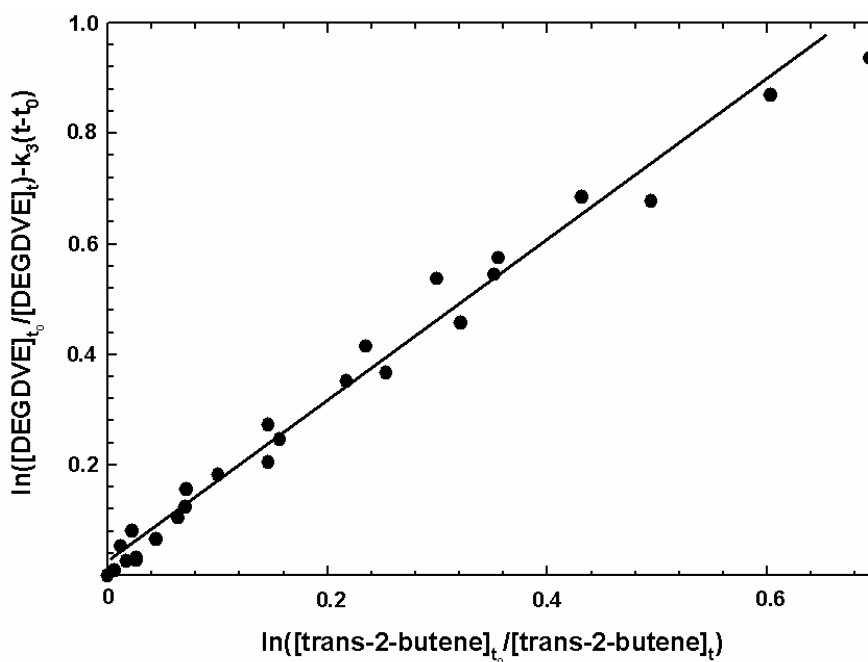


Figure 3.11 Plot of the kinetic data according to eq. (I) for the gas-phase reaction of O₃ with diethyleneglycol divinyl ether (DEGDVE).

The rate coefficients determined in this work for the reactions of ozone with alkyl vinyl ethers are compared with literature values in Table 3.7. The rate coefficients determined in the present work for the O₃ reactions with PVE and BVE and those measured by Barnes *et al.* [48] for the ozonolysis of iBVE and tBVE are in excellent agreement with the values determined by Mellouki and co-workers [50,51] from a best fit to concentration-time profiles measured in the EUPHORE chamber facility in Valencia, Spain (see Table 3.7). Using a pseudo-first-order kinetic method Grosjean and Grosjean [59] have determined a rate coefficient for the reaction of O₃ with EVE of $(1.54 \pm 0.3) \times 10^{-16} \text{ cm}^3 \text{ molecule}^{-1} \text{ s}^{-1}$ which is somewhat lower than the value determined by Thiault *et al.* [50] and Zhou *et al.* [53]. The value of Grosjean and Grosjean, however, does agree within the combined reported error limits of the other studies.

As seen in Table 3.7, using both a relative and absolute kinetic method, the rate coefficients measured by Al Mulla [55] for the ozonolysis of PVE and BVE are consistent with those from this work and the reported values of Mellouki [51].

Table 3.7 Comparison of the rate coefficients (in $\text{cm}^3 \text{molecule}^{-1} \text{s}^{-1}$) measured in the present work at 298 K for the reactions of O_3 with selected vinyl ethers with values reported in the literature at the same temperature.

| Vinyl ether | $k \times 10^{16}$ | Technique | References |
|---|---|---|--|
| EVE, $\text{C}_2\text{H}_5\text{OCH}=\text{CH}_2$ | 2.0±0.2 1.54±0.3 2.06±0.42 1.3 | Concentration fit p-f-o kinetics ⁱ⁾ Relative Relative and Absolute ⁱⁱ⁾ | Thiault <i>et al.</i> [50] Grosjean and Grosjean [59] Zhou <i>et al.</i> [53] Al Mulla [55] |
| PVE, $\text{C}_3\text{H}_7\text{OCH}=\text{CH}_2$ | 2.4±0.4 2.34±0.48 2.4 | Concentration fit Relative Rate Relative and Absolute ⁱⁱ⁾ | Mellouki [51] This work Al Mulla [55] |
| BVE, $n\text{-C}_4\text{H}_9\text{OCH}=\text{CH}_2$ | 2.9±0.2 2.59±0.52 2.3 | Concentration fit Relative Rate Relative and Absolute ⁱⁱ⁾ | Mellouki [51] This work Al Mulla [55] |
| iBVE, $i\text{-C}_4\text{H}_9\text{OCH}=\text{CH}_2$ | 3.1±0.2 2.85±0.62 2.3 | Concentration fit Relative Rate Relative and Absolute ⁱⁱ⁾ | Mellouki [51] Barnes <i>et al.</i> [48] Al Mulla [55] |
| tBVE, $t\text{-C}_4\text{H}_9\text{OCH}=\text{CH}_2$ | 5.0±0.5 5.30±1.07 2.4 | Concentration fit Relative Rate Relative and Absolute ⁱⁱ⁾ | Mellouki [51] Barnes <i>et al.</i> [48] Al Mulla [55] |
| EGMVE $\text{HOCH}_2\text{CH}_2\text{OCH}=\text{CH}_2$ | 2.02±0.41 | Relative Rate | This work |
| EGDVE $\text{H}_2\text{C}=\text{CHOCH}_2\text{CH}_2\text{O}-$ $\text{CH}=\text{CH}_2$ | 1.69±0.41 5.4 | Relative Rate Relative and Absolute ⁱⁱ⁾ | This work Al Mulla [55] |
| DEGDVE $\text{H}_2\text{C}=\text{CHOCH}_2\text{CH}_2\text{O}-$ $\text{CH}_2\text{CH}_2\text{OCH}=\text{CH}_2$ | 2.70±0.56 | Relative Rate | This work |

i) pseudo-first-order kinetic; ii) Absolute determination in a static system using chemiluminescence analysis to monitor the ozone decay in the presence of an excess of the vinyl ether

However, the value for EVE, iBVE and tBVE obtained by Al Mulla [55] are significantly lower than those determined by Barnes *et al.* [48] and Mellouki and co-workers [50,51].

To measure the rate coefficient for the ozone reaction with EGDVE two different reference compounds were used in the present work. The results from these two reference compounds are in good agreement (see Table 3.6). The rate coefficient for the ozonolysis of EGDVE determined by Al Mulla is higher than this work by a factor of about 3. As for the discrepancies which exist between this study and that of Al Mulla for the OH radical kinetic measurements the reasons for the discrepancies in the ozone kinetic studies are also unknown.

Table 3.8 compares the rate coefficients for the reactions of ozone with alkyl vinyl ethers, with those of the corresponding alkenes and other unsaturated oxygenated organic compounds.

Table 3.8 Comparison of the rate coefficients (in cm³ molecule⁻¹ s⁻¹) for the reactions of O₃ with alkyl vinyl ethers with values reported in the literature for corresponding alkenes and unsaturated carbonyls.

| Vinyl ether (k×10 ¹⁶) ^a | | Alkene (k×10 ¹⁷) ^b | | Unsaturated carbonyls (k×10 ¹⁸) | |
|---|------|---|-------------------|---|-------------------|
| EVE C ₂ H ₅ OCH=CH ₂ | 2.06 | 1-Butene C ₂ H ₅ CH=CH ₂ | 0.96 | Acrolein H(O)CCH=CH ₂ | 0.28 ^d |
| PVE n-C ₃ H ₇ OCH=CH ₂ | 2.34 | 1-Pentene n-C ₃ H ₇ CH=CH ₂ | 1.06 | Methacrolein H(O)CC(CH ₃)=CH ₂ | 1.12 ^d |
| BVE n-C ₄ H ₉ OCH=CH ₂ | 2.59 | 1-Hexene n-C ₄ H ₉ CH=CH ₂ | 1.13 | Methyl vinyl ketone CH ₃ C(O)CH=CH ₂ | 4.77 ^d |
| iBVE i-C ₄ H ₉ OCH=CH ₂ | 2.85 | 4-Methyl-1-pentene i-C ₄ H ₉ CH=CH ₂ | 1.00 | Vinyl acetate CH ₃ C(O)OCH=CH ₂ | 2.9 ^e |
| tBVE t-C ₄ H ₉ OCH=CH ₂ | 5.30 | 3,3-Dimethyl-1-butene t-C ₄ H ₉ CH=CH ₂ | 0.39 ^c | Methyl acrylate CH ₃ O(O)CCH=CH ₂ | 2.92 ^e |

a) Data for PVE and BVE taken from this work and those for iBVE and tBVE taken from Barnes *et al.* [48]; b) Data taken from Atkinson and Arey [15]; c) Data was given at 285 K; d) Data taken from Atkinson *et al.* [85]; e) Data taken from Grosjean *et al.* [86]

Although in the ozonolysis of alkyl vinyl ethers there is a tendency towards higher rate coefficients with increase in the carbon chain length with $EVE < PVE < BVE < iBVE < tBVE$, the increase from EVE to BVE is much less pronounced than that observed for the reactions of OH radicals with the alkyl vinyl ethers. As can be seen from Table 3.8 a very similar reactivity pattern has been observed for the reactions of ozone with the corresponding alkenes from 1-butene to 1-hexene [15], however, the rate coefficients for the ozonolysis of the alkyl vinyl ethers are much higher than those of the corresponding alkenes by factors of more than 20. This again reflects the strong electron donating effect of alkoxy groups, RO-, to the carbon-carbon double bond, which facilitates the electrophilic addition of ozone to the double bond.

The much higher rate coefficient for the reaction of tBVE with ozone could be explained by the stronger electron donating effect of the $(CH_3)_3CO-$ group compared to other alkyl groups. However, from Table 3.8 it is evident that this is not true for the corresponding alkenes where the rate coefficients for the ozonolysis drop off on proceeding from 1-hexene via 4-methyl-1-pentene to 3,3-dimethyl-1-butene. This can not be explained by simple electronic arguments since the more branched group will improve the stabilization of the radical character developing in the transition state. From a steric view of point, however, for the highly branched compound the steric effects hinder the approach of ozone towards the reactive double bond of the alkene which results in a lowering of the rate coefficient. In tBVE the extra O atom between the double bond and the tertiary butyl group lessens the steric hinderance and thus a higher reactivity is observed.

The rate coefficient for the ozonolysis of tBVE measured by Al Mulla [55] is lower than that reported by Barnes *et al.* [48] and Mellouki [51] by a factor of 2. It has to be noted that in his relative rate measurement of the ozonolysis of tBVE, Al Mulla used 1-methyl-1-cyclohexene and EVE as reference compounds and reported rate coefficients ratios k_1/k_2 of 1.16 and 2.04 for 1-methyl-1-cyclohexene and EVE, respectively. In combination with his measurement of $k_{ref} = 1.15 \times 10^{-16} \text{ cm}^3 \text{ molecule}^{-1} \text{ s}^{-1}$ for EVE he obtained a rate coefficient for the ozonolysis of tBVE of $2.35 \times 10^{-16} \text{ cm}^3 \text{ molecule}^{-1} \text{ s}^{-1}$, which was in agreement with the rate coefficient he obtained relative to 1-methyl-1-cyclohexene ($k_{ref} = 1.88 \times 10^{-16} \text{ cm}^3 \text{ molecule}^{-1} \text{ s}^{-1}$) and also that obtained using an absolute method ($2.65 \times 10^{-16} \text{ cm}^3 \text{ molecule}^{-1} \text{ s}^{-1}$). However, a rate coefficient of $2.06 \times 10^{-16} \text{ cm}^3 \text{ molecule}^{-1} \text{ s}^{-1}$ has been measured by Zhou *et al.* [53] for the ozonolysis of EVE. If this value is applied to Al Mulla's

determination a rate coefficient of $k_1(\text{O}_3+\text{tBVE}) = 4.20 \times 10^{-16} \text{ cm}^3 \text{ molecule}^{-1} \text{ s}^{-1}$ is obtained for the ozonolysis of tBVE, which is in line with the value of $(5.30 \pm 1.07) \times 10^{-16} \text{ cm}^3 \text{ molecule}^{-1} \text{ s}^{-1}$ obtained by Barnes *et al.* [48].

As can be seen in Table 3.8, when alkyl groups in alkenes are substituted by a carbonyl grouping (-C(O)R), ester grouping (-OC(O)R), or alkyl acrylate grouping (-C(O)OR), where R is an H atom or alkyl group, the rate coefficients for the ozonolysis of these type of compounds e.g. acrolein (CH₂=CHC(O)H), methacrolein (CH₂=C(CH₃)C(O)H), methyl vinyl ketone (CH₂=CHC(O)CH₃), vinyl acetate (CH₂=CHO(O)CCH₃) and methyl acrylate (CH₂=CHC(O)OCH₃), are lower than those of the structurally analogous alkenes and much lower than the corresponding alkyl vinyl ethers by around two orders of magnitude [1,15,72].

To date no other experimentally determined rate coefficients for the reactions of O₃ with EGMVE, EGDVE and DEGDVE have been reported in the literature with which the values determined in the present work can be compared. Table 3.9 lists the rate coefficients for the reactions of O₃ with the ethyleneglycol vinyl ethers together with the values reported in the literature for structurally similar alkenes at the same temperature.

Table 3.9 Comparison of the rate coefficients (in cm³ molecule⁻¹ s⁻¹) for the reactions of O₃ with ethyleneglycol vinyl ethers with values reported in the literature for alkenes at the same temperature.

| Vinyl ether ($k \times 10^{16}$) ^{a)} | | Alkenes ($k \times 10^{17}$) ^{b)} | | | |
|---|------|--|------|--|------|
| EGMVE HOCH ₂ CH ₂ OCH=CH ₂ | 2.02 | 1-Pentene CH ₃ CHCH ₂ CH=CH ₂ | 1.06 | | |
| EGDVE H ₂ C=CHOCH ₂ CH ₂ O- CH=CH ₂ | 1.69 | 1-Hexene CH ₃ CH ₂ CH ₂ CH ₂ CH=CH ₂ | 1.13 | 1,4-Pentadiene CH ₂ =CHCH ₂ CH=CH ₂ | 1.45 |
| DEGDVE H ₂ C=CHOCH ₂ CH ₂ O- CH ₂ CH ₂ OCH=CH ₂ | 2.70 | | | 2,5-Dimethyl-1,4-hexadiene CH ₂ =C(CH ₃)CH ₂ CH=C- (CH ₃)CH ₃ | 1.4 |

a) This work; b) Data taken from Atkinson and Arey [15]

The rate coefficients determined for ethyleneglycol vinyl ethers are somewhat higher than those of the structurally analogous terminal alkenes and non-conjugated dialkenes. This again reflects that electron donating groups neighboring the double bond strongly activate the double bond towards electrophilic addition of O_3 .

The result in this work for EGDVE is surprising since its rate coefficient with ozone is somewhat lower than EGMVE. It was expected that this reaction would be faster than EGMVE because the former contains two double bonds in its structure. Within the combined error limits the value of the rate coefficient for the ozonolysis of EGDVE is not significantly different to the values obtained for EVE and EGMVE. The reason for this anomaly is presently not known, it could be speculated that when an electron donating group is positioned between two double bonds that the electron donating ability is equally divided between each double bond entity such that the overall reactivity is not very different from the corresponding single double bonded alkyl analogue. It is to be expected that the theoretical calculations could possibly give more insight into the observed anomaly.

3.1.3 NO_3 radical reactions

Rate coefficients for the reactions of NO_3 with PVE, BVE, EGMVE, EGDVE and DEGDVE were measured at (298 ± 3) K and (740 ± 10) Torr total pressure of synthetic air using the relative kinetic technique. The reference compounds employed in the measurements are listed in Table 3.10.

The initial concentrations used in the NO_3 reactions were: vinyl ethers 5.0 ppm; reference compound(s) i.e. isoprene, 2,3-dimethyl-1,3-butadiene and 1,3-cycloheptadiene, 4.8-5.5 ppm. The reactants were monitored at the following wavenumbers (in cm^{-1}): PVE at 965, 1211.2 and 3129; BVE at 3128.9 and 1614; EGMVE at 1622.2; EGDVE at 1619.7; DEGDVE at 1617.2; isoprene at 893.4 and 905.9; 2,3-dimethyl-1,3-butadiene at 895; 1,3-cycloheptadiene at 1442.

For each reaction at least three experimental runs were performed.

Figures 3.12 to 3.16 show examples of the kinetic data plotted according to eq. (I) for NO_3 reactions with the selected vinyl ethers.

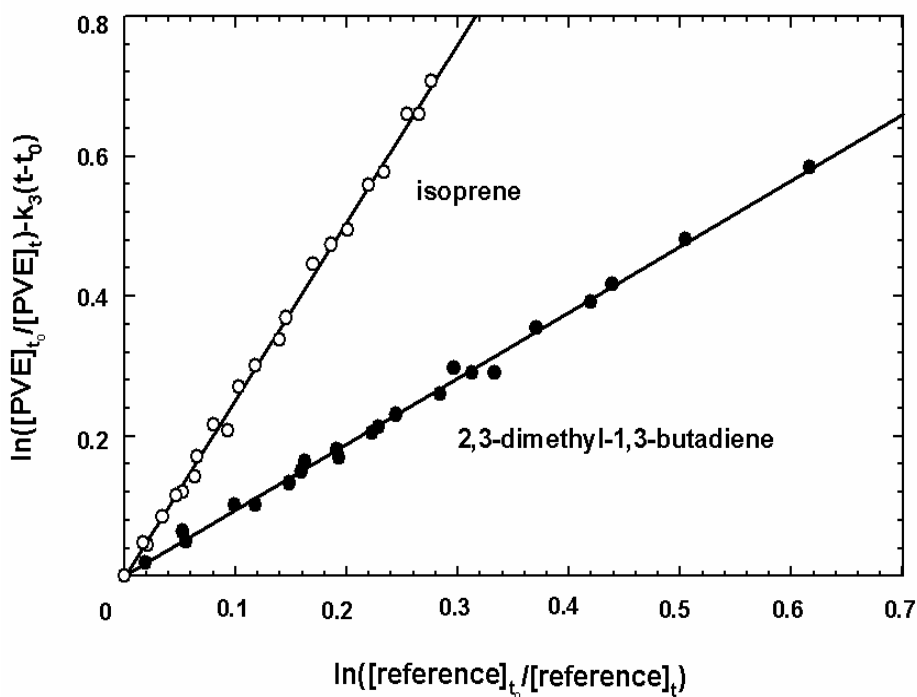


Figure 3.12 Plots of the kinetic data according to eq. (I) for the gas-phase reaction of NO₃ with propyl vinyl ether (PVE).

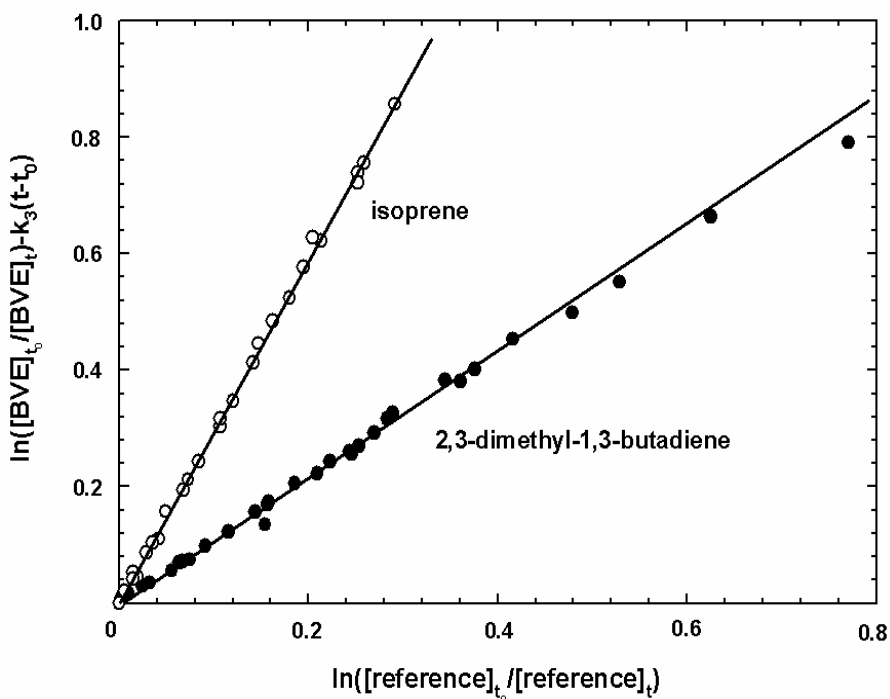


Figure 3.13 Plots of the kinetic data according to eq. (I) for the gas-phase reaction of NO₃ with butyl vinyl ether (BVE).

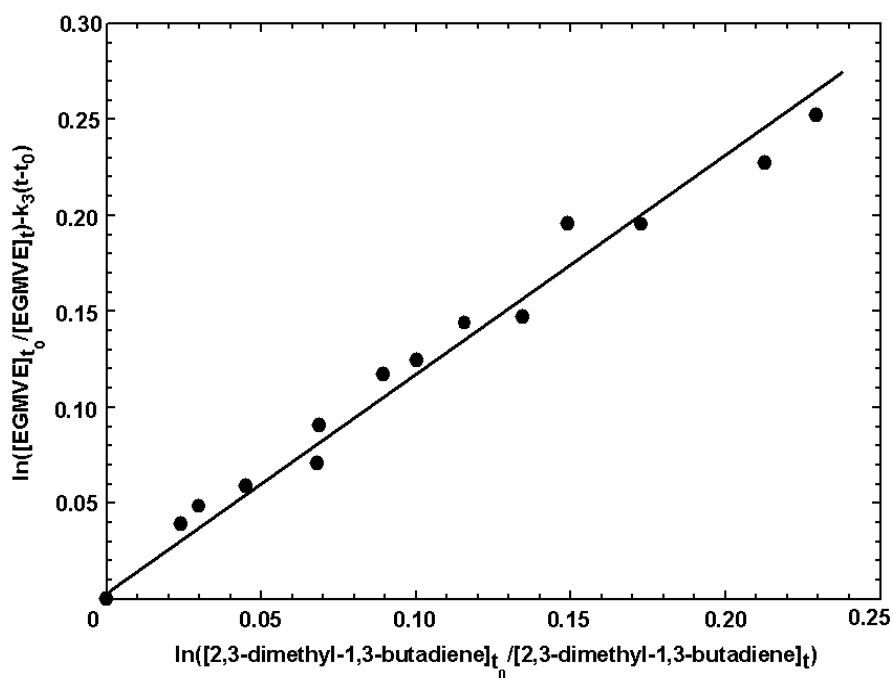


Figure 3.14 Plot of the kinetic data according to eq. (I) for the gas-phase reaction of NO_3 with ethyleneglycol vinyl ether (EGMVE).

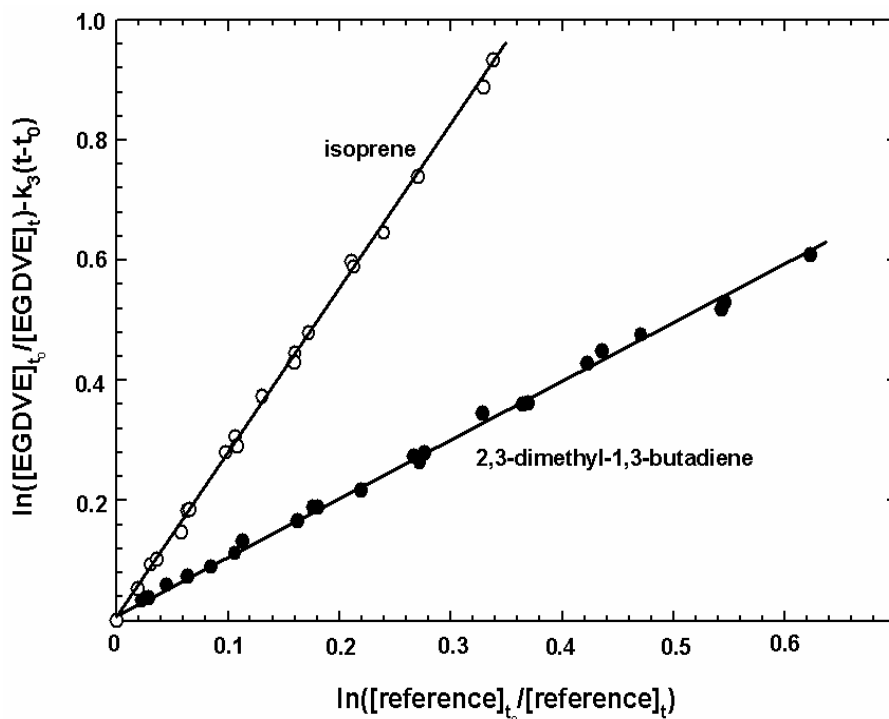


Figure 3.15 Plots of the kinetic data according to eq. (I) for the gas-phase reaction of NO_3 with ethyleneglycol divinyl ether (EGDVE).

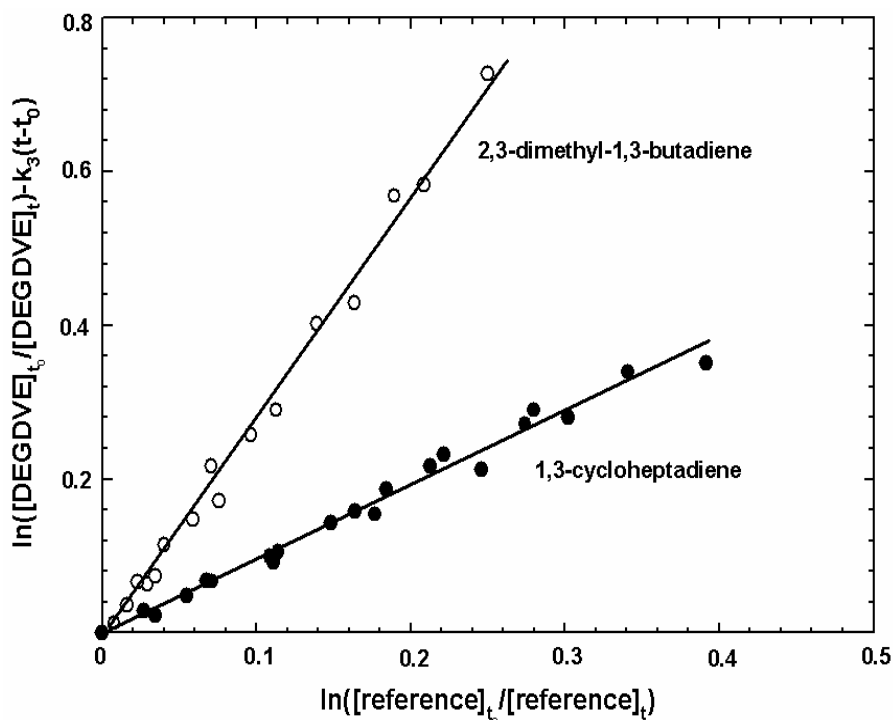


Figure 3.16 Plots of the kinetic data according to eq. (I) for the gas-phase reaction of NO₃ with diethyleneglycol divinyl ether (DEGDVE).

For all the vinyl ethers investigated good linear relationships were generally obtained. Difficulties were only encountered in measurements of the rate coefficient for the reaction of NO₃ with EGMVE due to the relatively high dark loss rate of the compound. The rate coefficient ratios, k_1/k_2 , obtained from these plots are listed in Table 3.10. Using these ratios in combination with $k_2(\text{isoprene}) = 6.78 \times 10^{-13} \text{ cm}^3 \text{ molecule}^{-1} \text{ s}^{-1}$, $k_2(2,3\text{-dimethyl-1,3-butadiene}) = 2.1 \times 10^{-12} \text{ cm}^3 \text{ molecule}^{-1} \text{ s}^{-1}$ and $k_2(1,3\text{-cycloheptadiene}) = 6.5 \times 10^{-12} \text{ cm}^3 \text{ molecule}^{-1} \text{ s}^{-1}$ [75] leads to the rate coefficients k_1 for the NO₃ reaction with the vinyl ethers which are also listed in Table 3.10. The contribution of the combined dark wall and dark reaction losses of the vinyl ethers to the measured overall losses were approximately 5% for PVE and BVE, 40-50% for EGMVE and 10-15% for EGDVE and DEGDVE. The errors are again the standard 2σ deviations plus an additional 20% to cover uncertainties in the values of the rate coefficients for the reference compounds. The rate coefficients obtained for the vinyl ether using the two reference compound(s) are in reasonable agreement (see Table 3.10).

Table 3.10 Measured rate coefficient ratios, k_1/k_2 , and rate coefficients k_1 (in $\text{cm}^3 \text{ molecule}^{-1} \text{ s}^{-1}$) for the reaction of NO_3 radical with PVE, BVE, EGMVE, EGDVE and DEGDVE obtained in the present work at 298 K using the relative kinetic technique

| Vinyl ether | Reference | k_1/k_2 | $k_1 \times 10^{12}$ | Average $k_1 \times 10^{12}$ |
|---|----------------------------|-----------------|----------------------|------------------------------|
| PVE, $n\text{-C}_3\text{H}_7\text{OCH}=\text{CH}_2$ | Isoprene | 2.54 ± 0.05 | 1.72 ± 0.35 | 1.85 ± 0.53 |
| | 2,3-Dimethyl-1,3-butadiene | 0.94 ± 0.02 | 1.98 ± 0.40 | |
| BVE, $n\text{-C}_4\text{H}_9\text{OCH}=\text{CH}_2$ | Isoprene | 2.94 ± 0.04 | 2.00 ± 0.40 | 2.10 ± 0.54 |
| | 2,3-Dimethyl-1,3-butadiene | 1.05 ± 0.02 | 2.20 ± 0.44 | |
| EGMVE $\text{HOCH}_2\text{CH}_2\text{O}-$ $\text{CH}=\text{CH}_2$ | 2,3-Dimethyl-1,3-butadiene | 1.06 ± 0.05 | 2.23 ± 0.46 | 2.23 ± 0.46 |
| EGDVE $\text{H}_2\text{C}=\text{CHOCH}_2\text{CH}_2-$ $\text{OCH}=\text{CH}_2$ | Isoprene | 2.73 ± 0.04 | 1.85 ± 0.38 | 1.96 ± 0.50 |
| | 2,3-Dimethyl-1,3-butadiene | 0.98 ± 0.02 | 2.06 ± 0.41 | |
| DEGDVE $\text{H}_2\text{C}=\text{CHOCH}_2\text{CH}_2\text{O}-$ $\text{CH}_2\text{CH}_2\text{OCH}=\text{CH}_2$ | 2,3-Dimethyl-1,3-butadiene | 2.89 ± 0.12 | 6.07 ± 1.24 | 6.14 ± 1.38 |
| | 1,3-cycloheptadiene | 0.96 ± 0.05 | 6.21 ± 1.31 | |

Since the last data evaluation on NO_3 kinetics [75], Kind *et al.* [87] have reported a rate coefficient of $1.4 \times 10^{-12} \text{ cm}^3 \text{ molecule}^{-1} \text{ s}^{-1}$ for the reaction of NO_3 with 2,3-dimethyl-1,3-butadiene which is one of the reference compounds used in this study. The value reported by Kind *et al.* is much lower than those reported in previous determinations. Using this value gives rate coefficients (in $\text{cm}^3 \text{ molecule}^{-1} \text{ s}^{-1}$) of $(1.32 \pm 0.28) \times 10^{-12}$, $(1.47 \pm 0.30) \times 10^{-12}$, $(1.48 \pm 0.31) \times 10^{-12}$, $(1.36 \pm 0.28) \times 10^{-12}$ and $(4.05 \pm 0.83) \times 10^{-12}$, for the reactions of NO_3 with PVE, BVE, EGMVE, EGDVE and DEGDVE, respectively. These values are not in as good agreement with those obtained with isoprene as reference compound when the currently recommended value of $2.1 \times 10^{-12} \text{ cm}^3 \text{ molecule}^{-1} \text{ s}^{-1}$ [75] is used as the rate coefficient for NO_3 reaction with 2,3-dimethyl-1,3-butadiene in the calculation of the rate coefficients for the reactions of NO_3 with the vinyl ethers.

To solve this reference problem, it was attempted to substitute 2,3-dimethyl-1,3-butadiene with another reference compound. Unfortunately, for all the potentially suitable substitute compounds selected, interferences in the FTIR data analyses were observed. Therefore, since Kind *et al.* could offer no explanation for the discrepancy, use the value of $2.1 \times 10^{-12} \text{ cm}^3 \text{ molecule}^{-1} \text{ s}^{-1}$ [75] for the rate coefficient for the reaction of NO₃ with 2,3-dimethyl-1,3-butadiene is preferred. Thus the following final rate coefficients (in units of $\text{cm}^3 \text{ molecule}^{-1} \text{ s}^{-1}$) at 298K are presented here:

$$\begin{aligned} k_1(\text{NO}_3+\text{PVE}) &= (1.85\pm 0.53) \times 10^{-12}, \\ k_1(\text{NO}_3+\text{BVE}) &= (2.10\pm 0.54) \times 10^{-12}, \\ k_1(\text{NO}_3+\text{EGMVE}) &= (2.23\pm 0.46) \times 10^{-12}, \\ k_1(\text{NO}_3+\text{EGDVE}) &= (1.96\pm 0.50) \times 10^{-12} \\ \text{and } k_1(\text{NO}_3+\text{DEGDVE}) &= (6.14\pm 1.38) \times 10^{-12}, \end{aligned}$$

which are averages of the values obtained using the two reference compounds (with the exception of EGMVE where only one reference was employed) with error limits which encompass the extremes of both determinations.

The rate coefficients for the NO₃ reaction with the alkyl vinyl ethers measured in this work are listed in Table 3.11 where they are compared with the available literature kinetic data at the same temperature.

From Table 3.11 it can be seen that the rate coefficients for the reaction of NO₃ with PVE and BVE measured in this study and those reported by Scarfogliero *et al.* [57] are in fair agreement when account is taken of the errors. The kinetic data plots of Scarfogliero *et al.* show much more scatter than those of the present work.

Recently, relative kinetic determinations of the rate coefficient for the NO₃ reaction with EVE have been reported by Zhou *et al.* [53], Scarfogliero *et al.* [57] and Pfrang *et al.* [60]. The value of $(1.7\pm 1.3) \times 10^{-12} \text{ cm}^3 \text{ molecule}^{-1} \text{ s}^{-1}$ measured by Pfrang *et al.* [60] has a large associated error, which the authors attributed to considerable difficulties with the measurements, and concluded that the data would benefit from refinement. Considering the experimental difficulties encountered in the measurements of Pfrang *et al.* and the larger scatter in their data points their measured k value for NO₃ + EVE is in fair agreement with the values of $(1.4\pm 0.35) \times 10^{-12}$ and $(1.31\pm 0.27) \times 10^{-12} \text{ cm}^3 \text{ molecule}^{-1} \text{ s}^{-1}$ determined by Zhou *et al.* [53] and Scarfogliero *et al.* [57], respectively.

Grosjean and Williams [49] have estimated a rate coefficient of $4.68 \times 10^{-13} \text{ cm}^3 \text{ molecule}^{-1} \text{ s}^{-1}$ for the reaction of NO_3 with MVE using structure-reactivity and linear free-energy relationships (SAR and LFER).

Table 3.11 Comparison of the rate coefficients (in $\text{cm}^3 \text{ molecule}^{-1} \text{ s}^{-1}$) for the reactions of NO_3 with the vinyl ethers with values reported in the literature at the same temperature.

| Vinyl ether | $k \times 10^{12}$ | Technique | References |
|---|-----------------------------------|---|---|
| MVE $\text{CH}_3\text{OCH}=\text{CH}_2$ | 0.47 0.72±0.15 | SAR and LFER ^{a)} Relative Rate | Grosjean and Williams [49] Scarfogliero <i>et al.</i> [57] |
| EVE, $\text{C}_2\text{H}_5\text{OCH}=\text{CH}_2$ | 1.40±0.35 1.7±1.3 1.31±0.27 | Relative Rate Relative Rate Relative Rate | Zhou <i>et al.</i> [53] Pfrang <i>et al.</i> [60] Scarfogliero <i>et al.</i> [57] |
| PVE, $\text{C}_3\text{H}_7\text{OCH}=\text{CH}_2$ | 1.85±0.53 1.33±0.30 | Relative Rate Relative Rate | This work Scarfogliero <i>et al.</i> [57] |
| BVE, $n\text{-C}_4\text{H}_9\text{OCH}=\text{CH}_2$ | 2.10±0.54 1.70±0.37 | Relative Rate Relative Rate | This work Scarfogliero <i>et al.</i> [57] |
| iBVE, $i\text{-C}_4\text{H}_9\text{OCH}=\text{CH}_2$ | 1.99±0.56 | Relative Rate | Barnes <i>et al.</i> [48] |
| tBVE, $t\text{-C}_4\text{H}_9\text{OCH}=\text{CH}_2$ | 4.81±1.01 | Relative Rate | Barnes <i>et al.</i> [48] |
| EGMVE $\text{HOCH}_2\text{CH}_2\text{OCH}=\text{CH}_2$ | 2.23±0.46 | Relative Rate | This work |
| EGDVE $\text{H}_2\text{C}=\text{CHOCH}_2\text{CH}_2\text{O}-$ $\text{CH}=\text{CH}_2$ | 1.95±0.50 | Relative Rate | This work |
| DEGDVE $\text{H}_2\text{C}=\text{CHOCH}_2\text{CH}_2\text{O}-$ $\text{CH}_2\text{CH}_2\text{OCH}=\text{CH}_2$ | 6.14±1.38 | Relative Rate | This work |

a) structure-reactivity and linear free-energy relationships (SAR and LFER)

The rate coefficients determined for the NO₃ reaction with EVE, PVE and BVE are factors of 3 to 4.5 higher than the estimated *k* value for NO₃ with MVE. Based on a comparison with the rate coefficients for the analogous OH radical reactions, where increases of a factor of between 2 to 3 are observed for the reactions of OH with EVE, PVE and BVE compared to OH with MVE, this seems fairly reasonable since the NO₃ radical reactions with the vinyl ethers appear to follow a similar reactivity trend to the OH radical reactions.

As for the analogous OH radical and ozone reactions, the rate coefficients determined for the NO₃ reactions show an increase with increasing carbon-chain length with $k(\text{MVE}) < k(\text{EVE}) < k(\text{PVE}) < k(\text{BVE}) \approx k(\text{iBVE}) < k(\text{tBVE})$, indicating that the order of reactivity of NO₃ towards alkyl vinyl ethers is similar to that observed for the OH and ozone reactions. As was the case for ozone reaction the relatively large increase in the NO₃ rate coefficient observed for tBVE compared with BVE and iBVE reflects the large increase in the positive inductive contribution to the electron density at the double bond caused by the increase in the branching complexity of the tert-butyl group which renders the bond more acceptive to electrophilic addition of the NO₃ radical.

To the best of my knowledge, at the time of writing, no other reports of experimentally determined rate coefficients for the reactions of NO₃ with alkyl vinyl ethers are published in the literature with which the values determined in this work can be compared.

Table 3.12 compares the rate coefficients for the reactions of NO₃ with alkyl vinyl ethers with those reported in the literature for the NO₃ reaction with structurally analogous alkenes and unsaturated carbonyls.

It can be seen from Table 3.12 that the rate coefficients for the reactions of NO₃ with EVE, PVE, BVE and iBVE are approximately two orders of magnitude higher than the corresponding rate coefficients for the reactions of NO₃ with propene, 1-butene, 1-pentene, 1-hexene and 3-methyl-1-butene [15], respectively. However, whereas an increase in rate coefficient is observed for the NO₃ reaction with the vinyl ethers with increase in the electron donating power of the alkyl group, this does not seem to be the case for the alkenes (at least on the basis of the available data), i.e., the rate coefficients for the NO₃ reaction with 1-pentene and 3-methyl-1-butene are very similar. This probably reflects the higher degree of steric hindrance associated with NO₃ addition to the alkenes compared with the vinyl ethers where an O atom

separates the double bond from the alkyl group.

In contrast to the analogue OH radical reactions the difference in the reactivity of the alkyl vinyl ethers toward electrophilic NO₃ addition to that of CH₂=CH-C(O)R, CH₂=CH-OC(O)R and CH₂=CH-C(O)OR compounds is much starker (see Table 3.12). For the few compounds for which data are available [1,15,60,72-76,88] the rate coefficients for the reactions of NO₃ with the alkyl vinyl ethers are an order of magnitude larger compared to those for CH₂=CH-OC(O)R compounds and 3-4 orders of magnitude higher compared to those for CH₂=CH-C(O)R and CH₂=CH-C(O)OR compounds.

Table 3.12 Comparison of the rate coefficients (in cm³ molecule⁻¹ s⁻¹) for the reactions of NO₃ with alkyl vinyl ethers with values reported in the literature for structurally similar alkenes and unsaturated carboxylic compounds at the same temperature

| Vinyl ether (k×10 ¹²) ^{a)} | | Alkene (k×10 ¹⁴) | | Unsaturated Carbonyls (k×10 ¹⁶) | |
|---|------|---|--------------------|--|--------------------|
| MVE CH ₃ OCH=CH ₂ | 0.72 | Propene CH ₃ CH=CH ₂ | 0.95 ^{b)} | Methyl vinyl ketone CH ₃ C(O)CH=CH ₂ | 4.7 ^{d)} |
| EVE C ₂ H ₅ OCH=CH ₂ | 1.40 | 1-Butene C ₂ H ₅ CH=CH ₂ | 1.35 ^{b)} | Ethyl vinyl ketone CH ₃ CH ₂ C(O)CH=CH ₂ | 0.94 ^{e)} |
| PVE n-C ₃ H ₇ OCH=CH ₂ | 1.85 | 1-Pentene n-C ₃ H ₇ CH=CH ₂ | 1.5 ^{b)} | Acrolein H(O)CCH=CH ₂ | 11 ^{d)} |
| BVE n-C ₄ H ₉ OCH=CH ₂ | 2.10 | 1-Hexene n-C ₄ H ₉ CH=CH ₂ | 1.8 ^{b)} | Methacrolein H(O)CC(CH ₃)=CH ₂ | 37 ^{d)} |
| iBVE i-C ₄ H ₉ OCH=CH ₂ | 1.99 | 3-Methyl-1-butene CH ₃ CH(CH ₃)CH=CH ₂ | 1.4 ^{c)} | Methyl acrylate CH ₃ O(O)CCH=CH ₂ | 1.0 ^{d)} |
| tBVE t-C ₄ H ₉ OCH=CH ₂ | 4.81 | | | | |

(a) Data taken from Table 3.11; b) Data taken from Atkinson and Arey [15]; c) Data taken from Noda *et al.* [34]; d) Data taken from Canosa-Mas *et al.* [88]; e) Data taken from Pfang *et al.* [60].

The rate coefficients for the reactions of the NO₃ radical with the alkyl vinyl ethers have been shown to increase with increasing electron donation to the double bond. This trend is fully in line with a mechanism involving electrophilic addition of NO₃ to the double bond. A comparison of the kinetic data with that for other structurally analogous compounds has demonstrated the high electron donating nature of alkoxy groups compared to alkyl groups as has also been seen for the reactions of unsaturated organics with OH and O₃.

Table 3.13 compares rate coefficients for the reactions of NO₃ with ethyleneglycol vinyl ethers with those for structurally similar alkenes. As was observed for the analogue O₃ reactions the rate coefficient for the reaction of NO₃ with EGDVE is somewhat lower than that of NO₃ with EGMVE, but agrees with that of NO₃ with EGMVE within the experimental error limits. The rate coefficient determined for DEGDVE is higher than that measured for EGDVE by a factor of about 3.

Table 3.13 Comparison of the rate coefficients (in cm³ molecule⁻¹ s⁻¹) for the reactions of NO₃ with ethyleneglycol vinyl ethers with values reported in the literature for structurally similar alkenes at the same temperature

| Vinyl ether (k×10 ¹²) ^a | | Alkene (k×10 ¹⁴) | |
|---|------|---|------------------|
| EGMVE HOCH ₂ CH ₂ OCH=CH ₂ | 2.23 | 1-Pentene n-C ₃ H ₇ CH=CH ₂ | 1.5 ^b |
| EGDVE H ₂ C=CHOCH ₂ CH ₂ O- CH=CH ₂ | 1.95 | 1,4-Pentadiene CH ₂ =CHCH ₂ CH=CH ₂ | 2.3 ^c |
| DEGDVE H ₂ C=CHOCH ₂ CH ₂ O- CH ₂ CH ₂ OCH=CH ₂ | 6.14 | | |

a) This work; b) Data taken from Atkinson and Arey [15]; c) Data taken from Bale *et al.* [94].

The rate coefficients for the NO₃ reaction with ethyleneglycol vinyl ethers are higher than those of structurally similar alkenes by about two orders of magnitude. Since

there are no other kinetic data available in the literature for the reactions of NO_3 radical with structurally similar oxygenated organic compounds a more detailed comparison is not warranted.

In the experiments on the reactions of NO_3 with EGDVE and DEGDVE the baselines of the FTIR spectra from 2000 cm^{-1} to 4000 cm^{-1} were elevated after introduction of N_2O_5 (see Figures 3.17 and 3.18). This is possibly due to the formation of secondary organic aerosols causing scattering of the IR light.

Oh and Andino [89-91] have reported an enhancement in the rate of reaction of OH radicals with methanol, ethanol and 1-propanol in the presence of aerosol in the system. In the presence and absence of $500\text{-}8000\mu\text{g}/\text{m}^3$ of NaCl , Na_2SO_4 or NH_4NO_3 aerosol, Sørensen *et al.* [92] studied the effect of aerosol on the reactivity of the OH radical toward methanol, ethanol and phenol. In contrast to the findings of Oh and Andino [89-91], Sørensen *et al.* found that there was no discernable effect of aerosol on the rate of loss of the organics via OH radical reactions. A theoretical calculation using gas-kinetic theory indicates that under the experimental conditions of Oh and Andino [89-91], OH radicals were at least a factor of 1000-9000 times more likely to react in the gas-phase than to collide with aerosol surface [92]. Therefore reaction on the aerosol surface would appear to be a negligible loss process.

This is also the case for the present work. From the kinetic data plots shown in Figure 3.15 and 3.16 an additional explanation is given here, i.e. that the formation of aerosol does not enhance the rate coefficients measured for the reactions of NO_3 radicals with the ethyleneglycol vinyl ethers. When the reaction is initiated, the reaction then generates semi-volatile products. After these products have reached their saturation vapor pressure, they start to nucleate homogeneously and aerosol is formed. If the aerosol formed had enhanced the loss of EGDVE and DEDVE, this would result in a faster decay of both compounds as the reaction proceeds compared to the initial stage of reaction. Therefore, in comparison with first few points in Figure 3.15 and Figure 3.16 the points measured at later stages in the reaction should result in curvature in the plot if aerosol formation was affecting the homogeneous reaction mechanism.

However, as seen in Figures 3.15 and 3.16 this was not the case for the measurements with both EGDVE and DEDVE, where all the plotted data show good linearity, indicating that the loss rate of both EGDVE and DEGDVE did not show any discernable differences with and without aerosol present in the system.

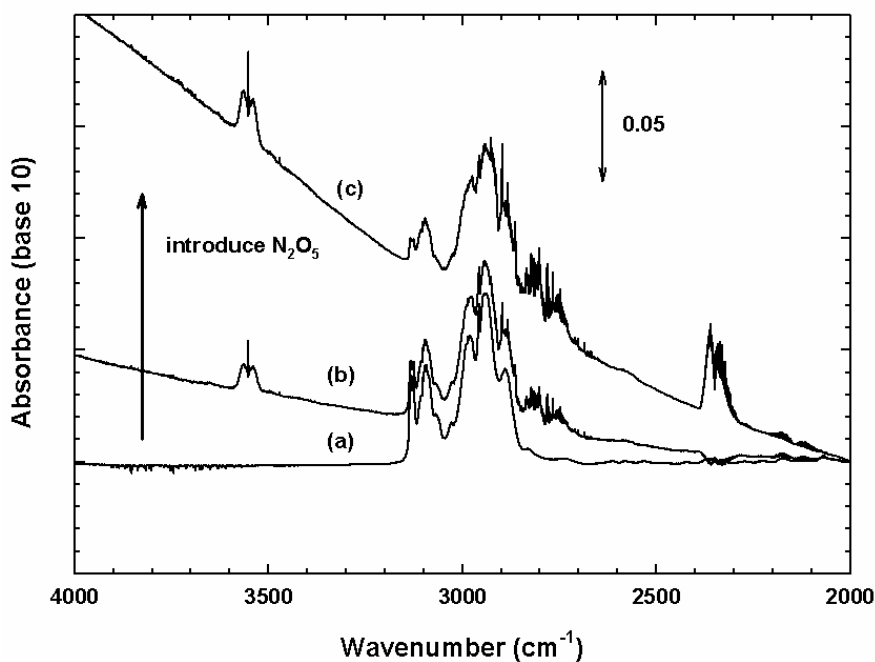


Figure 3.17 Baseline elevation in a study of the NO₃ radical reaction with ethyleneglycol divinyl ether (EGDVE): (a) before introduction of N₂O₅; (b) after introduction of N₂O₅ for 5 minutes; (c) after introduction of N₂O₅ for 8 minutes.

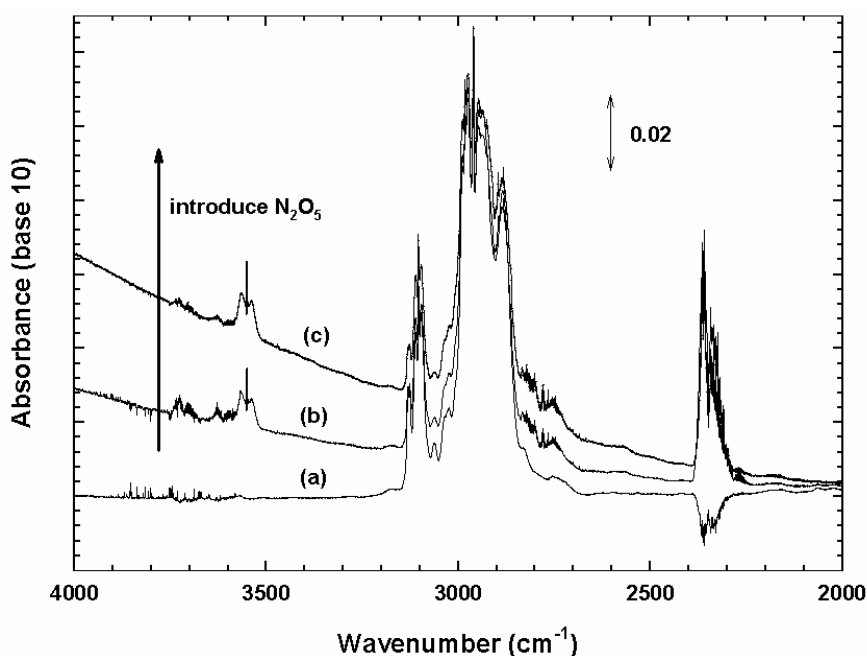


Figure 3.18 Baseline elevation in a study of the NO₃ radical reaction with diethyleneglycol divinyl ether (DEGDVE): (a) before introduction of N₂O₅; (b) after introduction of N₂O₅ for 5 minutes; (c) after introduction of N₂O₅ for 8 minutes.

Many types of correlations of kinetic data have been applied to highlight trends in chemical behavior and also to predict the rate coefficient for the reaction of a compound with the atmospheric reactive species such as OH, O₃ and NO₃ for which experimental data do not exist. For example, rate coefficients for the reactions of OH and NO₃ radicals with unsaturated organic compounds have often been correlated with the first vertical ionization potentials (E_v) of the compounds [93], whereby the logarithm of the rate coefficient for the particular reaction is plotted as a function of the corresponding E_v .

Other types of correlation that are typically applied, and are known as “linear free-energy relationships”, involve plotting the logarithm of the rate coefficient for reaction of the compound with, for example, OH ($\log(k_{OH})$), against the logarithm of the rate coefficient values for the corresponding reactions with another species, e.g., NO₃ ($\log(k_{NO_3})$) [93]. However, the data sets for the reactions of species such as OH, ozone and NO₃ with organic compounds are often not sufficiently large to allow reasonable rate coefficient recommendations to be made for the reactions of interest. Ionization potentials could not be found in the literature for vinyl ethers. The number of available rate coefficients for the reactions of OH and NO₃ radicals with the vinyl ethers is too small for the construction of a meaningful “linear free-energy relationship”; however, a plot using the available data suggests that a reasonable linear relationship exists between these reactants for C₁ to C₄ alkyl vinyl ethers.

It has been shown in recent years that it is possible to predict the rate coefficients for the reactions of OH, ozone and NO₃ with alkenes by perturbation frontier molecular orbital (PFMO) theory [93-98]. The natural logarithm of the room-temperature rate coefficients have been shown to correlate with the energy change, ΔE , when the highest occupied molecular orbital (HOMO) of the alkene perturbs the single occupied molecular orbital (SOMO) of the OH and NO₃ radical or the lowest unoccupied molecular orbital (LUMO) of O₃ as two reactant orbitals overlap. To the best of my knowledge this predictive technique has only been applied to unsubstituted alkenes [93,95] and chloroalkenes [96] and not to oxygenated alkenes. It would be interesting to extend the technique to the available database on oxygenated alkenes. Unfortunately, during the work the computer programs necessary to calculate the HOMO and SOMO energies for the correlations were not available.

3.2 Atmospheric implications

The atmospheric transformation processes for volatile organic compounds are initiated by reaction with OH radicals, ozone, NO₃ radicals, and under certain circumstances possibly Cl atoms, in addition to photolysis and wet / dry deposition.

Due to the presence of the alkene moiety vinyl ethers show high reactivity toward OH radicals, ozone and NO₃ radicals. Mellouki *et al.* [16] have concluded that reaction with these species represents the major degradation pathways of vinyl ethers in the troposphere.

The rate coefficients determined in this study for the reactions of OH radicals, O₃ and NO₃ radicals with PVE, BVE, EGMVE, EGDVE and DEGDVE can be used to estimate the atmospheric lifetimes of the vinyl ethers studied in this work with respect to chemical degradation by these species. The lifetime τ is defined as:

$$\tau = 1/k[\text{species}] \quad (\text{XV})$$

where k is the rate coefficient for the reaction of the reactive species (OH, O₃ or NO₃) with the vinyl ethers determined in this study and $[\text{species}]$ is the concentration of the reactive species.

The average tropospheric concentrations of OH radicals, ozone and NO₃ radicals used in calculations of the lifetimes were ca. 1.6×10^6 (12-h daytime average [99]), 7×10^{11} (24-hr average concentration [4]), and 5.0×10^8 molecule cm⁻³ (12-h nighttime average [100,101]), respectively. These are the values most commonly used in publications presenting calculations of the lifetimes of organic compounds with respect to reactions with OH radicals, ozone and NO₃ radicals. The atmospheric concentration of NO₃ radicals, however, is highly variable [101].

The atmospheric lifetimes of PVE, BVE, EGMVE, EGDVE and DEGDVE with respect to reactions with OH, ozone and NO₃ are shown in Table 3.14. The lifetimes for the reactions of the vinyl ethers with OH, ozone and NO₃ are all no more than a few hours in all cases. Thus all three loss processes can make significant contributions to the degradation of all the vinyl ethers investigated. The short lifetimes of the vinyl ethers show that they will be quickly degraded when emitted to the atmosphere and will only be actively involved in tropospheric chemistry on local to regional scales.

On the other hand, the losses of the vinyl ethers due to the catalyzed hydrolysis at the acidic chamber walls indicate the possibility of a contribution to the atmospheric removal of the vinyl ethers from catalyzed degradation on acidic aerosol surfaces. Work done here and within the EU project MOST [48] has shown that the photolysis of vinyl ethers is a negligible loss process for this class of organic compound in the troposphere.

Table 3.14 Estimated atmospheric lifetime (in hours) of PVE, BVE, EGMVE, EGDVE and DEGDVE with respect to degradation by OH radicals, ozone and NO₃ radicals

| Vinyl ether | $\tau_{\text{OH}}^{\text{a}}$ | $\tau_{\text{O}_3}^{\text{b}}$ | $\tau_{\text{NO}_3}^{\text{c}}$ |
|--|-------------------------------|--------------------------------|---------------------------------|
| PVE, C ₃ H ₇ OCH=CH ₂ | 1.78 | 1.70 | 0.30 |
| BVE, n-C ₄ H ₉ OCH=CH ₂ | 1.54 | 1.53 | 0.26 |
| EGMVE HOCH ₂ CH ₂ OCH=CH ₂ | 1.67 | 1.96 | 0.28 |
| EGDVE H ₂ C=CHOCH ₂ CH ₂ OCH=CH ₂ | 1.41 | 2.35 | 0.25 |
| DEGDVE H ₂ C=CHOCH ₂ CH ₂ OCH ₂ CH ₂ OCH=CH ₂ | 1.22 | 1.47 | 0.09 |

- a) Based on the average tropospheric concentrations of OH radicals of ca. 1.6×10^6 molecule cm⁻³ (12-h daytime average) [99];
- b) Based on the average tropospheric concentrations of ozone of ca. 7×10^{11} molecule cm⁻³ (24-hr average concentration) [4];
- c) Based on the average tropospheric concentrations NO₃ radicals of ca. 5.0×10^8 molecule cm⁻³ (12-h nighttime average) [100,101].

Chapter 4

Mechanisms of the Atmospheric Oxidation of Vinyl Ethers

As discussed in Chapter 3, the dominant atmospheric chemical loss processes for vinyl ethers are reactions with OH radicals, ozone and NO₃ radicals. Studies aimed at clarifying the oxidation mechanisms of the OH radical, ozone and NO₃ radical initiated oxidation of alkyl vinyl ethers were performed in the 405 l borosilicate glass chamber system at the University of Wuppertal.

4.1 Product studies of the OH radical initiated oxidation of vinyl ethers

In the studies on the OH radical reactions with vinyl ethers two types of OH radical source were employed, i.e. the photolysis of a NO_x-containing OH source, HONO, and the photolysis of a NO_x-free OH source, H₂O₂. After all the reactants were pre-mixed in the reactor the reactions were initiated by switching on the visible fluorescence lamps or UV lamps to irradiate the vinyl ethers and HONO or H₂O₂ in the bath gas. The contents of the chamber were monitored in the pre- and post-irradiations periods for a short time in order to establish the dark behaviors of the reactants and products for the data evaluation.

4.1.1 Experimental results

The product studies on the OH radical initiated oxidation of PVE and BVE were performed at (298 ± 3) K and (760 ± 10) Torr total pressure of synthetic air. For each reaction at least three experimental runs were performed.

The initial concentrations of the vinyl ethers, i.e. PVE and BVE, HONO and H_2O_2 were approximately 5.5, 1.9-4.7 and 20 ppm, respectively.

4.1.1.1 Results for the OH radical reaction with PVE

Figure 4.1 shows an example of a typical concentration-time profile of the reactants and products observed from an experiment on the OH radical reaction with PVE using the NO_x -containing OH radical source (HONO).

From Figure 4.1 it can be seen that the dark loss of PVE in the pre- and post- OH

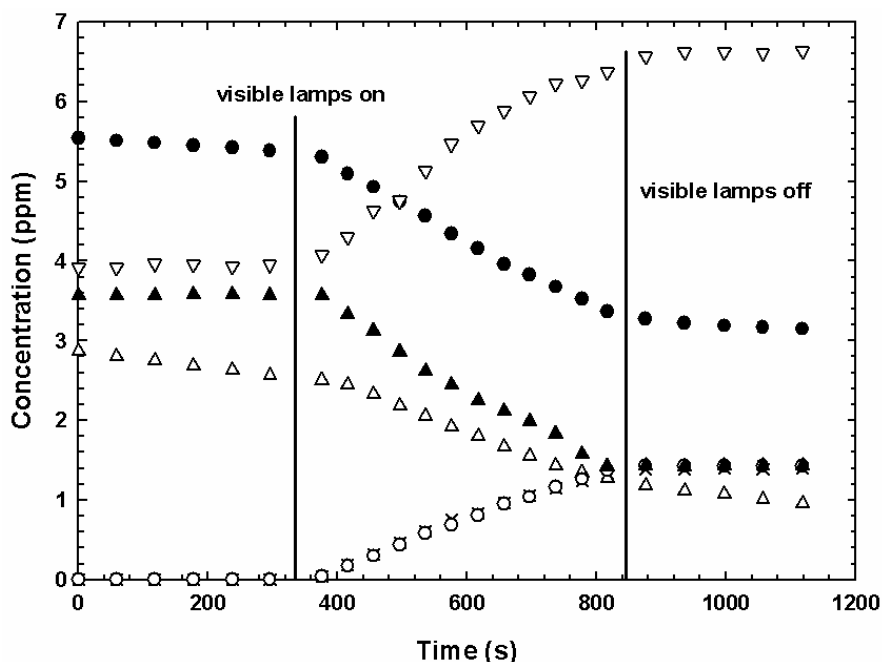


Figure 4.1 Concentration-time profiles of the reactants and products from the OH radical initiated oxidation of PVE obtained with the NO_x -containing OH radical source (HONO): (●)-PVE; (Δ)-HONO; (∇)- NO_2 ; (▲)-NO; (○)-propyl formate; (×)-HCHO.

radical reaction periods is the same.

With the photolysis of HONO as the OH radical source the wall loss for the identified products, HCHO and propyl formate, was negligible. From the plot it can also be seen that the amounts of formaldehyde and propyl formate formed in experiment are approximately the same.

Figure 4.2 gives an example of the concentration-time profiles of the reactants and products observed in an experiment on the OH radical reaction with PVE with the NO_x-free OH radical source (H₂O₂).

The shape of the curve for formaldehyde in Figure 4.2 shows that there is a secondary loss for this compound in the system. With H₂O₂ as the OH radical source a first order dark wall loss of formaldehyde was observed, and no dark loss was observed for propyl formate. Test experiments showed no evidence for photolysis of PVE, HCHO and propyl formate with either the visible fluorescence lamps or the UV lamps.

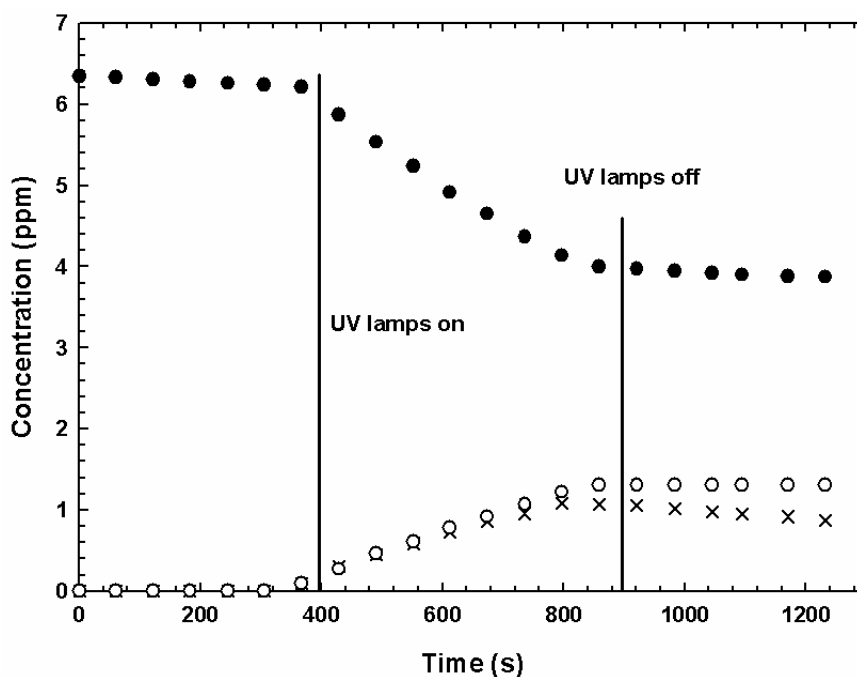


Figure 4.2 Concentration-time profiles of the reactants and products from an experiment on the OH radical initiated oxidation of PVE with the NO_x-free OH radical source (H₂O₂): (●)-PVE; (○)-propyl formate; (×)-HCHO.

Figure 4.3 shows typical product spectra recorded in the OH radical initiated oxidation of PVE. Trace (a) is a product spectrum obtained with the NO_x-containing

OH radical source and trace (b) shows a product spectrum obtained with the NO_x-free OH radical source.

It can be seen from a comparison of these spectra, with the reference spectra of propyl formate (trace (c)) and formaldehyde (trace (d)), that these two compounds are the main products of the reaction of OH with PVE in both systems. Traces (e) and (f) in Figure 4.3 show the residual spectra obtained from traces (a) and (b), respectively, after subtraction of the identified products. For easier comparison both spectra are expanded by a factor of 5.

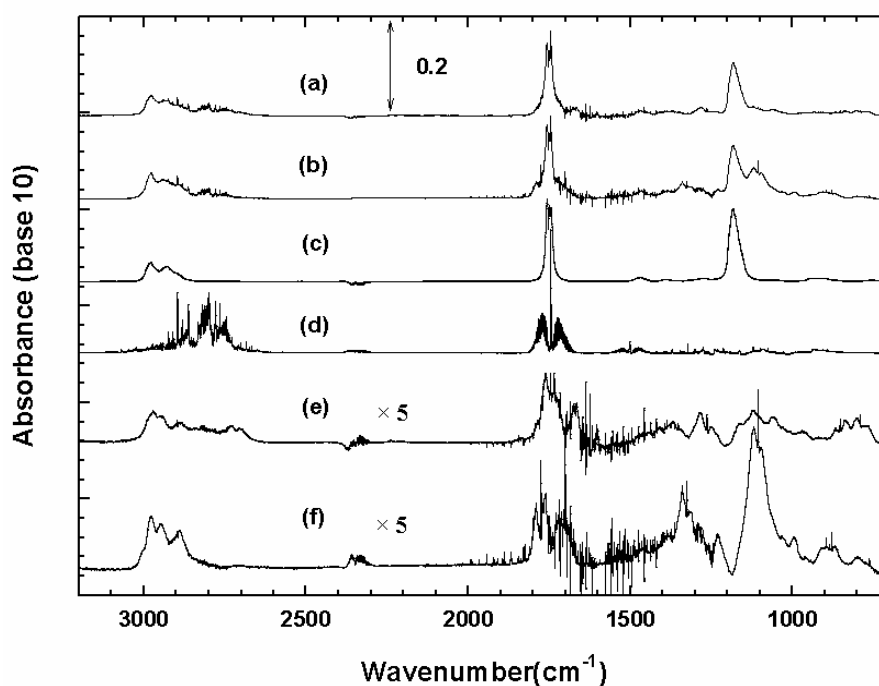


Figure 4.3 Product spectra recorded during the reaction of OH radicals with PVE; (a) product spectrum in the presence of NO_x; (b) product spectrum in the absence of NO_x; (c) scaled reference spectrum of propyl formate; (d) scaled reference spectrum of formaldehyde; (e) spectrum (a) after subtraction of all identified compounds; (f) spectrum (b) after subtraction of all identified products. For easier comparison all the spectra are offset and spectra (e) and (f) are expanded by a factor of 5.

In experiments using the NO_x-free OH radical source the concentration of formaldehyde has been corrected for dark loss and reaction with OH using the procedure outlined in the Section 2.2.3.1. The loss of formaldehyde due to reaction

with OH was only 2% because the rate coefficient for the reaction of PVE with OH is about 10 times higher than that of formaldehyde with OH. No correction was necessary for propyl formate due to its very low reactivity toward OH radicals.

Figure 4.4 presents examples of plots of the propyl formate and corrected formaldehyde concentrations as a function of reacted PVE for systems with and without NO_x present. The data points for propyl formate have been displaced for clarity. The slopes of the linear regression lines give the yields of the products. From a minimum of 3 experiments for each system averaged molar formation yields of (78.6±8.8)% and (75.9±8.4)% were obtained for propyl formate and formaldehyde, respectively, in the presence of NO_x and (63.0±9.0)% and (61.3±6.3)%, respectively, in the absence of NO_x.

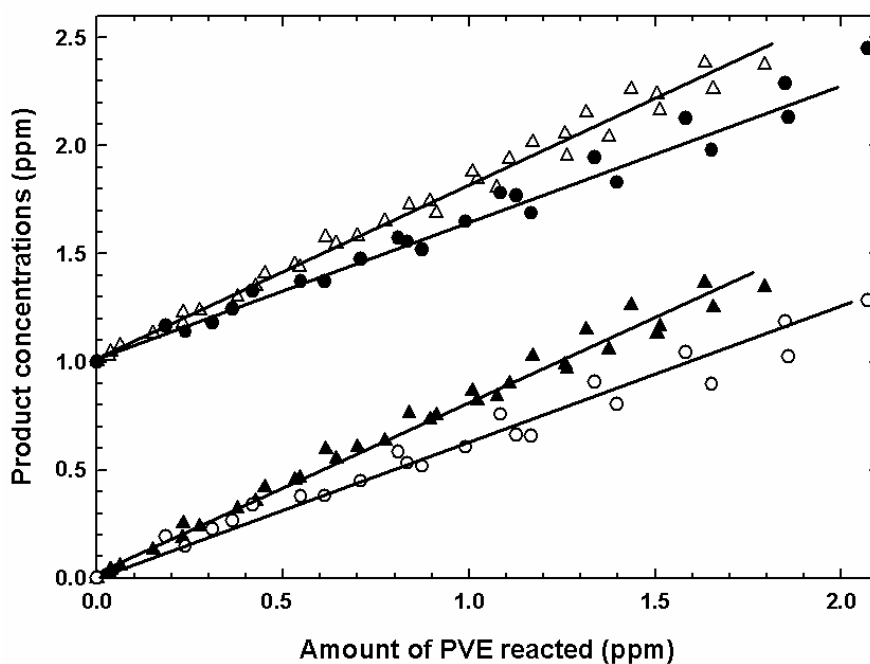


Figure 4.4 Plots of the measured product concentrations from the reaction of OH with PVE plotted as function of the amount of PVE reacted with OH radicals. (Δ)-propyl formate in the presence of NO_x; (\bullet)-propyl formate in the absence of NO_x; (\blacktriangle)-HCHO in the presence of NO_x; (\circ)-HCHO in the absence of NO_x. The propyl formate concentrations are offset by 1 ppm.

4.1.1.2 Results for the OH radical reaction with BVE

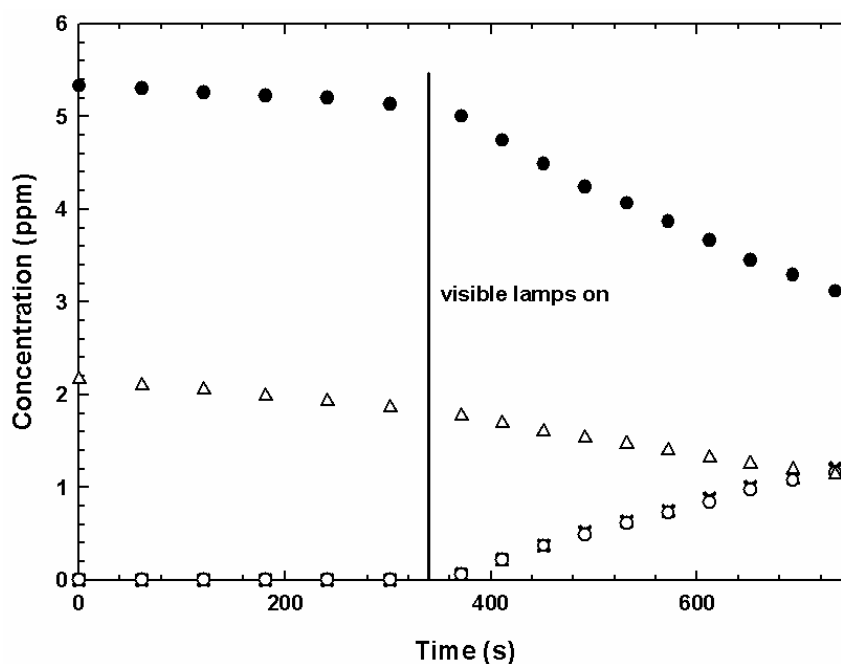


Figure 4.5 Concentration-time profiles of the reactants and products from an experiment on the OH radical initiated oxidation of BVE using a NO_x -containing OH radical source (HONO): (●)-BVE; (Δ)-HONO; (○)-butyl formate; (×)-HCHO.

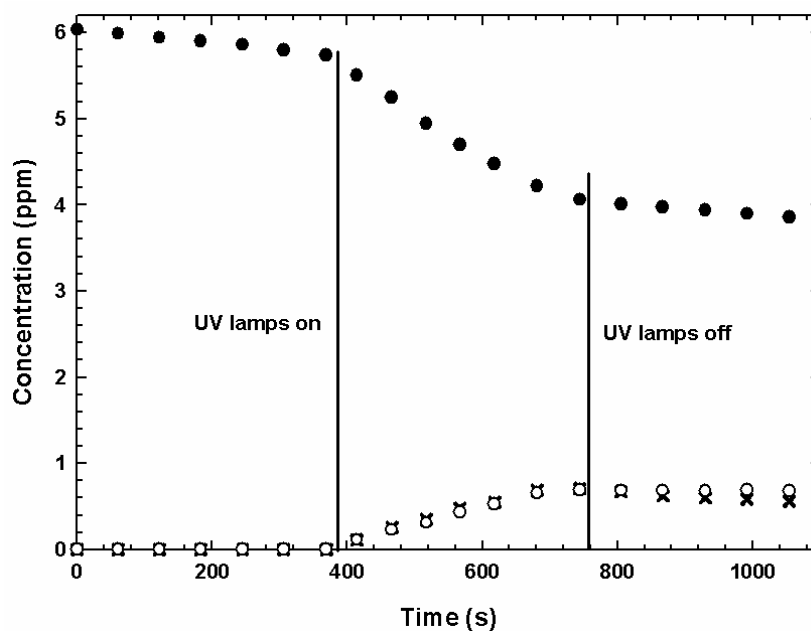


Figure 4.6 Concentration-time profiles of the reactants and products from an experiment on the OH radical initiated oxidation of BVE using a NO_x -free OH radical source (H_2O_2): (●)-BVE; (○)-butyl formate; (×)-HCHO.

The product studies on the reaction of OH with BVE were carried out exactly in the same manner as those on the reaction of OH with PVE.

Figure 4.5 and Figure 4.6 show the concentration-time profiles of the reactants and products for experiments on the reaction of OH with BVE with and without NO_x present in the system, respectively.

As for the studies on OH reaction with PVE, dark loss of BVE was observed and the data was corrected accordingly. As for PVE, the photolysis losses of BVE, butyl formate and HCHO were negligible with both the visible fluorescence and UV lamps. In the presence of NO_x no corrections for dark loss of butyl formate and HCHO were necessary. In contrast, in the presence of H₂O₂, dark loss of HCHO was observed. This was corrected using the procedure outlined in Section 2.2.3.1.

From the product spectra shown in Figure 4.7 it can be seen that butyl formate and HCHO are the main products in the OH radical reaction with BVE. Traces (e) and (f)

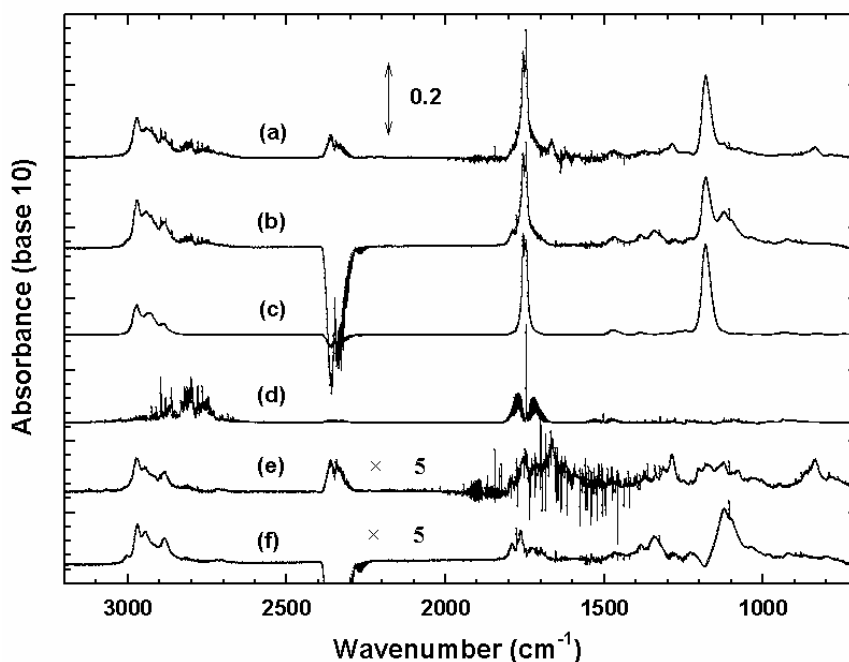


Figure 4.7 Product spectra recorded during studies on the OH radical reaction with BVE; (a) product spectrum in the presence of NO_x; (b) product spectrum in the absence of NO_x; (c) scaled reference spectrum of butyl formate; (d) scaled reference spectrum of formaldehyde; (e) spectrum (a) after subtraction of all identified compounds; (f) spectrum (b) after subtraction of all identified products. For easier comparison all the spectra are offset and spectra (e) and (f) are expanded by a factor of 5.

in Figure 4.7 give the residual spectra obtained for the NO_x -containing and NO_x -free systems, respectively, after subtraction of the identified products. For easier comparison both spectra are expanded by a factor of 5.

Figure 4.8 presents examples of the butyl formate and corrected formaldehyde concentrations, measured with and without NO_x present in the system, plotted as a function of the reacted BVE. The data points for butyl formate have been displaced in Figure 4.8 for clarity.

The slopes of the linear regression lines give the yields of the products. From a minimum of 3 experiments for each system averaged molar formation yields of $(64.7 \pm 7.1)\%$ and $(64.3 \pm 6.9)\%$ were obtained for butyl formate and formaldehyde, respectively, in the presence of NO_x and $(52.2 \pm 6.3)\%$ and $(52.9 \pm 6.3)\%$, respectively, in the absence of NO_x .

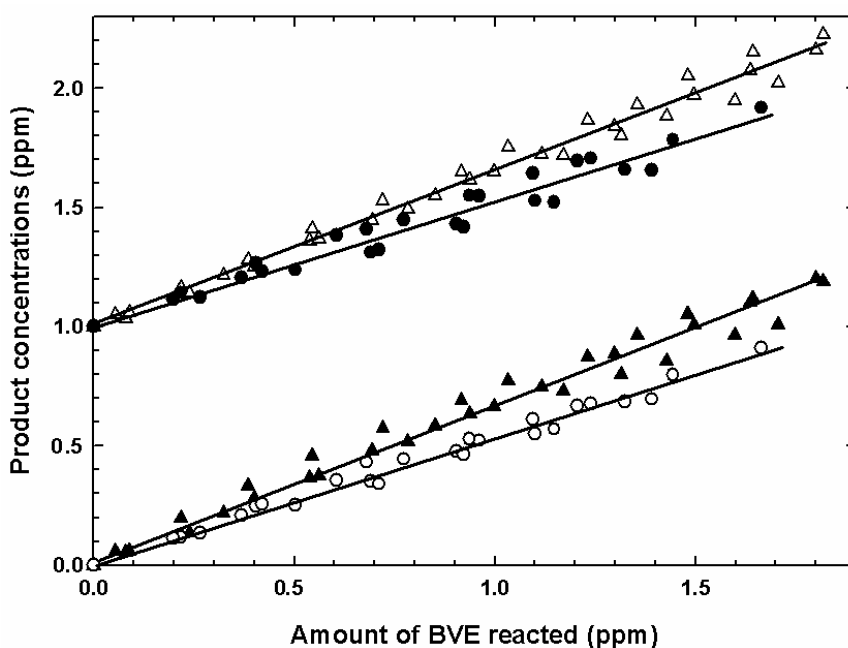


Figure 4.8 Plots of the measured product concentrations from the reaction of OH with BVE plotted as a function of the amount of BVE reacted with OH radicals. (Δ)-butyl formate in the presence of NO_x ; (\bullet)-butyl formate in the absence of NO_x ; (\blacktriangle)-HCHO in the presence of NO_x ; (\circ)-HCHO in the absence of NO_x . The butyl formate concentrations are offset by 1 ppm.

4.1.2 Discussion of the OH radical reactions

Alkyl formates and formaldehyde have been observed as major products in the reactions of OH with alkyl vinyl ethers [16,48,50-52,54]. Table 4.1 compares the yields of alkyl formates and formaldehyde determined in this study for the reactions of the OH radical with PVE and BVE with those reported in the literatures for alkyl vinyl ethers. It can be seen in Table 4.1 that high yields of alkyl formates and formaldehyde are observed for all of the vinyl ethers both with and without NO_x in the system.

Table 4.1 Comparison of the yields of alkyl formates (HC(O)OR) and HCHO/CH₃CHO from the reaction of OH radicals with vinyl ethers

| Vinyl ether | Formate yield (molar %) | HCHO yield (molar %) | Reference |
|---|--|--|---|
| MVE, CH ₃ OCH=CH ₂ | (80.9±8.2) ⁱ (50.2±5.1) ⁱⁱ | (76.6±7.9) ⁱ (57.0±6.0) ⁱⁱ | Klotz <i>et al.</i> [52] Klotz <i>et al.</i> [52] |
| EVE, C ₂ H ₅ OCH=CH ₂ | 76.8 ⁱ (92±7) ⁱ (83±7) ⁱⁱ | 71.8 ⁱ | Barnes <i>et al.</i> [48] Thiault <i>et al.</i> [50] Thiault <i>et al.</i> [50] |
| PVE, n-C ₃ H ₇ OCH=CH ₂ | (78.6±8.8) ⁱ (63.0±9.0) ⁱⁱ (72±6) ⁱ | (75.9±8.4) ⁱ (61.3±6.3) ⁱⁱ | This work This work Al Mulla [55] |
| BVE, n-C ₄ H ₉ OCH=CH ₂ | (64.7±7.1) ⁱ (52.2±6.3) ⁱⁱ (75±8) ⁱ | (64.3±6.9) ⁱ (52.9±6.3) ⁱⁱ | This work This work Al Mulla [55] |
| iBVE i-C ₄ H ₉ OCH=CH ₂ | (70.2±8.8) ⁱ (59.8±7.3) ⁱⁱ (63±6) ⁱ | (69.0±6.1) ⁱ (59.0±7.3) ⁱⁱ | Barnes <i>et al.</i> [48] Barnes <i>et al.</i> [48] Al Mulla [55] |
| tBVE t-C ₄ H ₉ OCH=CH ₂ | (56.8±6.2) ⁱ (50.9±6.0) ⁱⁱ (73±6) ⁱ | (60.4±6.4) ⁱ (56.7±5.8) ⁱⁱ (70±6) ⁱ | Barnes <i>et al.</i> [48] Barnes <i>et al.</i> [48] Al Mulla [55] |
| EPE, C ₂ H ₅ OCH=CHCH ₃ | 86.9 ⁱ | 56.9 ^{i & iii} | Barnes <i>et al.</i> [48] |

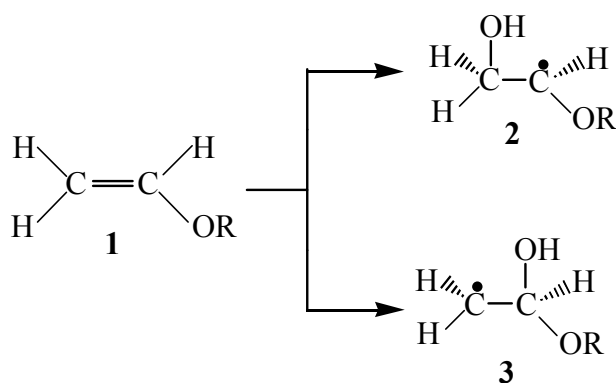
i) with NO_x present; ii) without NO_x present; iii) acetaldehyde

Al Mulla [55] has reported formate product yields for the reactions of OH with PVE, BVE and iBVE with NO_x present in the system which are in agreement with those determined in this work and by Barnes *et al.* [48]. The value reported by Al Mulla [55] for the yield of tert-butyl formate from the reaction of OH with tert-butyl vinyl ether (tBVE) is higher than that determined by Barnes *et al.* [48]; however, the values agree within the combined quoted errors limits.

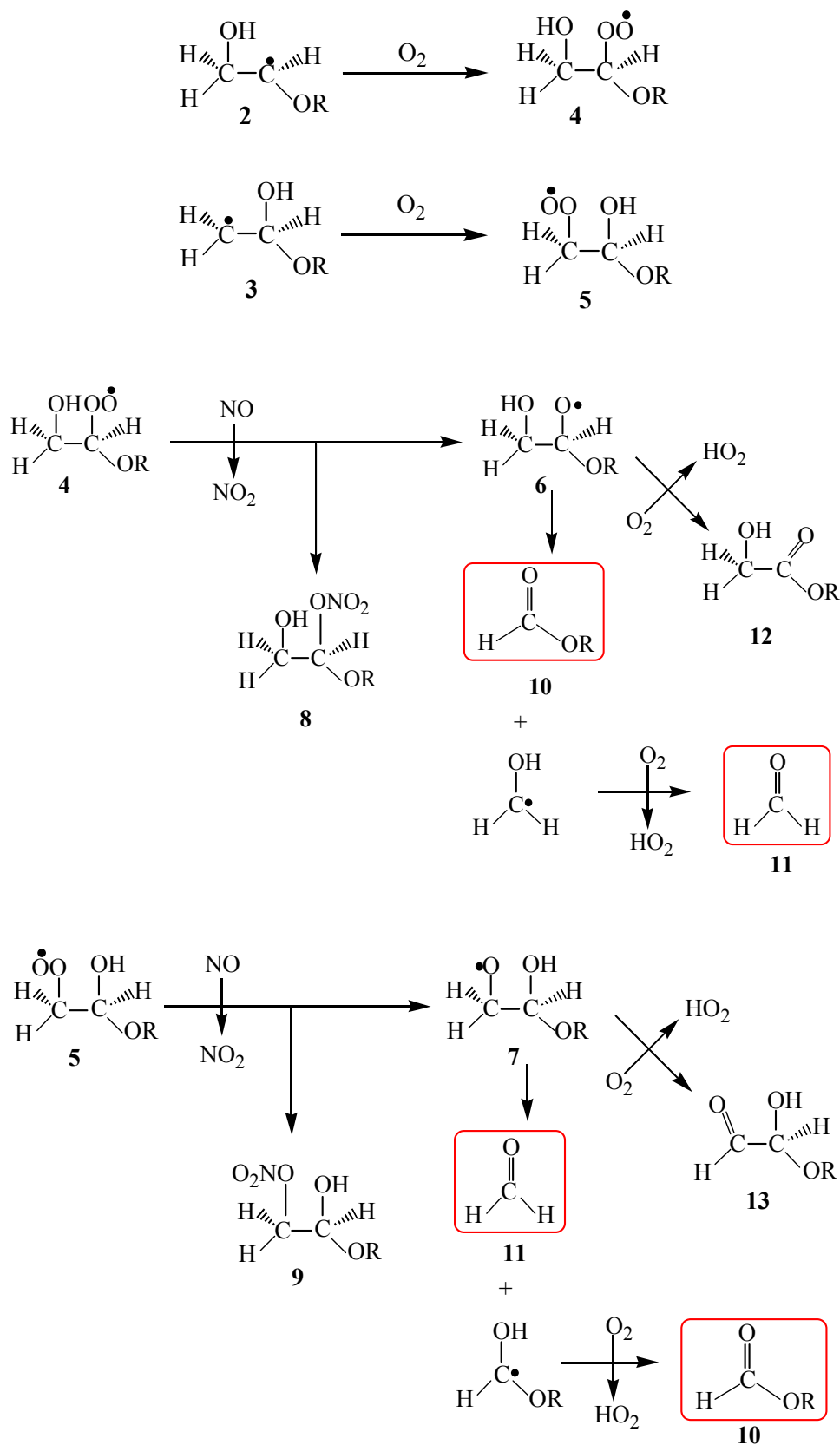
In the absence of NO_x the yields of both the alkyl formate and HCHO are lower than with NO_x present. The molar yields of both the alkyl formate and HCHO for the different vinyl ethers fall within the range of (70 ± 10) molar % for the NO_x -containing system and (60 ± 10) molar % for the NO_x -free system. The only exception is the very high formate yield reported for the reaction of the OH with ethyl vinyl ether (EVE) by Thiault *et al.* [50].

The reaction mechanisms for the OH radical initiated oxidation of PVE and BVE are expected to be very similar to that proposed by Klotz *et al.* [52] for the reaction of OH with MVE. The possible reactions of OH with alkyl vinyl ethers ($\text{CH}_2=\text{CHOR}$, where $\text{R} = -\text{CH}_2\text{CH}_2\text{CH}_3$ for PVE and $-\text{CH}_2\text{CH}_2\text{CH}_2\text{CH}_3$ for BVE) are addition of OH radical to the carbon-carbon double bond (2 possible addition sites) and H-atom abstraction from the alkyl group.

Addition results in formation of the radical β -hydroxy intermediates **2** and **3**, whereby formation of **2** is favored.



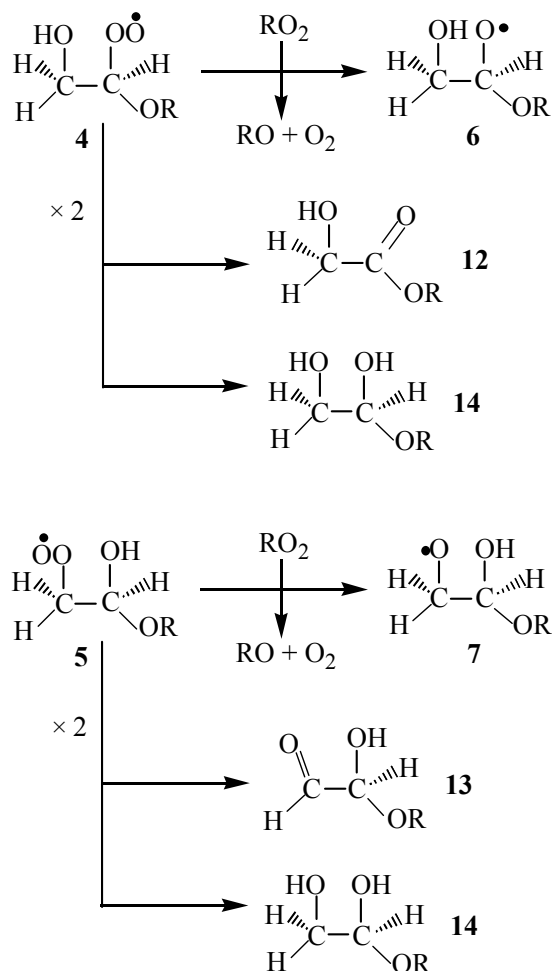
The intermediates **2** and **3** react with O_2 to give the organic β -hydroxy peroxy radicals **4** and **5**, respectively. In the presence of NO_x **4** and **5** react with NO to form either the β -hydroxy alkoxy radicals **6** and **7**, respectively, or the nitrates **8** and **9**, respectively.



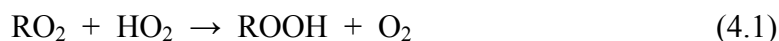
Subsequently the β -hydroxy alkoxy radicals **6** and **7** can react with O₂, unimolecularly decompose by C-C bond scission or isomerize by H atom shift. From the

products observed in the OH radical reaction with PVE and BVE, the major fate of **6** and **7** is decomposition to produce alkyl formate **10** and formaldehyde **11**, and the reaction of **6** and **7** with O₂ is of minor importance.

In the absence of NO_x the β-hydroxy peroxy radicals **4** and **5** can react with themselves or other RO₂ radicals to form the β-hydroxy alkoxy radicals **6** and **7**, respectively, which follow the reactions mentioned above to produce alkyl formate **10** and formaldehyde **11**. However, the self reaction of the β-hydroxy peroxy radicals **4** and **5** can also lead to the formation of multifunctional group compounds such as glycolic acid alkyl ester **12**, and hydroxy alkoxy acetaldehyde **13** and 1-alkoxy ethane-1,2-diol **14**.



Despite the relatively high production of HO₂ radicals in the NO_x-free system and their likely reaction with the peroxy radicals to give hydroperoxides shown below:



the modest drop in the alkyl formate and HCHO yields (from 75-80% to around 60-65% for OH with PVE and from 65-70% to around 50-55% for OH with BVE) suggests that the self- and cross-reactions of the β -hydroxy peroxy radicals **4** and **5** proceed predominately to give the corresponding β -hydroxy alkoxy radicals **6** and **7**, respectively.

In the NO_x-containing systems there were no discernible absorptions in the product spectrum which could be attributed to the -OH group, however, in the product spectrum obtained under NO_x-free conditions absorptions around 3600 cm⁻¹ attributable to an -OH group were clearly visible. The formation of hydroperoxides and the -OH group containing compounds such as glycolic acid alkyl ester **12**, hydroxy alkoxy acetaldehyde **13** and 1-alkoxy ethane-1,2-diol **14** could be responsible for this observation. The formation of these compounds can explain the reduced yields of the formates and HCHO observed in the absence of NO_x compared to the higher yields measured in the presence of NO_x.

As discussed in Section 3.1.1, 10-12% of the OH radical reaction proceeds via H-atom abstraction from the n-propyl group in PVE and n-butyl group in BVE. This in turn implies that around 10% and 20 % of OH addition to the double bond of PVE and BVE respectively, in the NO_x-containing system is leading to products other than alkyl formates and HCHO.

The H-atom abstraction channel for OH radical reactions with PVE leads to different radicals such as **15**, **16** and **17**, which in sequential reactions involving molecular oxygen, NO or RO₂ radicals can lead to the production of compounds such as vinyl formate **18**, acetaldehyde **19**, vinyl propionate **20**, ethenoxyacetone **21** and 3-ethenoxypropanal **22** in very low molar yields.

The analogue H-atom abstraction by OH radical for BVE produces vinyl formate **18**, propanal **19**, vinyl butyrate **20**, ethenoxy-2-butanone **21**, 4-ethenoxy-2-butanone **22** and 4-ethenoxybutanal **24**.

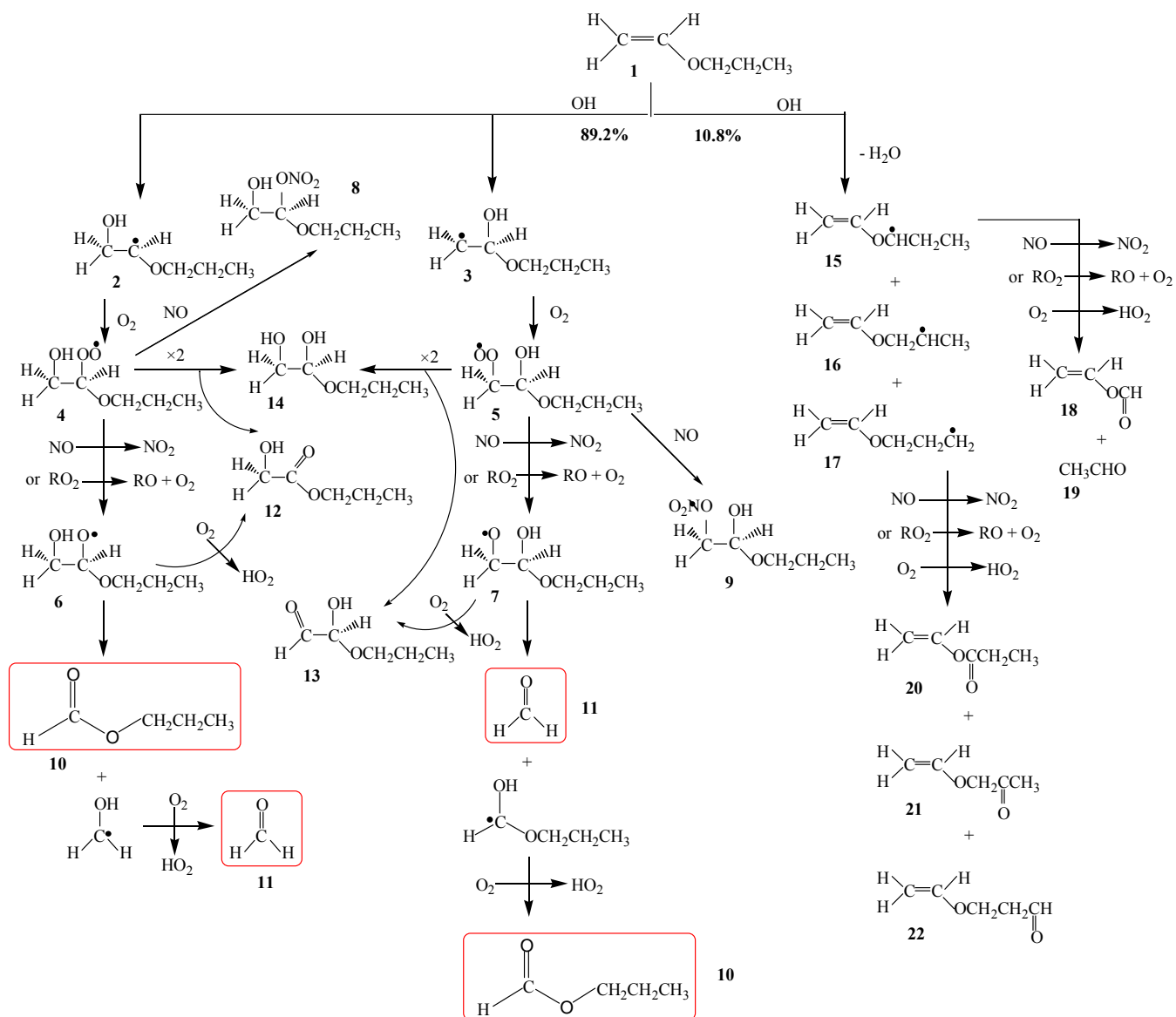
Simplified reaction mechanisms for the OH radical initiated oxidation of PVE and BVE are outlined in Scheme 4.1 and Scheme 4.2, respectively. Branching ratios (expressed in %) for OH radical addition to the double bond and H-atom abstraction from the alkyl group of 89.2 : 10.8 and 87.8 : 12.2 have been estimated for the reactions of OH radical with PVE and BVE, respectively, as mentioned in Chapter 3.

As discussed above the H-atom abstraction channel results in the formation of a variety of radicals. H-atom abstraction from the -CH₂- group adjacent to the ether oxygen to give radical **15** is the most favorable.

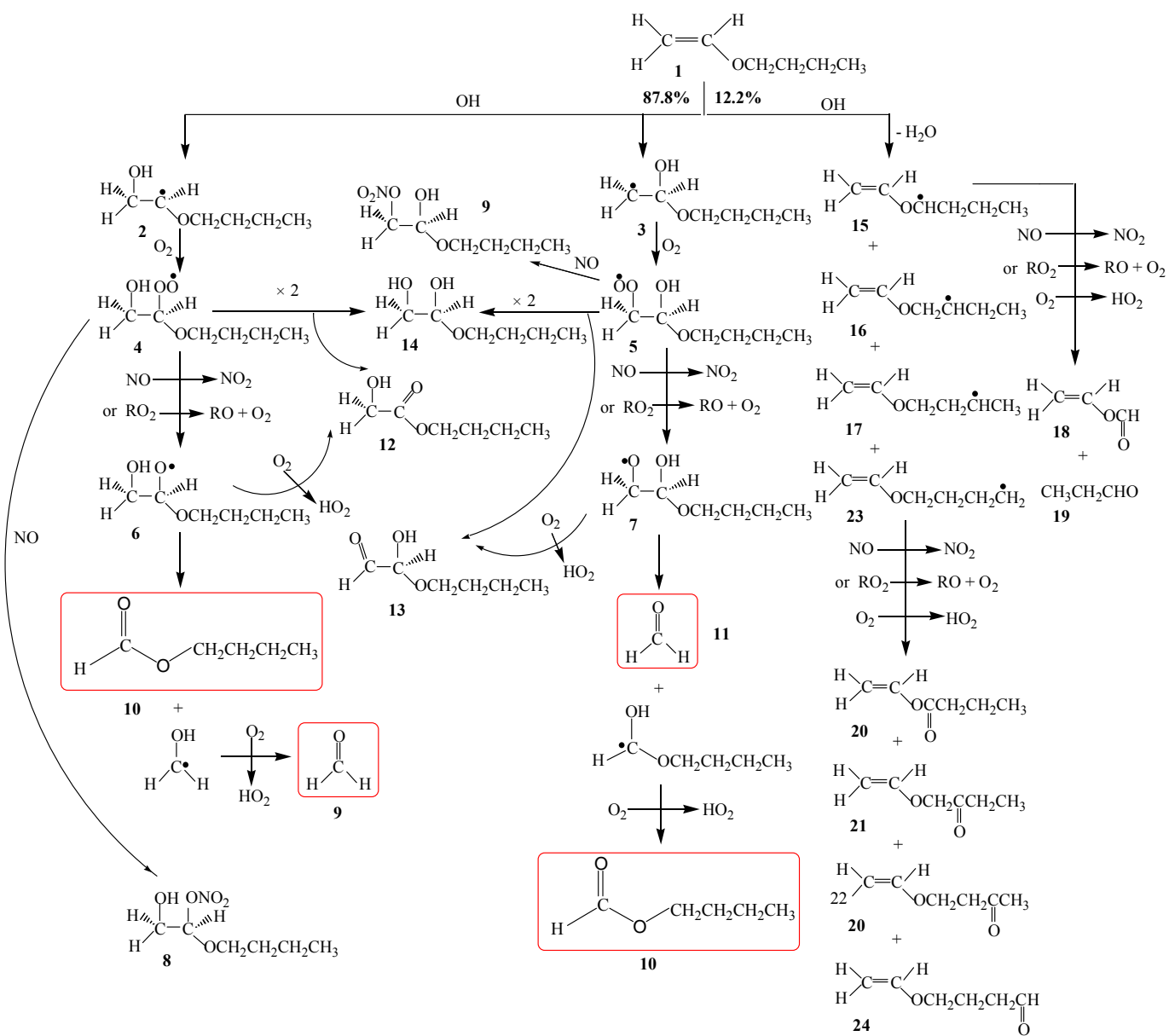
The subsequent reactions of **15** give rise to the production of vinyl formate **18** and the corresponding aldehyde **19** (acetaldehyde or propanal for PVE or BVE, respectively). As mentioned in Chapter 2, acetaldehyde is one of the products of the dark reaction of alkyl vinyl ethers, so it is not possible to say whether or not acetaldehyde is produced from the H-atom abstraction reaction of OH with PVE. However, in the OH + BVE reaction no absorptions were observed which could be attributed to propanal, with and without NO_x presence in the systems.

For the OH radical initiated oxidation of PVE, in the presence of NO_x, 77.0% C can be accounted for, compared to 63.4% C in the absence of NO_x. For the reaction of OH with BVE, in the presence of NO_x, 64.6% C can be accounted for, compared to 52.3% C in the absence of NO_x. In the presence of NO_x the residual product spectra (trace (e) in Figures 4.3 and 4.7), show an absorption in the carbonyl region around 1760 cm⁻¹. The absorptions in the regions around 1665 cm⁻¹, 1286 cm⁻¹ and 835 cm⁻¹ in trace (e), Figure 4.3 and those around 1664 cm⁻¹, 1284 cm⁻¹ and 834 cm⁻¹ in trace (e), Figure 4.7 are characteristic of compounds containing the nitrate group. Based on the known chemistry of RO₂ and NO_x it is reasonable to assume that multifunctional organic nitrate products comprise the majority of the missing carbon in the reaction systems of PVE + OH and BVE + OH containing NO_x.

The residual absorptions obtained in the NO_x-free system, trace (f) in both Figure 4.3 and Figure 4.7, are very similar to those observed by Klotz *et al.* [52] in their study of the reaction of OH with MVE. It is assumed that some of these absorptions stem from hydroxyl carbonyl compounds such as **12**, **13** and **14** shown in the reaction mechanisms Scheme 4.1 and 4.2 and also from hydroperoxides formed from the reactions of the peroxy radicals with HO₂. Unfortunately neither reference compounds nor the technical facilities for detection of these types of compounds were available to validate this assumption.



Scheme 4.1 Simplified reaction mechanism for the OH radical initiated oxidation of PVE



Scheme 4.2 Simplified reaction mechanism for the OH radical initiated oxidation of BVE

4.2 Product studies of the ozone initiated oxidation of vinyl ethers

As described in Chapter 2, two types of experiments were conducted for the product studies on the reactions of ozone with PVE and BVE, i.e. i) in the presence of an OH radical scavenger, cyclohexane, and ii) in the presence of an OH radical tracer, 1,3,5-trimethyl-benzene (TMB).

4.2.1 Experimental results

The product studies on the ozone initiated oxidation of PVE and BVE were performed at (298 ± 3) K and (733 ± 4) Torr total pressure of synthetic air. For each reaction at least three experimental runs were performed.

The approximate reactant concentrations were vinyl ether 3.2-6.5 ppm, O_3 1.0-1.8 ppm, cyclohexane 290 ppm and TMB 4.0 ppm.

4.2.1.1 Results for the reaction of ozone with PVE

Figure 4.9, trace (a), shows the product spectrum obtained from the reaction of O_3 with PVE in an excess of cyclohexane used to trap the OH radicals produced in the system. Traces (b) and (c) in Figure 4.9 are reference spectra of PVE and propyl formate, respectively.

In the presence of the OH radical scavenger, the only product that could be positively identified was propyl formate. The infrared absorption regions of other products were either saturated by absorptions due to cyclohexane or were subject to strong overlap by absorptions from cyclohexane.

Trace (a) in Figure 4.10 is the residual product spectrum obtained from the ozonolysis of PVE in the presence of TMB after subtraction of the identified products propyl formate, HCHO and CO. Traces (b) and (c) in Figure 4.10 show reference spectra of

hydroxyperoxy methyl formate (HPMF) and formic anhydride (FA), respectively, while trace (d) is the residual spectrum obtained from trace (a) after the subtraction of HPMF and FA. For easier visual comparison spectra (a) and (d) are multiplied by a factor of 5.

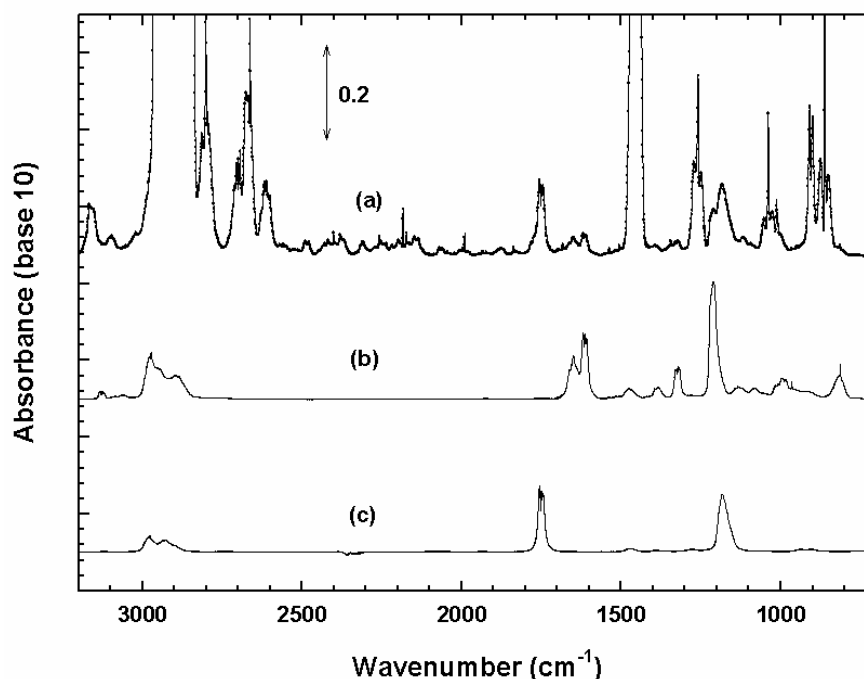


Figure 4.9 Product spectra recorded during the ozonolysis of PVE in the presence of excess cyclohexane: (a) spectrum recorded after reaction of O₃ with PVE; (b) scaled reference spectrum of PVE; (c) scaled reference spectrum of propyl formate.

Figure 4.11 gives the concentration-time profiles of PVE and the identified products from a typical experiment performed in the presence of the OH radical tracer TMB. It can be seen that propyl formate is the major product in the ozone reaction with PVE. Figure 4.12 shows examples of the concentration of propyl formate formed i) in the presence of the OH radical scavenger and ii) in the presence of the OH radical tracer, plotted as a function of the reacted PVE. The data points for the propyl formate formation measured in the presence of the OH radical scavenger have been offset by 0.3 ppm in Figure 4.12 for clarity.

From the slopes of the linear regression lines in Figure 4.12 molar yields for propyl

formate formation of $(88.3 \pm 9.3)\%$ in the presence of the OH scavenger and $(89.7 \pm 9.9)\%$ in the presence of the OH radical tracer are obtained. Since both yields are in excellent agreement it is preferred to quote a value of $(89.0 \pm 11.4)\%$ for the yield of propyl formate, which is an average of the two determinations with error limits which encompass the extremes of both determinations.

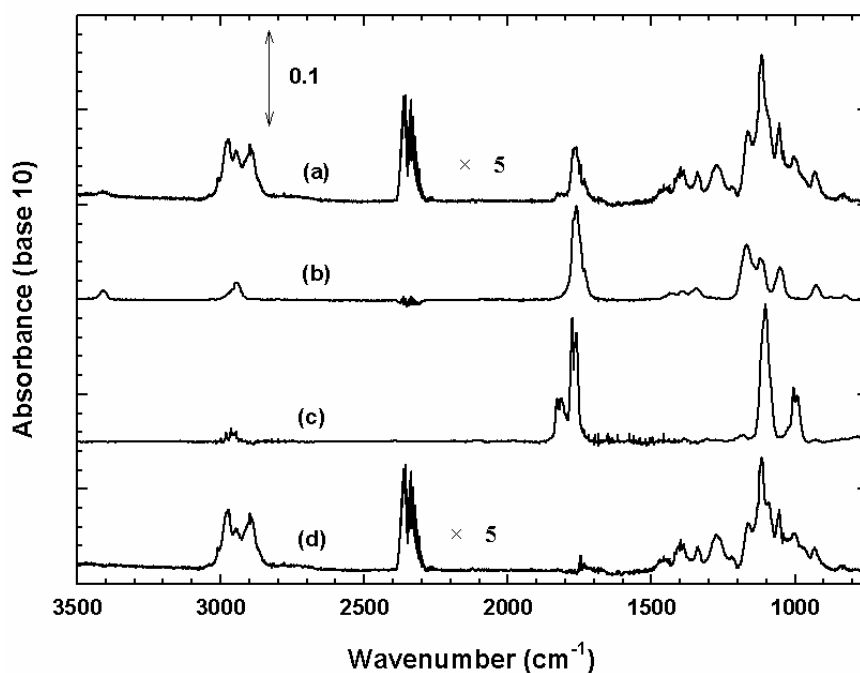


Figure 4.10 Product spectra obtained for the reaction of ozone with PVE in the presence of an OH radical tracer: (a) product spectrum after subtraction of the products propyl formate, HCHO and CO; (b) scaled reference spectrum of hydroxyperoxy methyl formate (HPMF); (c) scaled reference spectrum of formic anhydride (FA); (d) spectrum (a) after subtraction of (b) and (c). For easier comparison (a) and (d) are multiplied by a factor of 5.

Figure 4.13 presents a plot of the concentrations of the other products identified in the ozonolysis of PVE versus the amount of consumed PVE for a typical experiment performed in the presence of the OH radical tracer. Formaldehyde and CO could be measured and were formed in significant yields with values (corrected for reaction with OH radicals) of (12.9 ± 4.0) and (10.9 ± 2.6) molar %, respectively. Formaldehyde and CO are thought to stem entirely from the ozonolysis of PVE since they have not been observed as products in the reaction of the OH radical with TMB [102-104].

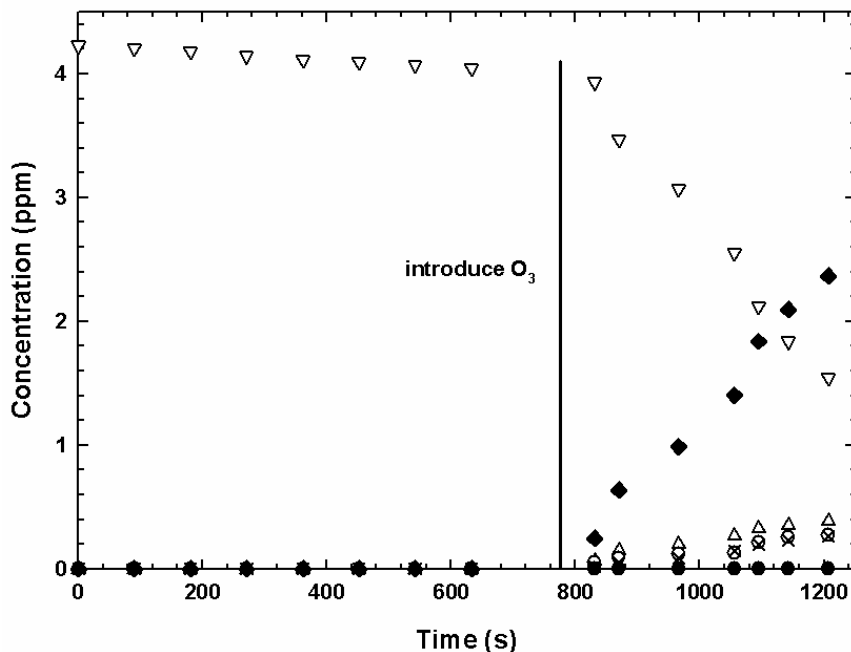


Figure 4.11 Concentration-time profiles of PVE and identified products from the ozone initiated oxidation of PVE: (∇)-PVE; (Δ)-HCHO; (\times)-CO ; (\blacklozenge)-propyl formate; (\bullet)-FA; (\circ)-HPMF.

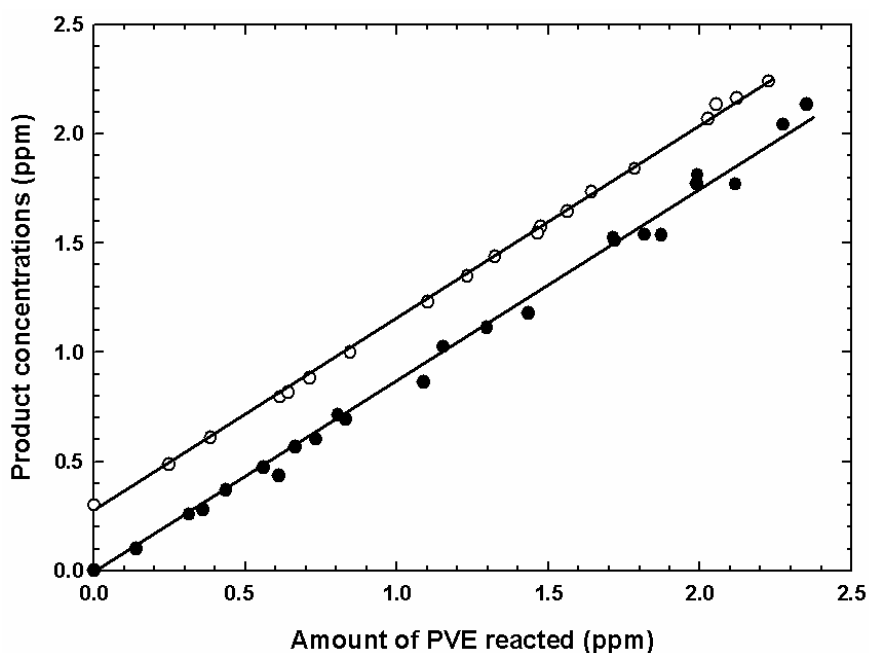


Figure 4.12 Plots of the measured product concentrations of propyl formate as a function of the amount of PVE reacted with ozone. (\circ)-propyl formate produced in the presence of the OH radical scavenger; (\bullet)-propyl formate produced in the presence of the OH radical tracer. The propyl formate concentration measured in the presence of the OH radical scavenger is offset by 0.3 ppm.

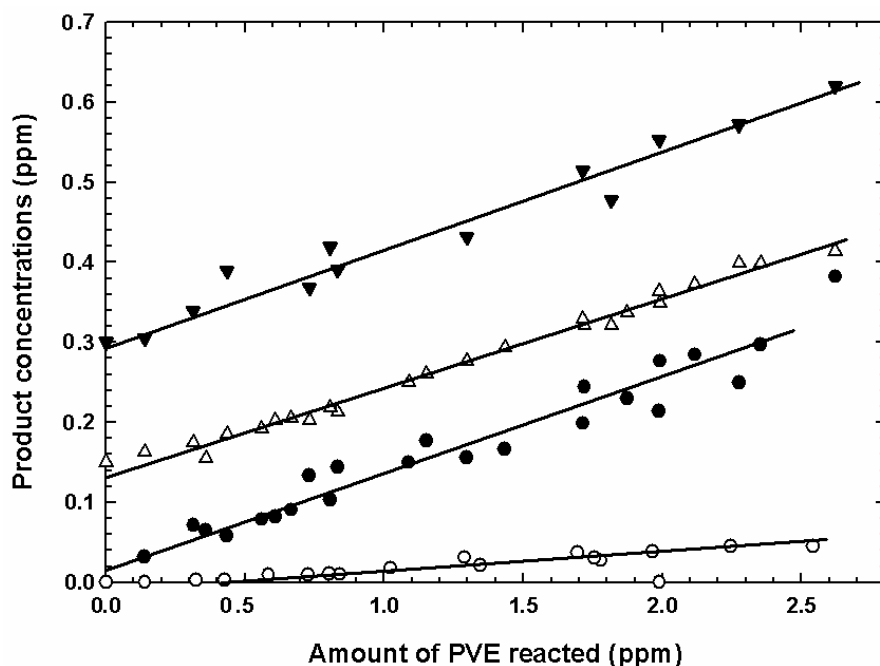


Figure 4.13 Plots of the measured product concentrations as a function of the amount of PVE reacted with ozone from experiments performed in the presence of an OH tracer. (\blacktriangledown)-HPMF; (Δ)-CO; (\bullet)-HCHO; (\circ)-FA. The concentrations of CO and HPMF are offset by 0.15 ppm and 0.3 ppm respectively.

From Figure 4.13 a molar yield of $(13.0 \pm 3.4)\%$ has been determined for HPMF. Formation of FA was only observed after the formation of HPMF and its yield was very low $(1.94 \pm 0.59)\%$.

4.2.1.2 Results for the reaction of ozone with BVE

The product studies on the ozonolysis of BVE were conducted exactly in the same manner as those on the ozone reaction with PVE.

Figure 4.14, trace (a), is the product spectrum obtained from the reaction of O_3 with BVE performed in an excess of cyclohexane to trap the OH radicals produced in the system. Traces (b) and (c) in Figure 4.14 show reference spectra of BVE and butyl formate, respectively.

As in the ozonolysis of PVE, in the presence of an OH radical scavenger the only

product that could be positively identified was an alkyl formate, i.e. butyl formate in the case of BVE. The infrared absorption regions of other products were either saturated or strongly overlapped by cyclohexane absorptions.

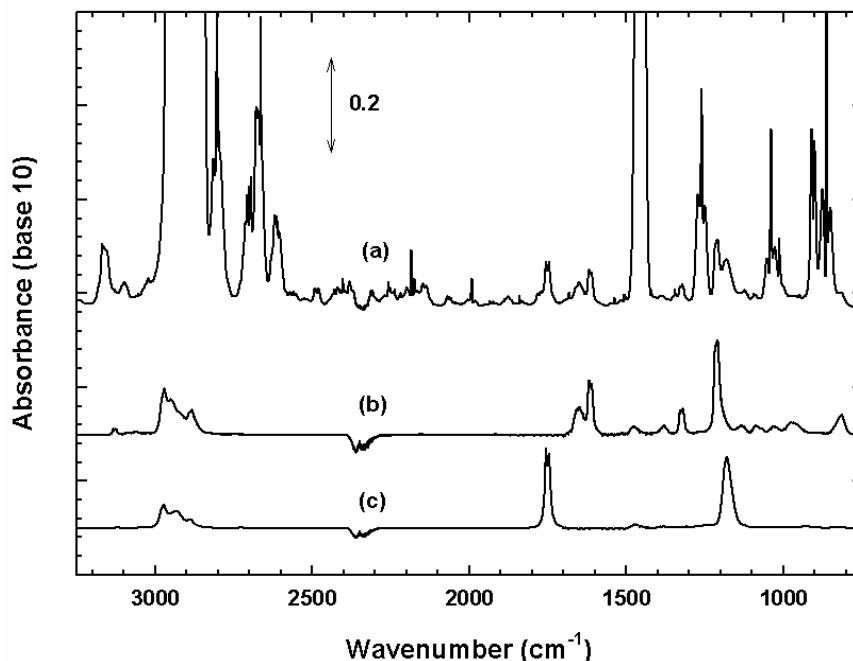


Figure 4.14 Product spectra recorded during the ozonolysis of BVE in the presence of excess cyclohexane: (a) reaction mixture spectrum; (b) scaled reference spectrum of BVE; (c) scaled reference spectrum of butyl formate.

Trace (a) in Figure 4.15 is the residual product spectrum obtained from the ozonolysis of BVE in the presence of the OH radical tracer TMB after subtraction of the identified products: butyl formate, HCHO and CO. Traces (b) and (c) in Figure 4.15 are again reference spectra of HPMF and FA, respectively, while trace (d) is the residual spectrum obtained from trace (a) after the subtraction of HPMF and FA.

The concentration-time profile of the reactants and the products identified in a typical experiment on the ozonolysis of BVE are shown in Figure 4.16. It is obvious that butyl formate is the major product in the ozone reaction with BVE.

Figure 4.17 presents plots of the amount of butyl formate formed i) in the presence of an OH scavenger and ii) in the presence of the OH tracer, versus the amount of reacted BVE. The data points for butyl formate measured in the presence of the OH scavenger have been offset by 0.3 ppm in Figure 4.17 for clarity. From the slopes of

the linear regression lines molar yields for butyl formate formation of $(78.5 \pm 8.8)\%$ and $(76.7 \pm 8.9)\%$ have been obtained in the presence of the OH scavenger and the OH radical tracer, respectively. Since both yields are in good agreement it is preferred to quote a value of $(77.6 \pm 9.8)\%$ for the yield of butyl formate, which is again an average of the two determinations with error limits which encompass the extremes of both determinations.

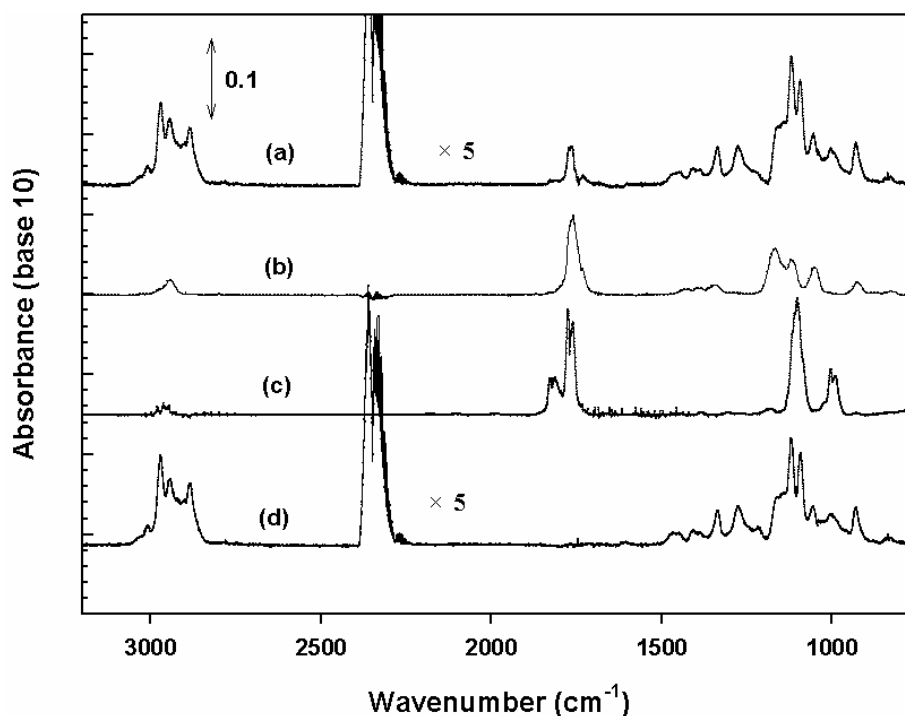


Figure 4.15 Product spectra from an experiment on the reaction of ozone with BVE in the presence of an OH radical tracer: (a) residual product spectrum after subtraction of butyl formate, HCHO and CO; (b) scaled reference spectrum of hydroxyperoxy methyl formate (HPMF); (c) scaled reference spectrum of formic anhydride (FA); (d) spectrum (a) after subtraction of (b) and (c). For easier comparison (a) and (d) is multiplied by a factor of 5.

Figure 4.18 shows plots of the concentrations of the other quantified products versus the amount of consumed BVE for an ozonolysis experiment performed with the OH radical tracer. Formaldehyde, CO, HPMF and FA could be quantified and were formed with molar yields of $(10.5 \pm 1.8)\%$, $(8.2 \pm 1.3)\%$, $(12.0 \pm 2.9)\%$ and $(2.6 \pm 0.54)\%$, respectively. FA was again observed after the formation of HPMF.

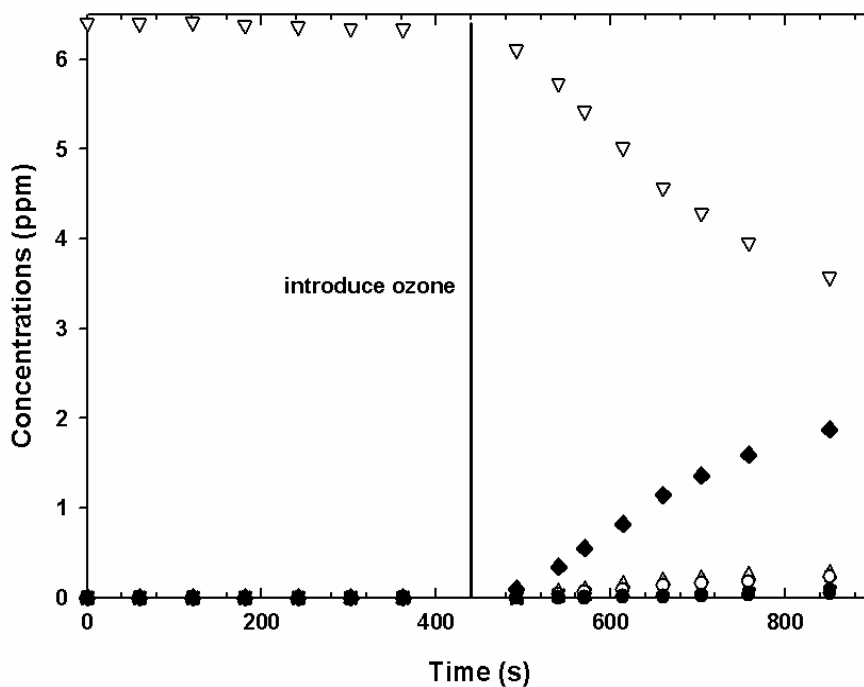


Figure 4.16 Concentration-time profiles of reactants and products for the ozone initiated oxidation of BVE: (∇)-BVE; (Δ)-HCHO; (\times)-CO ; (\blacklozenge)-butyl formate; (\bullet)-FA; (\circ)-HPMF.

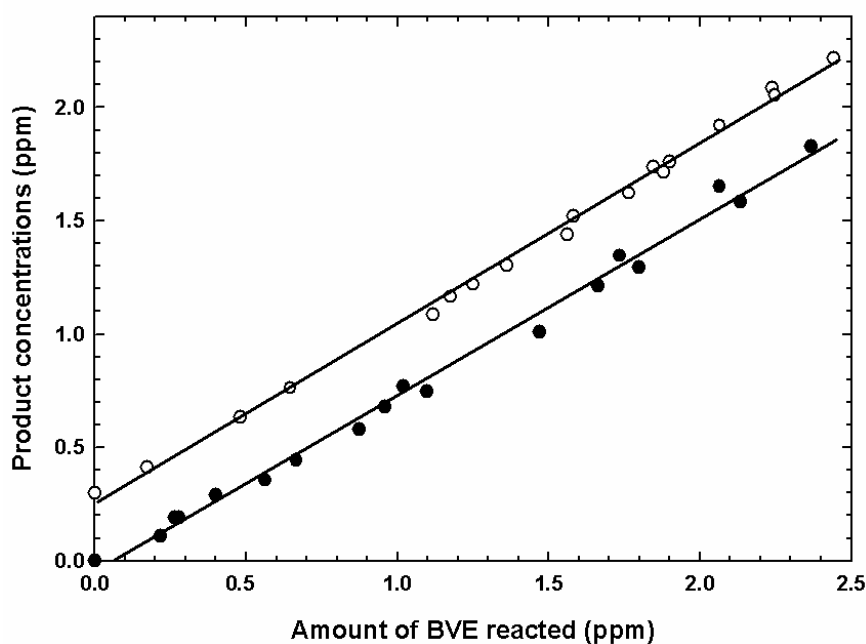


Figure 4.17 Plots of the measured butyl formate concentrations as function of the amount of BVE reacted with ozone. (\circ) n-butyl formate produced in the presence of the OH radical scavenger; (\bullet) n-butyl formate produced in the presence of the OH radical tracer. The n-butyl formate concentration measured in the presence of the OH scavenger is offset by 0.3ppm.

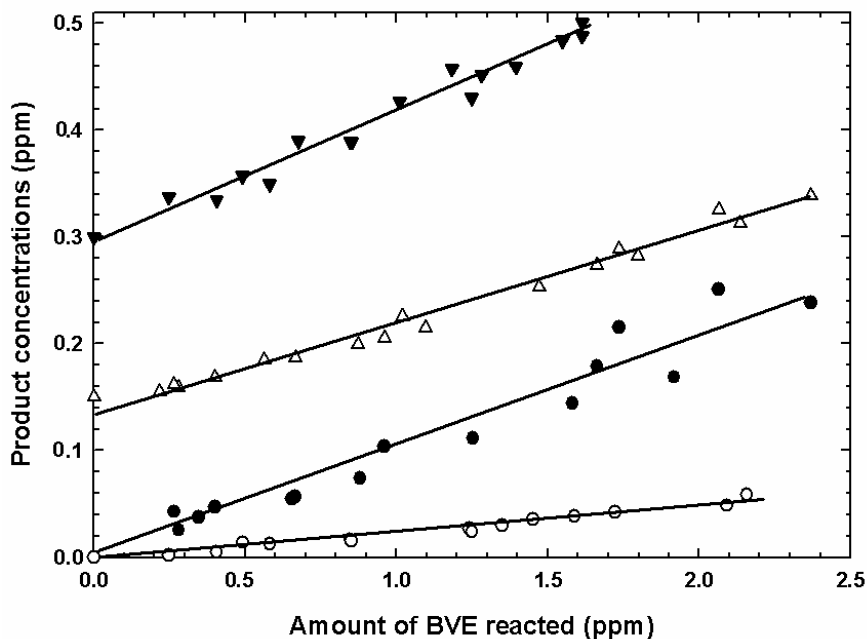


Figure 4.18 Plots of the measured product concentrations as a function of the amount of BVE reacted with ozone for experiments performed in the presence of the OH tracer. (\blacktriangledown)-HPMF; (Δ)-CO; (\bullet)-HCHO; (\circ)-FA. The concentrations of CO and HPMF are offset by 0.15 ppm and 0.3 ppm, respectively.

4.2.2 Discussion on the ozone reactions

The products identified in the ozonolysis of PVE and BVE presented above account for 81.9% and 70.2% of reacted carbon, respectively.

The yields of the products for the reaction of O_3 with PVE and BVE are listed in Table 4.2 where they are compared with the results from product studies on the ozonolysis of alkyl vinyl ethers. From Table 4.2 it can be seen that the yields of the formates and formaldehyde determined within this study for the vinyl ethers fall within the ranges (75 ± 15) and (20 ± 10) molar %, respectively. The values reported by Klotz *et al.* [52] for MVE, Mellouki [51] for EVE and Barnes *et al.* [48] for iBVE, tBVE and EPE also fall within these ranges.

The formate and HCHO yields for the reactions of ozone with EVE and EPE reported by Grosjean and Grosjean [29] do not fall within these ranges, the formate yields are much lower (factor of 2) and the HCHO yields much higher (factor of 2 or more) than those measured in this work and reported by other authors.

Table 4.2 Comparison of the product yields reported in the literature for the ozonolysis of alkyl vinyl ethers

| Vinyl ether | Formate yield (molar %) | HCHO yield (molar %) | HPMF yield (molar %) | CO yield (molar %) | FA yield (molar %) | Reference |
|---|-------------------------|-------------------------|----------------------|--------------------|--------------------|-----------------------------|
| MVE, CH ₃ OCH=CH ₂ | 73.5±7.5 | 27.8±6.6 | 19.6±6.2 | 14.2±1.5 | | Klotz <i>et al.</i> [52] |
| EVE, C ₂ H ₅ OCH=CH ₂ | 87±6 | 19±4 | - | - | | Thiault [50,51] |
| | 86.5 | 21 | 20.5 | 11.2 | | Barnes <i>et al.</i> [48] |
| | >38.8 ⁱ⁾ | 48.7±5.2 | - | - | | Grosjean <i>et al.</i> [29] |
| | 80±8 | 46±7 | - | - | | Grosjean <i>et al.</i> [58] |
| PVE, n-C ₃ H ₇ OCH=CH ₂ | 89.0±11.4 | 12.9±4.0 | 13±3.4 | 10.9±2.6 | 1.94±0.59 | This work |
| | 60±8 | 40±4 | | | | Al Mulla [55] |
| BVE, n-C ₄ H ₉ OCH=CH ₂ | 77.6±9.8 | 10.5 ±1.8 | 12.0±2.9 | 8.2±1.3 | 2.6±0.54 | This work |
| | 59±8 | 41±6 | | | | Al Mulla [55] |
| iBVE, i-C ₄ H ₉ OCH=CH ₂ | 81.1±11.2 | 11.9±5.0 | 14.2±4.4 | 9.4±2.2 | 2.5±0.54 | Barnes <i>et al.</i> [48] |
| | 55±6 | 38±6 | | | | Al Mulla [55] |
| tBVE, t-C ₄ H ₉ OCH=CH ₂ | 65.9±8.9 | 11.5±3.4 | 11.8 | 7.4 | 1.5±0.4 | Barnes <i>et al.</i> [48] |
| | 68±8 | 32±4 | | | | Al Mulla [55] |
| EPE, C ₂ H ₅ OCH=CHCH ₃ | 83.1 | 11.7 ⁱⁱ⁾ | - | 13.3 | | Barnes <i>et al.</i> [48] |
| | >43.3 ⁱ⁾ | 35.3±1.4 ⁱⁱ⁾ | | | | Grosjean <i>et al.</i> [29] |

i) lower limit; ii) this yield refers to acetaldehyde formation from the split of the propenyl bond; formation of HCHO was also observed

Grosjean and Grosjean [29] collected their samples on C₁₈ cartridges coated with 2,4-dinitrophenylhydrazine (DNPH) and analyzed them by liquid chromatography with UV detection. Although they reported that their formate yields were probably lower limits due to difficulties with the analysis this can not explain the difference in the HCHO yields. The yields reported by other authors in Table 4.2 were determined using mainly *in situ* long path FTIR and well established infrared cross sections for HCHO and the formates. The consistency of the FTIR data obtained with the different experimental systems would tend to suggest that the method employed by Grosjean and Grosjean [29] to study the ozonolysis products of EVE and EPE is in some way flawed, at least as far as the analysis of the ozonolysis products from these particular compounds is concerned.

Al Mulla [55] has used FTIR to measure product formation yields for the reactions of ozone with a series of vinyl ethers. The yields were not measured directly; gas samples from a photoreactor were expanded into an evacuated long path multi-reflection cell mounted in the sample compartment of the spectrometer and spectra were recorded at a resolution of 4 cm⁻¹. The product yields reported by Al Mulla [55] for EVE are in good agreement with those determined by Barnes *et al.* [48] and Thiault [50]. For tBVE the formate yield reported by Al Mulla [55] is in excellent agreement with the yield determined by Barnes *et al.* [48] but his formaldehyde yield is over a factor of 3 times higher. For the other vinyl ethers studied by Al Mulla [55], i.e. PVE, BVE and iBVE, the reported formate yields are approximately 30% lower than other determinations and the formaldehyde yields are between factors of 3 to 4 higher. At present the reason for these discrepancies are not clear. The sampling system used by Al Mulla [55] could give rise to sampling artifacts which would influence the product yields; however, until more information on the work of Al Mulla [55] becomes available this is merely speculation.

HPMF has been detected previously in the ozonolysis of MVE [52], iBVE, tBVE and EPE [48]. The yields determined here for HPMF formation in the reactions of O₃ with PVE and BVE are very similar to those measured for the reactions of O₃ with iBVE and tBVE but a little lower than the values of approximately 20% reported for MVE and EPE.

FA is a decomposition product of HPMF; observation of its formation in the decomposition of HPMF has been reported previously in the literature [52,105].

Formation of formic acid (HCOOH), an expected product of the ozonolysis of PVE

and BVE, was not observed in the present product studies. Klotz *et al.* [52] reported very low yields (0.75 ± 0.13)% of formic acid in their study on the ozonolysis of MVE. From the known reactions of the Criegee biradicals [105] formation of formic acid would be expected either by the decomposition of excited Criegee biradicals or the reaction of stable Criegee biradical with water. Klotz *et al.* [52] attributed the low formic acid yield in ozonolysis of MVE to the known fast reaction of formic acid with Criegee biradicals to produce HPMF [52]. It is assumed that this is also the case in this study on the ozonolysis of PVE and BVE and that the concentration of formic acid remains below the detection sensitivity of the FTIR set-up employed for the investigations.

Carbon monoxide yields have been reported for the ozonolysis of MVE [52], EVE, EPE, iBVE and tBVE [48], the measured yields are very similar to those determined here for the ozonolysis of PVE and BVE.

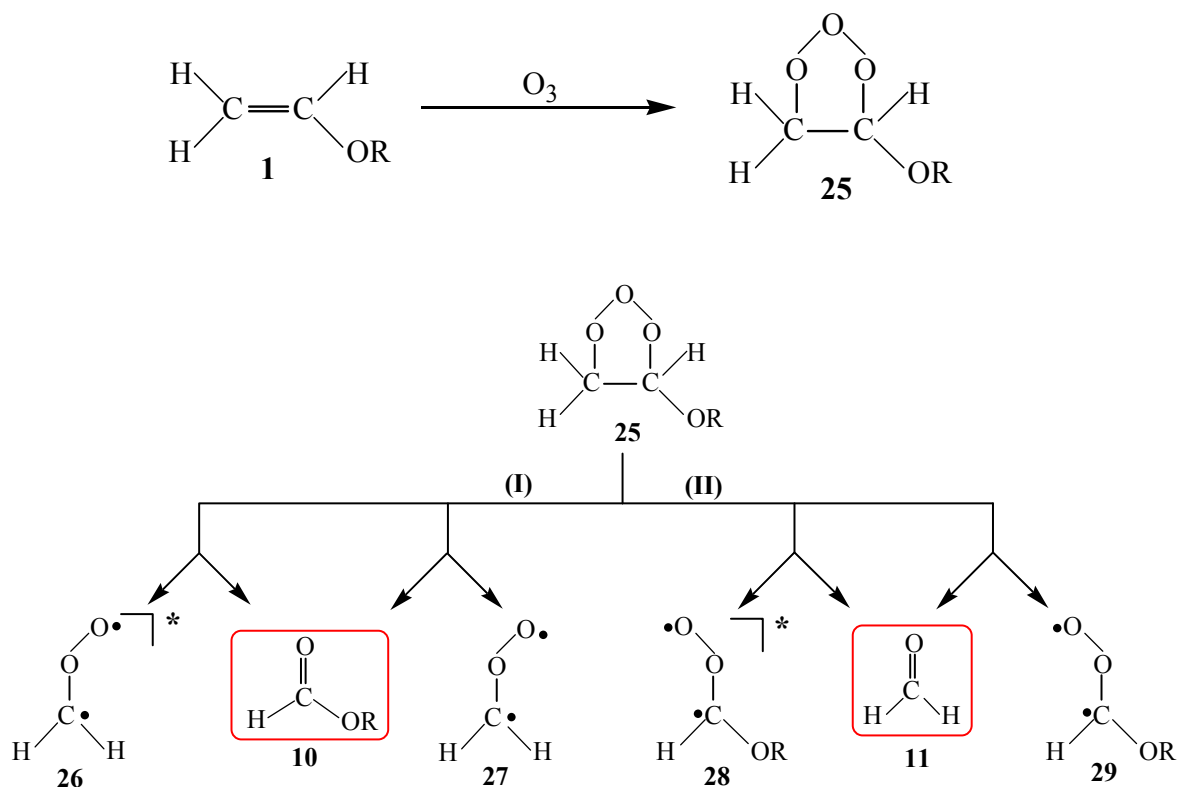
In the OH tracer type of experiment averaged OH radical concentrations of $(1.3 \pm 0.38) \times 10^6$ and $(2.5 \pm 0.72) \times 10^6$ molecules cm^{-3} have been calculated for the ozonolysis of PVE and BVE, respectively. The total concentration of OH radicals formed in the ozonolysis of PVE and BVE can be calculated using the procedures described in Section 2.2.3.3. The OH formation yield is given by the ratio of the total amount of OH radicals formed against the amount of vinyl ethers reacted. Using this procedure OH radical yields of $(17 \pm 9)\%$ and $(18 \pm 9)\%$ have been estimated for the ozonolysis of PVE and BVE, respectively. These yields are similar to that determined for the ozonolysis of MVE [52], where an OH formation yield of $(14 \pm 7)\%$ was found. As not all the possible sinks for the OH radicals can be included in the calculations, the OH formation yields should be considered as lower limits.

There are large discrepancies in the reported OH formation yields for the ozonolysis of alkenes [106,107], and structure activity relationships regarding OH formation in ozonolysis reactions are still unclear. The work from this study and that of Klotz *et al.* [52] show that the ozonolysis of MVE, PVE and BVE result in similar OH radical yields. The yields are also similar to that found for the ozonolysis of ethene. It would, therefore, appear that the OH formation yield in the ozonolysis of alkyl vinyl ethers is comparatively independent of the nature of the alkoxy group.

As for other carbon-carbon double bond containing compounds, the reaction of O₃ with alkyl vinyl ethers is initiated by addition of O₃ to the double bond in the vinyl ether ($\text{CH}_2=\text{CHOR}$, where R = $-\text{CH}_2\text{CH}_2\text{CH}_3$ for PVE or $-\text{CH}_2\text{CH}_2\text{CH}_2\text{CH}_3$ for BVE)

1.

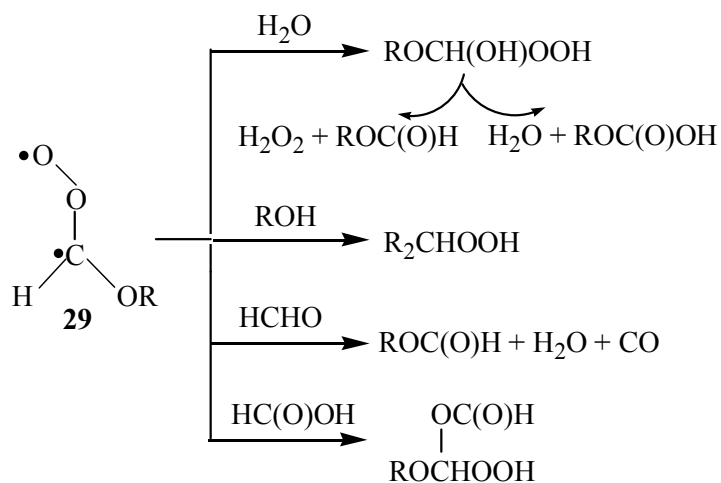
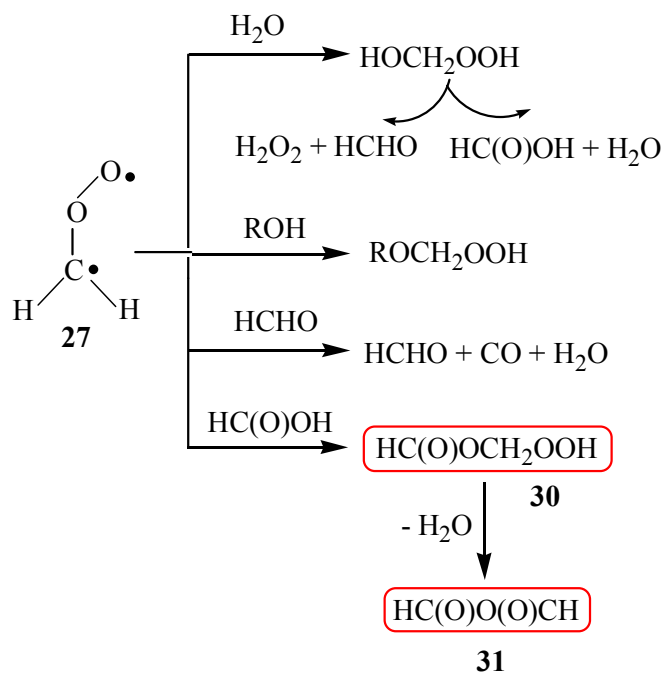
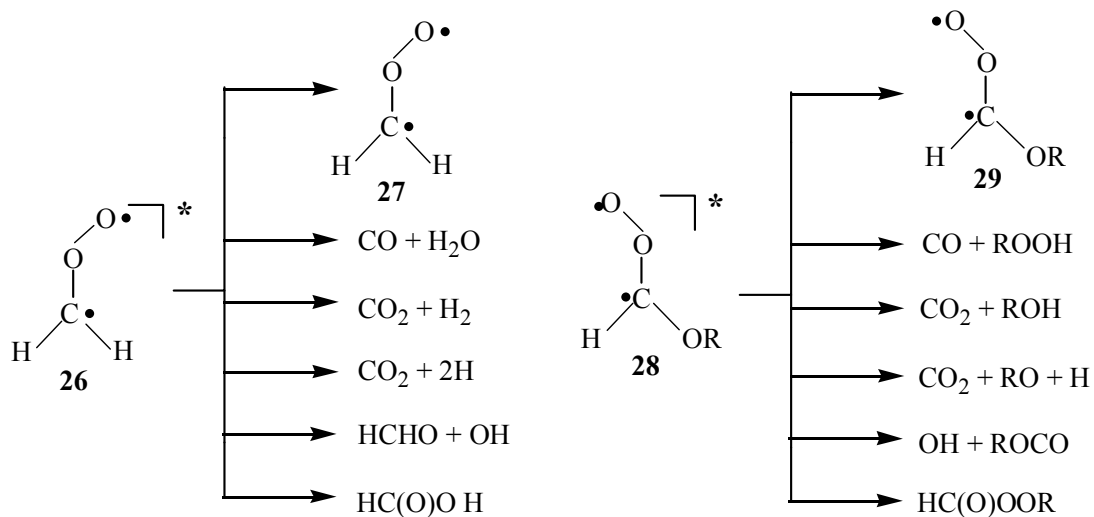
The addition results in the formation of an energy rich primary ozonide **25** which can decompose in two ways (I) and (II). The decomposition can lead to formation of an alkyl formate **10** and the Criegee biradical CH_2OO **26** or **27**, by pathway (I) or formaldehyde **11** and the alkoxy Criegee biradical RO-CHOO **28** or **29**, by pathway (II).



Criegee intermediates **26** and **28** are excited and **27** and **29** are stabilized forms.

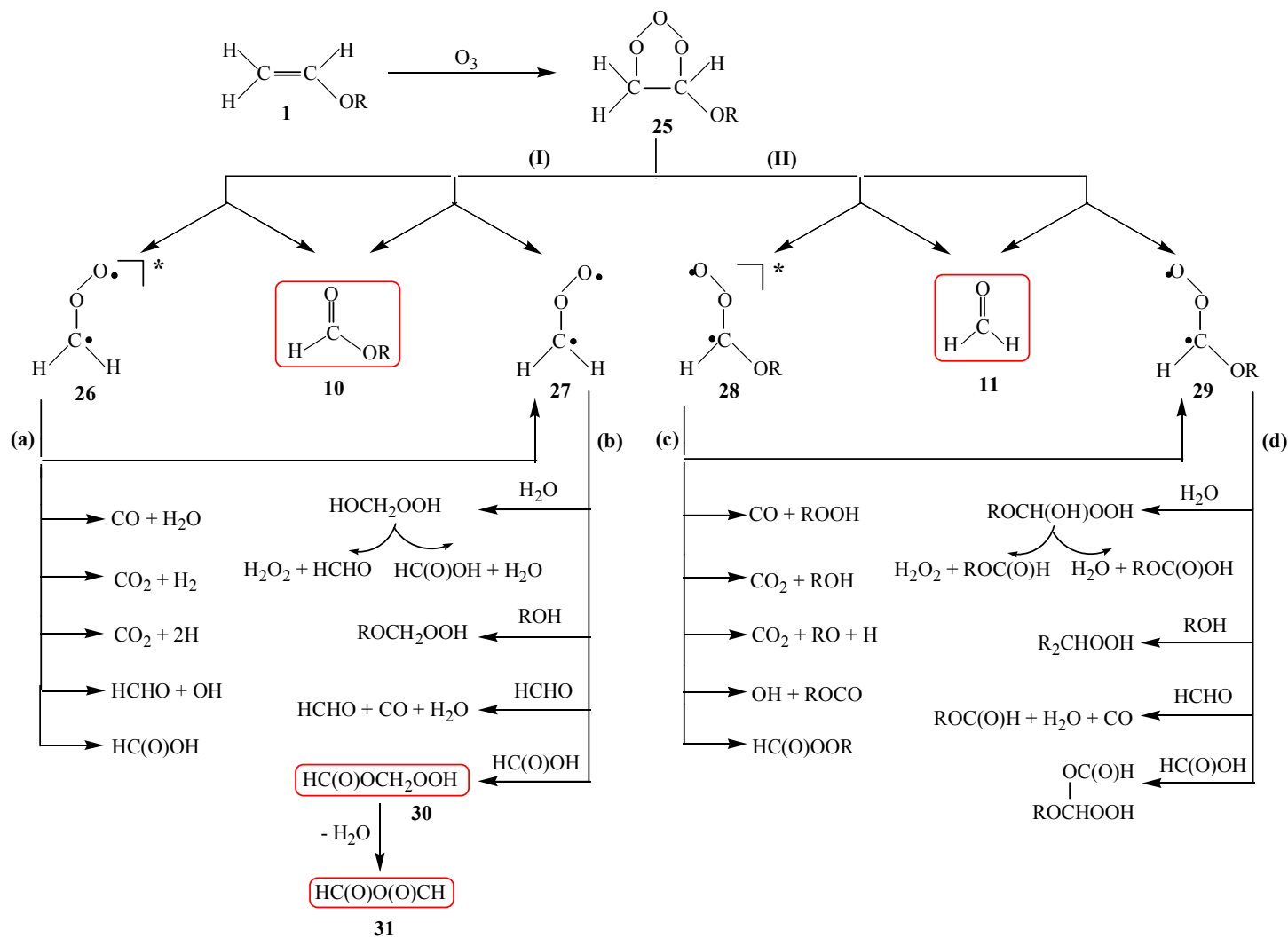
The excited forms **26** and **28** are generally regarded to largely decompose with the formation of the products shown above, while the stabilized Criegees **27** and **29** are thought to react with various components in the system. As discussed above the formation of HPMF **30** is attributed to the reaction of the stable radical **27** with formic acid, which decomposes to give FA **31**.

According to the reaction mechanism shown above (decomposition of excited Criegee biradicals **26** and **28**) and product studies of the reaction of ozone with MVE [52] and terminal alkenes [72] CO_2 will be a product in the ozonolysis of PVE and BVE and will account for some of the unidentified carbon.



Unfortunately due to the presence of CO₂ in the external optics of the FTIR setup used in this work CO₂ could not be quantified. Klotz *et al.* [52], however, have reported a molar CO₂ yield of (30.3±6.0)% for the ozonolysis of MVE, and molar yields of around 20% and 31.9% have been reported for the ozonolysis of EVE and EPE, respectively [48]. Based on the narrow range of the reported yields of the major products from the ozonolysis of vinyl ethers it is assumed that the yields of CO₂ from the ozone reactions with PVE and BVE will be fairly similar to those reported for MVE, EVE and EPE.

Based on the product yields of alkyl formates and HCHO the branching ratios for channels (I) and (II) must be of the order of approximately (89.0±11.4)% and (12.9±4.0)% for ozonolysis of PVE and (77.6±9.8)% and (10.5±1.8)% for that of BVE, respectively, giving a total yield of (101.9±16.9)% and (88.1±13.7)% for the reactions of ozone with PVE and BVE, respectively. Of the products listed in the overall reaction mechanism in Scheme 4.3 it has only been possible to identify and quantify the alkyl formate, HPMF, HCHO, CO and FA (Table 4.2). Trace (d) in Figure 4.10 and Figure 4.15 show typical residual spectra acquired after subtraction of all the identified products from a spectrum obtained from the ozonolysis of PVE and BVE, respectively. The identities of the products giving rise to the absorption bands are presently unclear; potential candidates are shown in a tentative simplified reaction mechanism outlined in Scheme 4.3.



Scheme 4.3 Simplified reaction mechanism for the ozonolysis of vinyl ethers (R=-CH₂CH₂CH₃ for PVE and -CH₂CH₂CH₂CH₃ for BVE)

4.3 Product studies on the NO_3 radical initiated oxidation of vinyl ethers

4.3.1 Experimental results

The product studies on the NO_3 radical initiated oxidation of PVE and BVE were conducted at (298 ± 3) K and (733 ± 4) Torr total pressure of synthetic air. For each reaction at least three experimental runs were performed to test the reproducibility of the results. The approximate vinyl ether concentrations were 5.5 ppm.

4.3.1.1 Results for the reaction of NO_3 with PVE

Figure 4.19, trace (a) shows a typical spectrum obtained upon addition of N_2O_5 to PVE; trace (b) is the residual product spectrum obtained after subtraction of the absorptions due to PVE, propyl formate, formaldehyde, HNO_3 and NO_2 from the spectrum shown in trace (a); trace (c) is the product spectrum obtained from (b) after addition of NO to the reaction mixture.

Figure 4.20 presents the concentration-time profile for the decay of PVE and the formation of products after addition of N_2O_5 to the system. It can be seen from Figure 4.20 that after the addition of N_2O_5 was terminated no further decay of PVE due to reaction with NO_3 was observed. However, the concentrations of formaldehyde and propyl formate were both observed to increase at the same slow rate. On injection of NO there was a fast drop in the PVE concentration accompanied by increases in the concentrations of both HCHO and propyl formate.

Figure 4.21 shows plots of the concentrations of the identified products versus the amount of consumed PVE for a NO_3 experiment. From Figure 4.21 molar formation yields for propyl formate and formaldehyde of $(52.7\pm 5.9)\%$ and $(55.0\pm 6.3)\%$, respectively, have been determined.

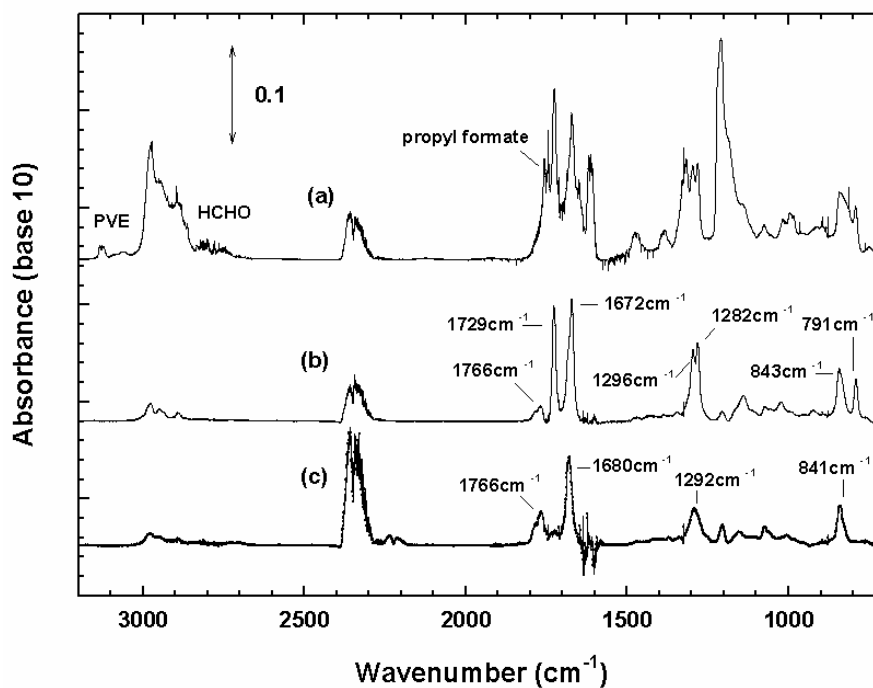


Figure 4.19 Product spectra for the reaction of NO₃ radicals with PVE: (a) reaction mixture spectrum after reaction with NO₃; (b) spectrum (a) after subtraction of all identified organic and inorganic compounds (PVE, HCHO, propyl formate, NO₂, HNO₃, H₂O); (c) spectrum (b) after addition of NO to the reaction system.

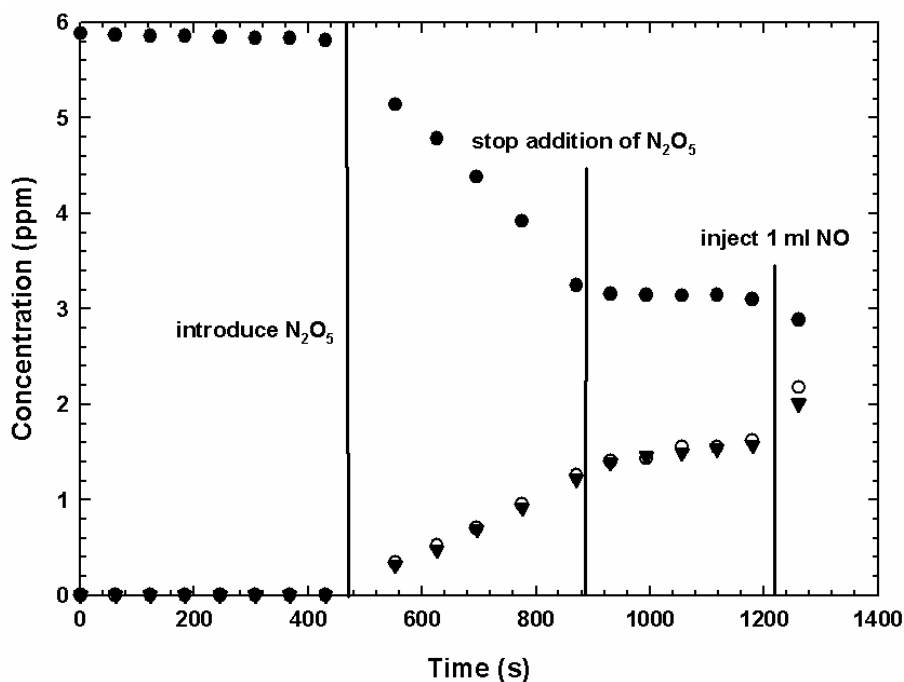


Figure 4.20 Typical concentration-time profiles obtained from an experiment on the NO₃ radical initiated oxidation of PVE: (●)-PVE; (○)-HCHO; (▼)-propyl formate.

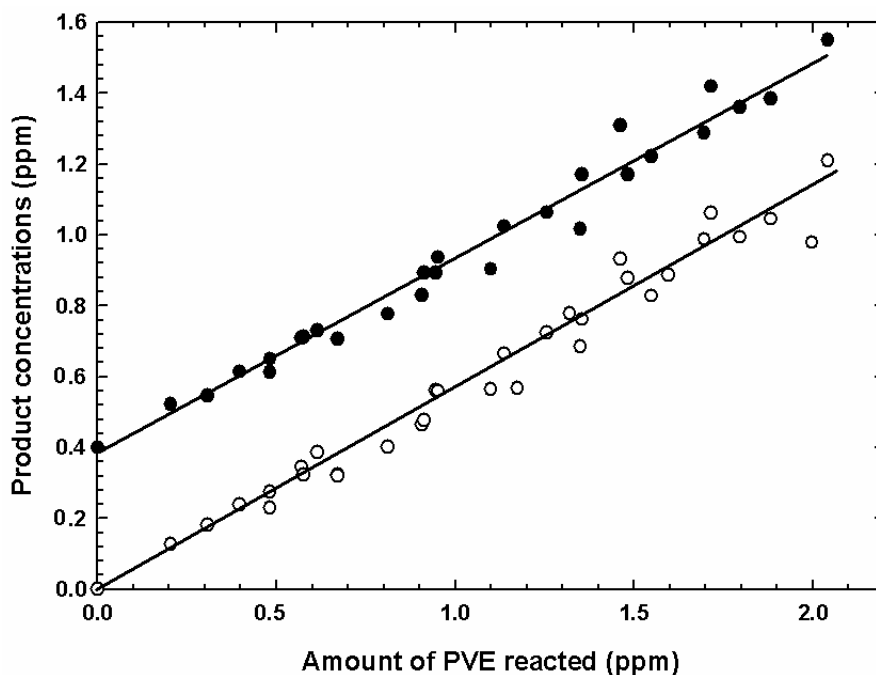


Figure 4.21 Plots of the measured product concentrations as function of the amount of PVE reacted with NO_3 radicals: (●)-propyl formate; (○)-HCHO. For clarity the propyl formate concentration is offset by 0.4ppm.

4.3.1.2 Results for the reaction of NO_3 with BVE

Figure 4.22, trace (a), shows a typical spectrum obtained upon addition of N_2O_5 to BVE in air; trace (b) is the residual product spectrum obtained after subtraction of the absorptions due to butyl formate, formaldehyde, HNO_3 and NO_2 from the spectrum shown in trace (a); trace (c) is the product spectrum obtained from (b) after addition of NO to the reaction mixture.

Figure 4.23 gives the concentration-time profiles for BVE and the identified products in the NO_3 initiated oxidation of BVE. As was observed in the PVE reaction after the addition of N_2O_5 was terminated no further decay of BVE was observed. However, the concentrations of formaldehyde and butyl formate both showed a slow increase. After injection of NO into the reaction system there was a sharp drop in the concentration of BVE decayed and a fast elevation in the concentrations of both HCHO and butyl formate.

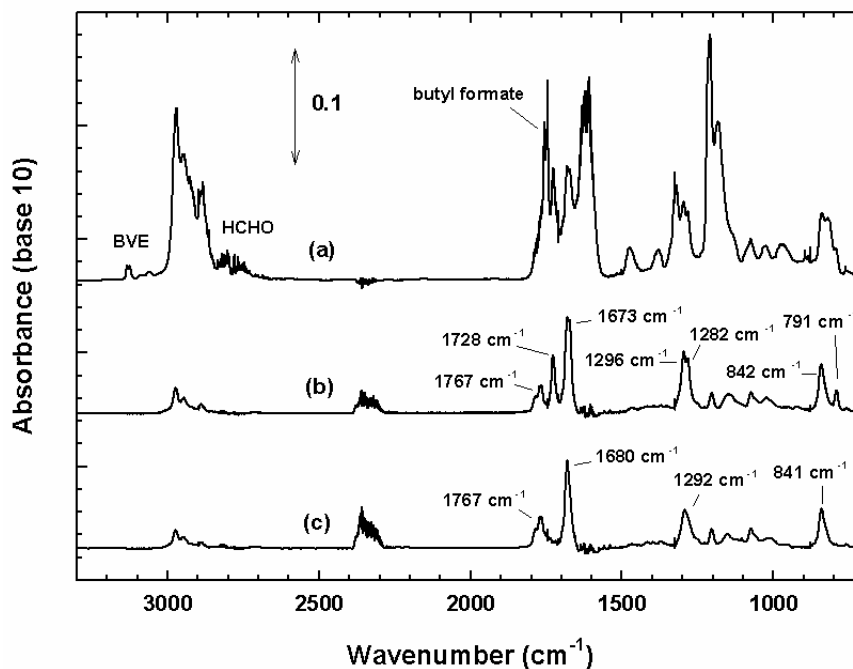


Figure 4.22 Product spectra for the reaction of NO₃ radical with BVE: (a) spectrum after addition of N₂O₅ to BVE in air; (b) spectrum (a) after subtraction of all identified organic and inorganic compounds such as BVE, HCHO, butyl formate, NO₂, HNO₃, H₂O; (c) spectrum (b) after addition of NO to the reaction system.

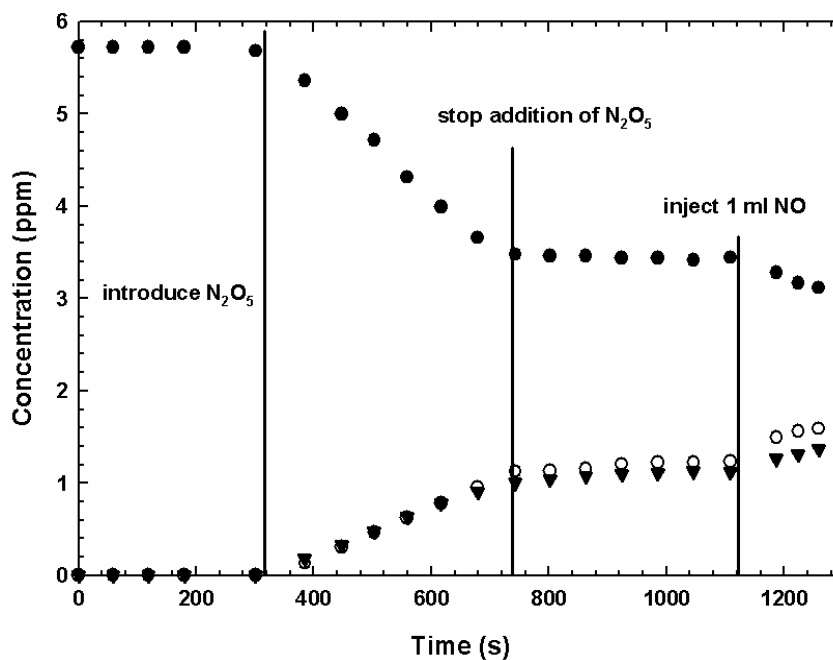


Figure 4.23 Concentration-time profiles obtained from a typical experiment on the NO₃ radical initiated oxidation of BVE: (●)-BVE; (○)-HCHO; (▼)-butyl formate.

Molar formation yields for butyl formate and formaldehyde of $(43.6\pm 4.5)\%$ and $(48.0\pm 5.6)\%$, respectively, have been obtained from the slopes of the linear regression lines in Figure 4.24, where the product concentrations versus the amount of reacted BVE were plotted.

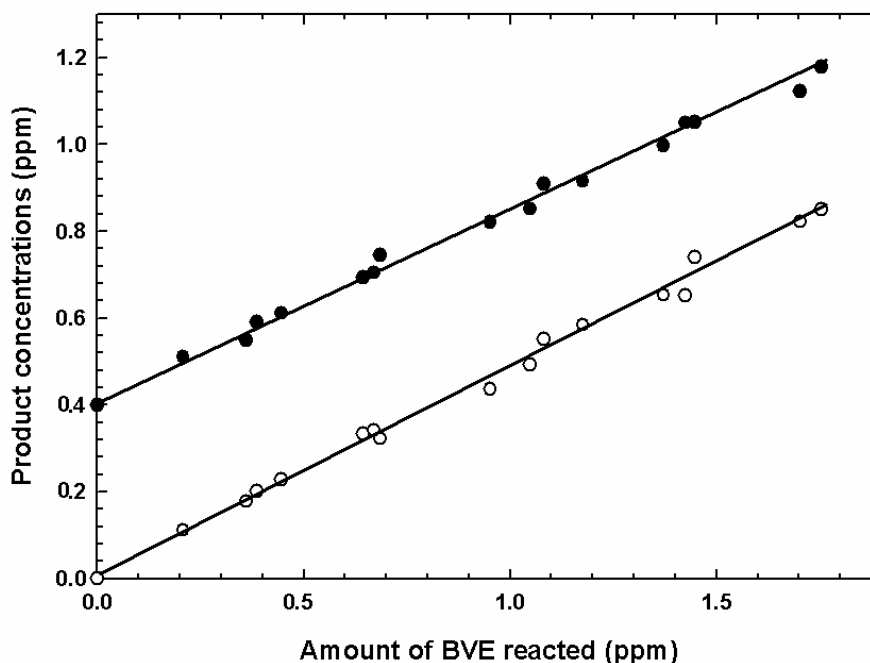


Figure 4.24 Plots of the measured product concentrations as function of the amount of BVE reacted with NO_3 radical: (●)-butyl formate; (○)-HCHO. For clarity the butyl formate concentration is offset by 0.4 ppm.

4.3.2 Discussion on the reactions of the NO_3 radical with vinyl ethers

The formation yields obtained for the formates and formaldehyde for the NO_3 radical initiated oxidation of PVE and BVE are listed in Table 4.3 together with those reported in the literature for the NO_3 radical reaction with alkyl vinyl ethers.

It can be seen from Table 4.3 that the formation of the alkyl formate and HCHO for the different vinyl ethers are both being formed with molar yields within the range of (55 ± 10) molar % with the exception of tBVE and EPE [48], where the formation yield of HCHO for tBVE is much higher than other vinyl ethers and the yields of ethyl formate and formaldehyde for EPE are considerably lower than the corresponding

products from other vinyl ethers. To the best of my knowledge there are no other product studies presently available in the literature with which the results obtained in the present work for PVE and BVE and those determined by Barnes *et al.* [48] for iBVE, tBVE and EPE can be further compared.

Table 4.3 Comparison of the yields of formate (HC(O)OR) and HCHO/CH₃CHO from the reaction of NO₃ radical with vinyl ethers

| Vinyl ether | Formate yield (molar %) | HCHO yield (molar %) | Reference |
|---|-------------------------|----------------------|--|
| MVE, CH ₃ OCH=CH ₂ | 52.5±6.3 57±17 | 51.4±6.2 56±23 | Klotz <i>et al.</i> [52] Scarfogliero <i>et al.</i> [57] |
| EVE, C ₂ H ₅ OCH=CH ₂ | 50.1 60±7 | 52.7 68±13 | Barnes <i>et al.</i> [48] Scarfogliero <i>et al.</i> [57] |
| PVE, n-C ₃ H ₇ OCH=CH ₂ | 52.7±5.9 52±14 | 55.0±6.3 52±14 | This work Scarfogliero <i>et al.</i> [57] |
| BVE, n-C ₄ H ₉ OCH=CH ₂ | 43.6±4.5 52±4 | 48.0±5.6 49±8 | This work Scarfogliero <i>et al.</i> [57] |
| iBVE, i-C ₄ H ₉ OCH=CH ₂ | 47.4±5.0 | 50.2±5.0 | Barnes <i>et al.</i> [48] |
| tBVE, t-C ₄ H ₉ OCH=CH ₂ | 58.8±6.6 | 74.0±8.4 | Barnes <i>et al.</i> [48] |
| EPE, C ₂ H ₅ OCH=CHCH ₃ | 32.2 | 38.3 ⁱ⁾ | Barnes <i>et al.</i> [48] |

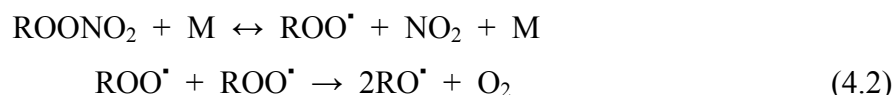
i) acetaldehyde

The absorptions with maximums around 1766, 1729, 1672, 1296, 1282, 843 and 791 cm⁻¹ in Figure 4.19, trace (b), and 1767, 1728, 1673, 1296, 1282, 842 and 791 cm⁻¹ in Figure 4.22, trace (b), are indicative of the formation of different types of organic nitrates such as dinitrates, carbonyl nitrates and peroxy nitrates [108]. Absorption bands around 1729 (-NO₂ asymmetric stretch), 1296 (-NO₂ symmetric stretch) and 791 (-NO₂ deformation) cm⁻¹ are characteristic for peroxy nitrate-type compounds [108,109] while absorptions around 1672, 1296 and 843 cm⁻¹ are characteristic for alkyl nitrates/ dinitrates [108,110]. The absorption band at 1766/1767 cm⁻¹ indicates

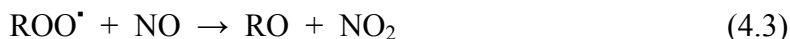
the presence of a carbonyl group in addition to the nitrate group.

As described previously, on leaving the products to stand in the dark no further decay in both PVE and BVE was observed (see Figure 4.20 and Figure 4.23) but the concentrations of the alkyl formates and formaldehyde increased slowly and the intensities of the bands at 1729 and 791 cm^{-1} for $\text{NO}_3 + \text{PVE}$ and 1728 and 791 cm^{-1} for $\text{NO}_3 + \text{BVE}$ decreased faster than those of the other bands. Figures 4.19, trace (c) and 4.22, trace (c), are the product spectra obtained from the respective (b) traces after addition of NO to the reaction mixture. The addition of NO to the reaction mixture resulted in the rapid disappearance of the bands at 1729/1728 and 791 cm^{-1} , changes in the maxima and shapes of the bands at 1672, 1296, 1282 and 843 cm^{-1} for $\text{NO}_3 + \text{PVE}$, 1673, 1296, 1282 and 842 cm^{-1} for $\text{NO}_3 + \text{BVE}$, and increases in the concentrations of the alkyl formate and HCHO.

Thermal instability is a typical characteristic of peroxyxynitrate-type compounds:



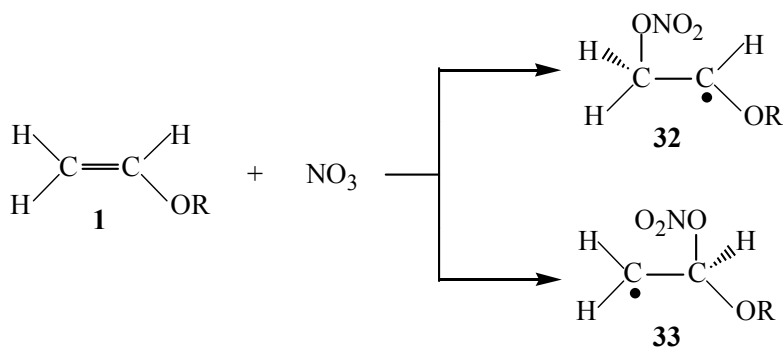
and in the presence of NO, the peroxy radical ROO^\bullet will react rapidly as follows:



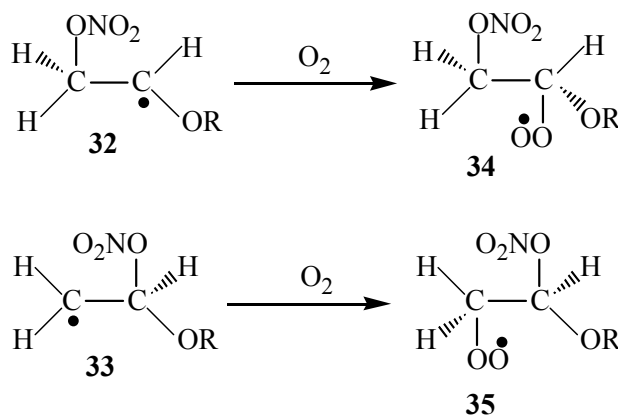
Reaction (4.3) disturbs the equilibrium in reaction (4.2) which leads to a rapid decomposition of the peroxyxynitrates.

The remaining absorptions at around 1766, 1680, 1292 and 841 cm^{-1} in Figure 4.19 trace (c) and Figure 4.22 trace (c) are most probably due to the formation of organic carbonyl nitrate and/or dinitrate compounds.

As with other carbon-carbon double bond containing compounds the NO_3 radical reaction with vinyl ethers mainly proceeds by addition of NO_3 to the double bond (2 possible addition sites) to produce the β -nitrooxyalkyl radicals **32** and **33** [72].



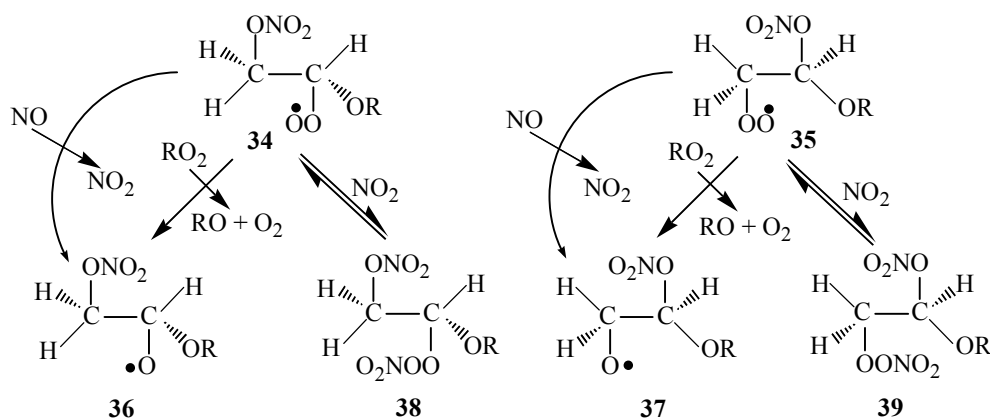
In the presence of O₂ radicals **32** and **33** react with O₂ to form the nitrooxyalkyl-peroxy radicals **34** and **35**, respectively.

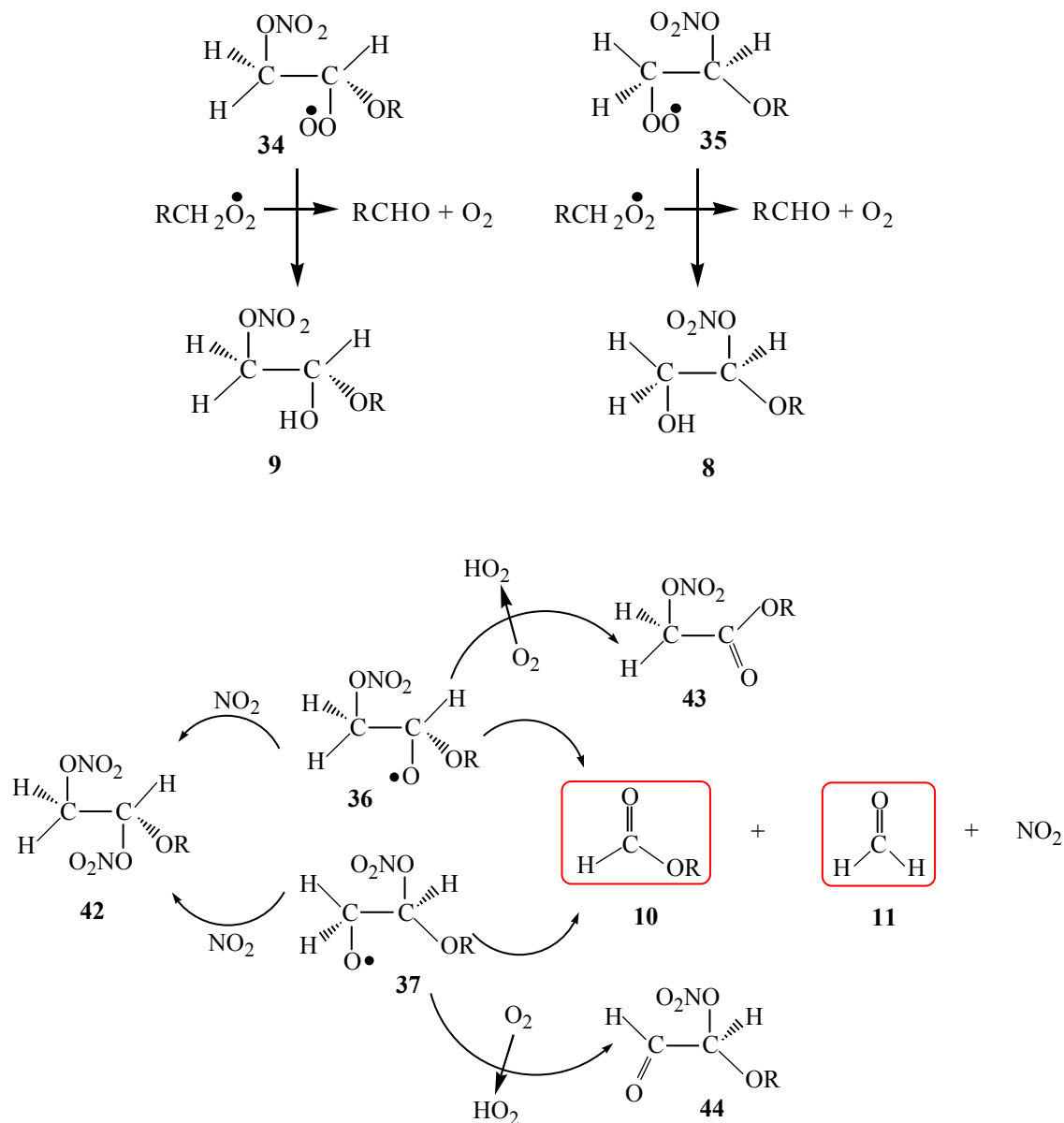


The further reactions of the nitrooxyalkyl-peroxy radicals are either with RO₂ to produce the β-nitrooxy alkoxy radicals **36** and **37**, respectively, or reversibly with NO₂ to form the thermally unstable nitrooxy-peroxy nitrates **38** and **39**, respectively. The strong absorptions in the product spectrum (Figure 4.19, trace (b) and Figure 4.22, trace (b)) at around 1729, 1296 and 791 cm⁻¹ are probably attributable to the peroxy-nitrate-type compounds **38** and **39**. When NO is injected into the reaction system nitrooxy-peroxy radicals **34** and **35** react rapidly with NO to form the nitrooxy-alkoxy radicals **36** and **37**, respectively.

Nitrooxy-peroxy radicals **34** and **35** may also react with RCH₂OO radicals to form the hydroxy nitrates **9** and **8**, respectively.

There are several reaction channels open to β-nitrooxy alkoxy radicals **36** and **37**: i) a carbon-carbon bond scission to give the observed major products propyl formate **10** and formaldehyde **11**; ii) reaction with NO₂ to form a dinitrate **42**; iii) reaction with molecular oxygen to give the corresponding carbonyl nitrates **30** and **31**, respectively.



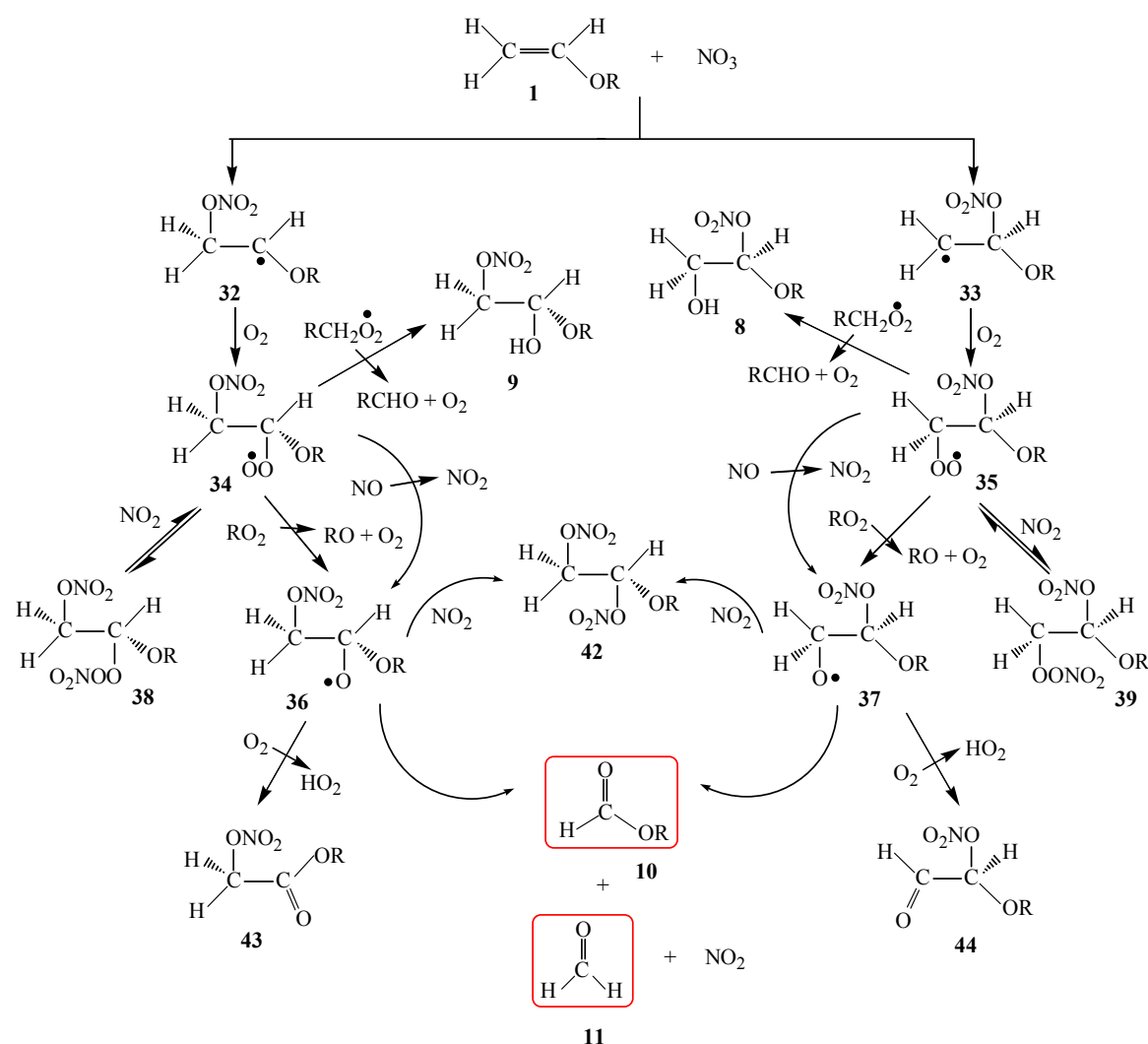


As mentioned above the residual absorptions at around 1766 ($-\text{C}(\text{O})-$ stretch), 1680 ($-\text{NO}_2$ asymmetric stretch), 1292 ($-\text{NO}_2$ symmetric stretch) and 841 (O-N stretch) cm^{-1} in Figure 4.19 trace (c) and Figure 4.22 trace (c) are attributed to a carbonyl nitrate [109], probably mainly the alkyl nitroxyacetate ($\text{ROC}(\text{O})\text{CH}_2(\text{ONO}_2)$) **43**, with possible minor contributions from a dinitrate **42**.

From the formation yields of the alkyl formates and HCHO carbon balances of 53.2% and 44.3% are obtained for the reactions of NO_3 with PVE and BVE, respectively. Based on the analysis of 14 nitrate compounds Barnes *et al.* [109] have estimated an averaged absorption cross section of $\sigma = (6.4 \pm 1.4) \times 10^{-19} \text{ cm}^2 \text{ molecule}^{-1}$ for the $-\text{ONO}_2$ symmetric stretching band located around 1285 cm^{-1} . Using this cross section

total nitrate formation yields of (56.0±12.3)% and (57.1±12.3)% have been estimated for the reactions of NO₃ with PVE and BVE, respectively. Simple addition of the carbon balance yields and the estimated nitrate yields results in values of 109.2% and 101.4% for the overall carbon balance for NO₃ + PVE and NO₃ + BVE, respectively. This would suggest that most unidentified nitrates are probably mono-functional nitrates since the nitrates and carbonyl nitrates **8**, **9**, **43** and **44** shown above contain the same number of carbon atoms as the alkyl vinyl ethers. However, the estimation technique is subject to substantial errors and confirmation using calibrated spectra of the authentic nitrate compounds is desirable.

Scheme 4.4 shows a tentative simplified reaction mechanism for the reaction of NO₃



Scheme 4.4 Simplified reaction mechanism for the NO₃ radical initiated oxidation of an alkyl vinyl ether (R = -CH₂CH₂CH₃ for PVE and R = -CH₂CH₂CH₂CH₃ for BVE).

radicals with alkyl vinyl ether where for PVE $R = -CH_2CH_2CH_3$ and for BVE $R = -CH_2CH_2CH_2CH_3$.

4.4 Atmospheric implications

It is known that the reactions of vinyl ethers with OH radical, ozone and NO_3 radical make a significant contribution to their losses in the troposphere. The product distributions for the OH, ozone and NO_3 initiated oxidation of vinyl ethers in the present investigations were carried out in reaction chambers under simulated atmospheric conditions, which are similar but not identical to those found in the troposphere.

The OH radical reactions performed in the present work were carried out both in the presence of a high level of NO_x and under NO_x -free conditions. Both sets of conditions are not representative for the real troposphere. However, the presence of NO_x does not seem to have a very significant effect on the main product yields; the yields of the alkyl formate and HCHO for the different vinyl ethers are both being formed with molar yields within the range of (70 ± 10) molar % for the NO_x -containing system and (60 ± 10) molar % for the NO_x -free system.

Due to the levels of NO_x presence in the regions of the troposphere in which the vinyl ethers are emitted, it is expected that the organic peroxy radicals will mainly react with NO, not undergo self-reaction or reaction with other RO_2 radicals. In the OH radical initiated oxidation of PVE and BVE in the presence of NO_x about 23% and 36% of carbon still remains unidentified for PVE and BVE, respectively. From a consideration of the radical chemistry it is likely that hydroxyl carbonyls comprise the majority of the missing carbon in the reactions of PVE + OH and BVE + OH in the troposphere with the remainder being made up of multifunctional organic nitrates.

The experiments for the reactions of ozone with the vinyl ethers were carried out under “dry” conditions. However, under the “humid” conditions prevailing in the troposphere, based on the available data, the dominant loss of the thermalized $\cdot CH_2OO\cdot$ Criegee biradical will be reaction with water vapor [111,112] to produce hydroxymethyl hydroperoxide ($HOCH_2OOH$) as shown in channels (b) and (d), Scheme 4.3, while the formation of HPMF will be a minor process.

The NO₃ radical initiated oxidation of vinyl ethers performed in this work were carried out under conditions of high NO₂ concentrations that are not representative of the troposphere. As a result, the formation of the thermally unstable peroxy nitrates and dinitrate observed in this work are not expected to be significant under atmospheric conditions. To derive product formation yields for the NO₃ radical reaction with MVE under atmospheric conditions Klotz *et al.* [52] assumed in their studies that the nitrooxyperoxy radicals behave similarly to their hydroxyl peroxy radical analogues in an NO_x-free system and a branching ratio of 0.33:0.67 for the molecular versus the peroxy radical formation channels of RO₂+RO₂ [55,113] reaction shown in Scheme 4.4. If the same assumption is made in the present work the following formation yields can be estimated for the reaction of NO₃ with PVE under tropospheric conditions: propyl formate and HCHO 62.2%, hydroxyl nitrates 16%, carbonyl nitrates 21.8%. Similarly, for the reaction of NO₃ with BVE: butyl formate and HCHO 55.5%, hydroxyl nitrates 16%, carbonyl nitrates 28.5%.

The OH radical, ozone and NO₃ radical initiated oxidation of alkyl vinyl ethers leads to the formation of carbonyl compounds, alkyl formates and formaldehyde as demonstrated in the present work. As shown in the kinetic studies, these short-lived vinyl ethers, based purely on the tropospheric lifetimes can have atmospheric impacts on local and regional scales, however, the atmospheric impacts are not only be determined solely by the persistence of these unsaturated ethers but also by the fate of their oxidation products. HCHO will be removed by photolysis or by reaction with OH radicals and has a lifetime of less than a day; therefore its effect will remain local. The formates, on the other hand, will be oxidized mainly by reaction with OH radicals leading to formic acid and acetic formic anhydride which are highly soluble and can be rapidly incorporated into cloud droplets. Formates have lifetimes ranging from 3 days to 2 months [48], therefore, the formation of formates from the oxidation of vinyl ethers, if used on a large industrial scale, could lead to atmospheric acidification on an extensive tropospheric scale.

As discussed in Chapter 2 an acid catalyzed hydrolysis of the vinyl ethers on the glass walls of the chambers was observed. This is very likely also to occur on acidic surfaces in the atmosphere. An assessment of the atmospheric relevance/importance of this phenomenon requires further investigation.

Chapter 5

Exploratory Studies on Secondary Organic Aerosol Formation in Ozonolysis of Alkyl Vinyl Ethers

Secondary organic aerosol (SOA) is ubiquitous in the atmosphere, being present in both urban and remote locations. SOA is formed when a parent volatile organic compound is oxidized to form semi-volatile organic products with sufficiently low vapor pressures so that the products undergo absorptive partitioning between the gas and particle phases.

In 2001 the Intergovernmental Panel on Climate Change [114] estimated global biogenically derived SOA to be in the range of 8-40 Tg/yr, while SOA from anthropogenic precursors was estimated to be in the range from 0.3 to 1.8 Tg/yr. As urban areas continue to grow the interaction between their emissions and those from the rural biosphere is of increased importance.

After Klotz *et al.* [52] reported SOA formation from the ozonolysis of MVE, the smallest compound studied that produces aerosol during its atmospheric degradation, Sadezky *et al.* [64] investigated the SOA formation from the gas-phase reactions of ozone with a series of alkyl vinyl ethers and observed formation of oligomers in the SOA. The mechanism of the formation of the oligomers is so far unknown but is thought to involve reaction of the Criegee biradicals formed in the ozonolysis of the vinyl ethers with the double bond of the compounds. The observed aerosol profiles in

both studies showed typical behavior associated with homogeneous nucleation.

5.1 SOA formation from the ozonolysis of PVE and BVE

5.1.1 Size distribution of SOA

The experiments on the SOA formation in the ozonolysis of PVE and BVE were carried out at (298 ± 3) K and 1000mbar of synthetic air. Excess amounts (~ 150 ppm) of cyclohexane were introduced to scavenge the OH radical produced in the systems. The initial vinyl ether conditions for the reaction of ozone with PVE and BVE are given in Table 5.1.

Figure 5.1 and 5.2 show typical time evolution profiles of the particle number size distribution during the ozonolysis of PVE and BVE, respectively.

Table 5.1 Experimental conditions and results for the reaction of ozone with PVE and BVE at 298K and atmospheric pressure

| Vinyl ether | Initial concentration (ppm) | Y(%) | α_i (%) | K_i ($m^3/\mu g$) | P_i^0 (μ Torr) |
|-------------|-----------------------------|------|----------------|-----------------------|-----------------------|
| PVE | 2.6 | 0.42 | 0.40 | 0.1050 | 0.44 |
| | 1.0 | 0.45 | 0.46 | 0.2233 | 0.21 |
| | 0.69 | 0.48 | 0.47 | 0.2716 | 0.17 |
| BVE | 1.87 | 0.63 | 0.64 | 0.1069 | 0.43 |
| | 1.68 | 1.09 | 1.12 | 0.057 | 0.82 |
| | 0.95 | 0.31 | 0.31 | 0.5289 | 0.09 |

From Figure 5.1 and Figure 5.2, the SOA formed in the ozonolysis of PVE and BVE appears to be mono modal in both cases. The formation of detectable particles (>14 nm) was observed a few minutes after initiation of the ozonolysis (6 and 4 minutes for

PVE and BVE, respectively). No seed aerosol was used in the experiments and the background particle concentration was less than 300 particles/cm³. The observed aerosol profiles showed typical behavior associated with homogeneous nucleation.

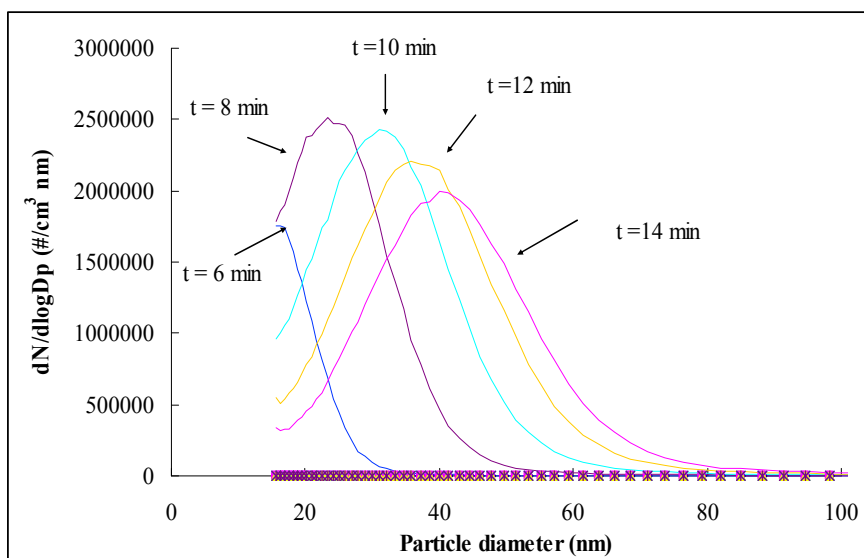


Figure 5.1 Evolution of the SOA distribution with reaction time (t) during the ozonolysis of PVE.

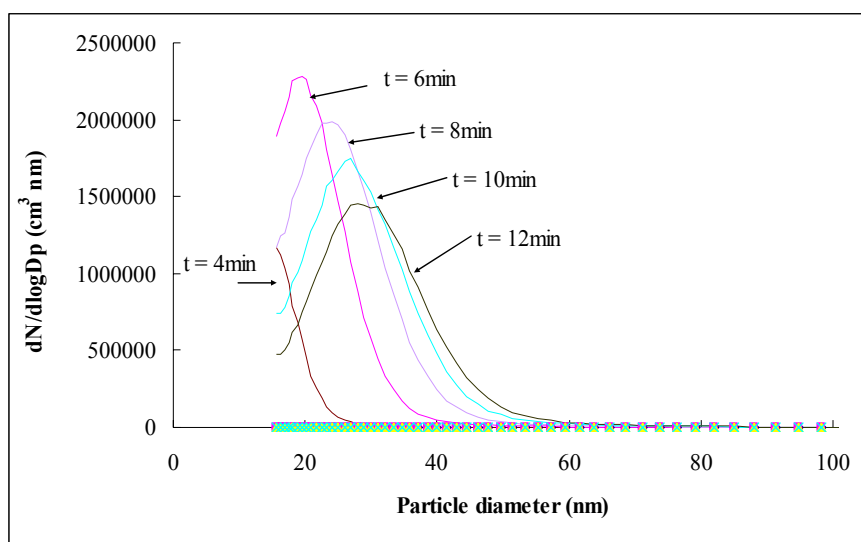


Figure 5.2 Evolution of the SOA distribution with reaction time (t) during ozone reaction with BVE.

A maximum total particle concentration of $(2-2.5) \times 10^6$ particles cm^{-3} was reached. As seen in Figure 5.1 and 5.2 the particle number concentrations decreased with increasing reaction time and the mean particle diameter increased from an initial value of 20 nm to around 40 nm due to particle coagulation and/or evaporation of small particles followed by re-condensation on the larger particle surfaces.

5.1.2 Aerosol yields and partition coefficients for SOA in the ozonolysis of PVE and BVE

Figure 5.3 presents a typical plot of the total aerosol mass concentration as a function of the amount of PVE reacted while Figure 5.4 gives a plot of the aerosol formation yield as a function of the aerosol mass concentration for the same reaction, assuming only one partitioning semi-volatile compound. The solid line is a fit to the data points using the adsorption/partitioning model developed by Odum *et al.* [8]. As described in Chapter 2 the slope of the straight line of Figure 5.3 gives the aerosol yield Y (eq. IX).

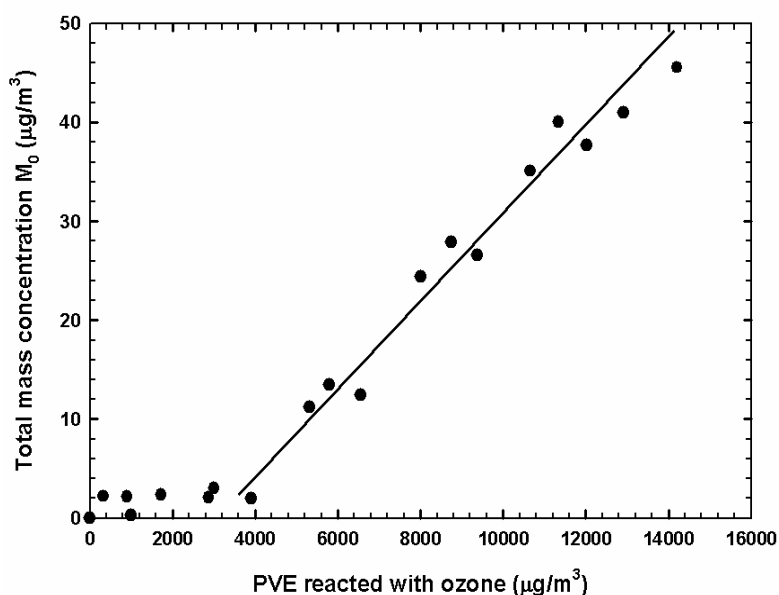


Figure 5.3 Typical plot of the aerosol mass concentration M_0 as a function of the mass of reacted PVE

The mass-based stoichiometric coefficient α_i as well as partitioning coefficients K_i for

semi-volatile compound i can also be obtained from a fit of the points in Figure 5.4 (equation XIII), by assuming spherical particles with a density of 1 g cm^{-3} .

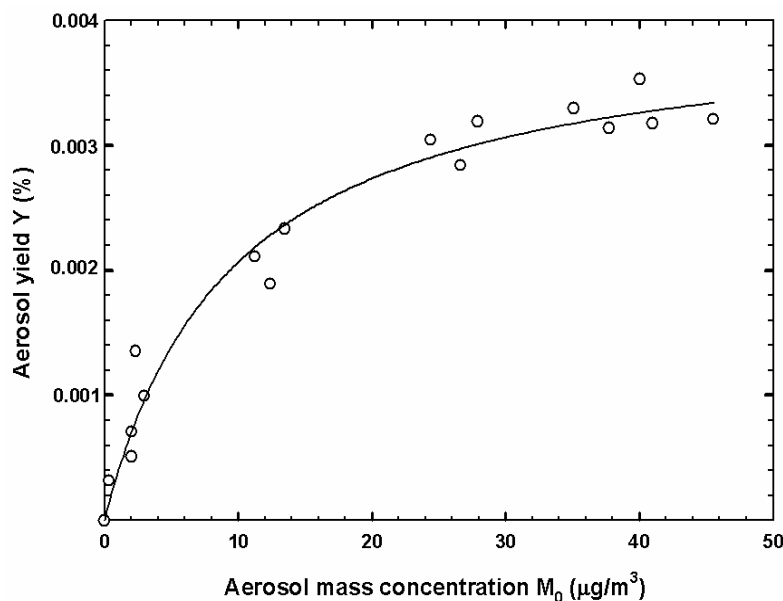


Figure 5.4 Typical plot of the aerosol yield for the reaction of ozone with PVE as a function of the aerosol mass concentration M_0 . The solid line is a fit based on the adsorption/partitioning model.

Figure 5.5 and 5.6 are the typical profiles of SOA formation obtained from the ozonolysis of BVE. The SOA yields and the partitioning coefficients calculated for the ozonolysis of PVE and BVE are listed in Table 5.1.

From Figure 5.3 and 5.5 it is clear that a certain amount of vinyl ethers must react before detectable aerosol is observed. This is an indication of mass of reacted vinyl ethers necessary to produce enough semi-volatile products to reach the saturation vapor pressure P_i^0 . The saturation vapor pressure P_i^0 of the hypothetical semi-volatile compound can be derived from the partitioning coefficient K_i , which is calculated using the following equation,

$$P_i^0 = \frac{760RT}{M_i \times 10^6 K_i \zeta_i} \quad (\text{XVI})$$

where R is the universal gas constant, T is the temperature in Kelvin; M_i is the molar mass of the aerosol and ζ_i is the activity coefficient. As discussed by Sadezky *et al.* [64] M_i and ζ_i were assumed to be 400 g/mol and 1 , respectively.

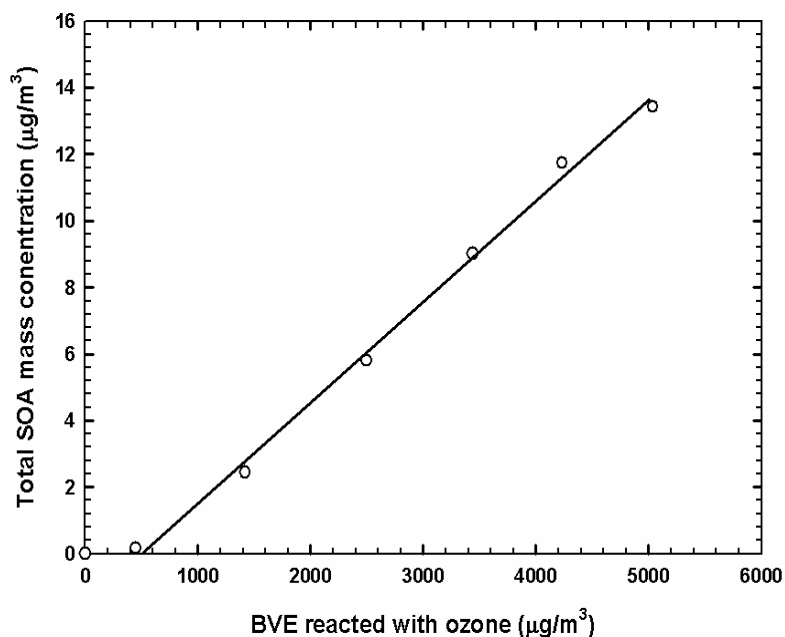


Figure 5.5 Typical plot of the aerosol mass concentration M_0 as a function of the mass of reacted BVE

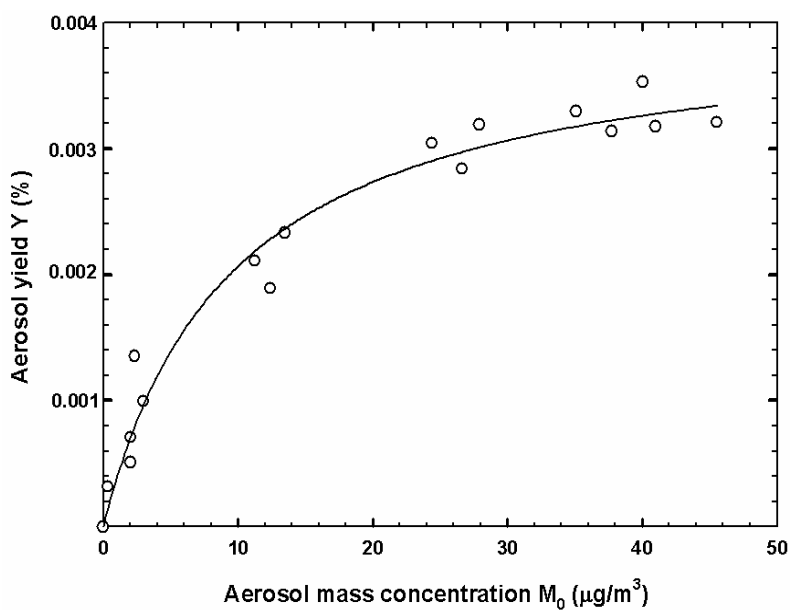


Figure 5.6 Typical plot of the aerosol yield as a function of the aerosol mass concentration M_0 for BVE. The solid line is a fit based on the adsorption/partitioning model.

The calculated values of P_1^0 are also listed in Table 5.1. The calculated saturation vapor pressures should be considered as estimated upper limits, since the calculations

are based on liquid compounds with flat surfaces and does not take into account the curved surface of the liquid droplets. According to Kelvin's law, the smaller the radius of the droplet, the higher is the vapor pressure over the droplet surface. The observed particle size is expected to be several nanometers so the real saturation vapor pressures of the SOA formed should, therefore, be much lower.

5.2 Discussion on SOA formation in the ozonolysis of PVE and BVE

As can be seen in Table 5.1 the aerosol formation yields Y are in excellent agreement with the calculated mass-based stoichiometric coefficient α , indicating near ideal behavior of the hypothetical semi-volatile products. According to the adsorption/partitioning model, if condensation plays a significant role in SOA formation higher initial concentrations of the reactants will give rise to higher SOA yields. However, as seen in Table 5.1 variation in the initial PVE concentrations did not affect the aerosol yields which are all around 0.4%. In contrast, the aerosol yields for the ozonolysis of BVE were found to vary between 0.3 to 1.1% under the conditions applied; however, the aerosol yields are not proportional to the initial concentration of BVE as predicted by the model.

The SOA yields are very low and are associated with relatively large errors. More experiments, under a wider range of conditions, are necessary in order to determine whether or not the results for BVE are statistically relevant. Artifacts in the experimental system can also not be excluded.

Table 5.2 compares the results for SOA formation from the reaction of ozone with PVE and BVE from the present study with values reported in the literature for alkyl vinyl ethers.

It is clearly evident from Table 5.2 that the presence of an OH radical scavenger (cyclohexane) significantly reduces aerosol formation in the ozonolysis of alkyl vinyl ethers.

It is well established that the OH radical is a product of the ozonolysis of unsaturated organics. The OH radical can be produced from various reactions of the Criegee intermediates (CI). Therefore, an OH radical scavenger is commonly used to isolate

the ozone reaction. To date, the effects of the addition of an OH radical scavenger and a stabilized CI scavenger on SOA formation in chemical systems are not well understood.

Table 5.2 Comparison of the SOA yields obtained in the present study with those reported in literature for the ozonolysis of alkyl vinyl ethers.

| Vinyl ether | Initial concentration (ppm) | OH tracer | OH scavenger | α_i (%) |
|-------------|-----------------------------|------------------|--------------|-------------------------|
| MVE | 4.9-8.9 | di-n-butyl ether | - | 0.66 ^{a)} |
| EVE | 0.2-0.4 | - | - | 3.5 ^{b)} |
| PVE | 0.69-2.6 | | Cyclohexane | 0.44 ^{c)} |
| | 0.2-0.4 | - | - | 3.8 ^{b)} |
| BVE | 0.95-1.87 | | Cyclohexane | 0.31-1.12 ^{c)} |
| | 0.2-0.4 | - | - | 4.3 ^{b)} |
| iBVE | 0.2-0.4 | | Cyclohexane | 0.9 ^{b)} |
| | 0.2-0.4 | - | - | 4.4 ^{b)} |
| tBVE | 0.2-0.4 | - | - | 1.6 ^{b)} |

a) Data taken from Klotz *et al.* [52] b) Data taken from Sadezky *et al.*[64] c) Present work

Recent studies aimed at investigating the effects of OH radical and CI scavengers on SOA formation in the ozonolysis of alkenes have been performed by several laboratories.

Docherty and Ziemann *et al.* [115-118] have studied the effect of an OH scavenger on the SOA formation from the ozonolysis of several alkenes and established that the OH radical scavenger definitely plays a role. They have demonstrated that the extent and direction of the influence is dependent on the specific alkene. For example, in a β -pinene/ozone reaction system Ziemann [116] observed a higher SOA yield when cyclohexane was used as the scavenger compared to propanol. In a cyclohexene/ozone reaction system, using three different OH radical scavengers, Keywood *et al.* [117] observed that the SOA yield was highest with CO, intermediate with 2-butanol and the lowest with cyclohexane.

To explain the OH scavenger effects on SOA formation in the ozonolysis of alkenes Docherty *et al.* [115,118] and Keywood *et al.* [117] have proposed that the main influence of the scavengers arises from their independent production of HO₂ radicals, which apparently enhances the rate of reaction of hydroperoxy radicals with key radical intermediates in SOA formation.

The effect of water vapor, an effective CI scavenger, on the SOA formation from the reaction of ozone with several monoterpenes has been investigated recently [119-125]. Regarding the mass of SOA, most studies found an increase in SOA on adding water to the system [120,122,125]. However, with regard to the number of the particles, the results are more contradictory. The study performed by Jonsson *et al.* [125] showed an increase in the number of particles with increase in humidity, while most of the other studies found either a slight decrease or no effect [119,120,123,124]. The increase in mass could be partly explained by physical water uptake, but not the observed increase in the number concentration.

The water dependence of the SOA formation from ozonolysis of monoterpenes observed by Jonsson *et al.* [125] was attributed by the authors to water influence on: i) the gas-phase reactions, e.g. reaction of the stabilized CI with water producing carboxylic acids, ii) the HO_x chemistry, and iii) the partitioning and condensed phase chemistry.

Docherty *et al.* [115,118], on the other hand, observed that the aerosol mass spectrum and the yields were relatively insensitive to the identity of the CI scavenger (water, alcohols and aldehydes) in the ozonolysis of β-pinene, indicating that the association reactions of the stabilized CI contribute minimally to the SOA formation, at least, in this system.

The present work in combination with that of Sadezky *et al.* [64], clearly show that the presence of an OH radical scavenger affects the SOA formation from the ozonolysis of alkyl vinyl ethers. As with the other ozonolysis systems, the effect of the OH radical scavenger on the mechanism of the SOA formation from ozonolysis of vinyl ethers is not clear.

In the ozonolysis of alkyl vinyl ethers Sadezky *et al.* [64] have also shown that the SOA formation is dramatically reduced in the presence of HCOOH and water. The reactions of the stabilized CI with HCOOH and water are discussed in Chapter 4. From the above results it would appear on first glance, that the influence of a CI scavenger on SOA formation from the ozonolysis of alkyl vinyl ethers is completely

different to that observed for ozone/monoterpene systems, and that different mechanisms leading to SOA formation must be operative in the systems. However, the SOA yields from the ozone/monoterpene systems are much higher than those observed in the ozonolysis of alkyl vinyl ethers. It is, therefore, more likely that the mechanism leading to the small SOA yields in the ozonolysis of the vinyl ethers is also operative in the ozone/monoterpene systems but is going undetected because of the large variability in the SOA yields from the ozone/monoterpene systems.

The formation of oligomers in the ozonolysis of alkyl vinyl ethers observed by Sadezky *et al.* [64], which contain the Criegee biradical structural entity, and the large decrease in the SOA yield on adding a CI scavenger to the reaction systems strongly support a major role of CI in the SOA formation observed in the “dry” ozonolysis of alkyl vinyl ethers. If this is the case, addition of an OH radical scavenger such as cyclohexane to the ozone/alkyl vinyl ether systems will increase the HO₂ radical level in the system. These radicals can react with the CI to form hydroperoxides, which will reduce the amount of attack of the CI at the double bond. The hydroperoxides are relatively small and highly volatile compared to those formed in terpene ozonolysis systems and will not form SOA, thus the overall SOA yield would be expected to decrease in the presence of cyclohexane compared to that in its absence if reaction of CI with the alkyl vinyl ether is the SOA formation route as is observed experimentally.

Similarly, the presence of CI scavengers, such as water and HCOOH, will very effectively transform the CI to highly volatile hydroperoxides thus hindering reaction of the CI with the alkyl vinyl ether double bond and reducing SOA formation.

If reaction of the CI with the double bond in the ozonolysis of alkyl vinyl ethers is the major route to the SOA formation as the results of Sadezky *et al.* [64] suggested the SOA formation from the ozonolysis of alkyl vinyl ethers will be of negligible importance under atmospheric conditions due to scavenging of the CI by the high concentrations of water vapour constantly present in the troposphere. However, if the SOA observed in the ozonolysis of alkyl vinyl ethers via reaction of the CI with the double bond is a general phenomena for alkenes then it needs to be taken into account in all SOA studies on the ozonolysis of alkenes performed under dry conditions.

Chapter 6

Summary

Vinyl ethers are used increasingly as organic solvents, additives and in different types of coatings in industry. Because of their fairly high volatility this class of compound will result in a significant emission into the urban atmosphere and hence will be oxidized by OH radical, ozone and NO₃ radical.

The objectives of present work were: i) to determine the rate coefficients for the reactions of selected vinyl ethers with atmospheric reactive species, i.e. OH radical, ozone and NO₃ radicals, ii) to elucidate the atmospheric reaction mechanisms for the OH, ozone and NO₃ initiated oxidation of alkyl vinyl ethers, and iii) to study the secondary organic aerosol (SOA) formation from the ozonolysis of alkyl vinyl ethers. This study has successfully addressed these objectives.

The kinetic studies performed in the present work were carried out in a 405 l borosilicate glass chamber at Wuppertal University, Germany. Relative rate coefficients have been measured for the reactions of OH radical, ozone and NO₃ radicals with propyl vinyl ether (PVE), butyl vinyl ether (BVE), ethylene glycol monovinyl ether (EGMVE), ethylene glycol divinyl ether (EGDVE) and diethylene glycol divinyl ether (DEGDVE). The rate coefficients (in cm³ molecule⁻¹ s⁻¹) obtained in the present work are listed in the following table.

| Vinyl ether | $k_{\text{OH}} \times 10^{11}$ | $k_{\text{O}_3} \times 10^{16}$ | $k_{\text{NO}_3} \times 10^{12}$ |
|--|--------------------------------|---------------------------------|----------------------------------|
| Propyl vinyl ether, n-C ₃ H ₇ OCH=CH ₂ | 9.73±1.94 | 2.34±0.48 | 1.85±0.53 |
| Butyl vinyl ether n-C ₄ H ₉ OCH=CH ₂ | 11.3±3.1 | 2.59±0.52 | 2.10±0.54 |
| Ethyleneglycol monovinyl ether HOCH ₂ CH ₂ OCH=CH ₂ | 10.4±2.15 | 2.02±0.41 | 1.95±0.50 |
| Ethyleneglycol divinyl ether H ₂ C=CHOCH ₂ CH ₂ OCH=CH ₂ | 12.3±3.25 | 1.69±0.41 | 2.23±0.46 |
| Diethyleneglycol divinyl ether H ₂ C=CHOCH ₂ CH ₂ OCH ₂ CH ₂ OCH=CH ₂ | 14.2±3.00 | 2.70±0.56 | 6.14±1.38 |

In addition, the rate coefficient for OH radical reaction with 2-methyl-1,3-dioxolane, the only product of the dark reaction of EGMVE, was measured as $(1.05 \pm 0.25) \times 10^{11} \text{ cm}^3 \text{ molecule}^{-1} \text{ s}^{-1}$.

The present kinetic data has considerably supplemented the kinetic database required to develop structure-reactivity relationships for the reactions of OH radical, ozone and NO₃ radicals with oxygenated volatile organic compounds. Using the rate coefficients obtained in this work, in combination with tropospheric concentrations (in molecule cm⁻³) of [OH] = 1.6×10^6 (12 hour daytime average), [O₃] = 7.0×10^{11} (24 hour average) and [NO₃] = 5.0×10^8 (12 hour nighttime average) the atmospheric lifetimes of the selected vinyl ethers with respect to their reactions with OH radical, ozone and NO₃ radicals range from few minutes for reaction with NO₃ to a few hours for reaction with OH and ozone. Thus all three reactions can make significant contributions to the degradation of the selected vinyl ethers. The short lifetimes of the vinyl ethers show that they will be quickly degraded when emitted to the atmosphere and will only be actively involved in tropospheric chemistry on local to regional scales. Results from laboratory studies show that photolysis of vinyl ethers is a negligible loss process for this class of organic compound in the troposphere.

As mentioned above the tropospheric degradation of vinyl ethers is initiated by

reactions with OH radical, ozone and NO₃ radicals. Product studies of the OH, ozone and NO₃ initiated oxidation of alkyl vinyl ethers were performed in the 405 l borosilicate glass reactor at Wuppertal University.

In the case of the OH radical initiated oxidation of PVE and BVE alkyl formate and formaldehyde are the main products. The molar yields of both the alkyl formate and HCHO for the different vinyl ethers fall within the range of (70±10) molar % for the NO_x-containing system and (60±10) molar % for the NO_x-free system. The reduced yields of the formates and HCHO observed in the absence of NO_x compared to the higher yields measured in the presence of NO_x can be explained by different mechanisms.

The reactions of the OH radical with alkyl vinyl ethers is mainly initiated by the addition of the OH radical to the carbon-carbon double bond of the vinyl ethers to form β-hydroxy alkyl radicals. Further reactions of the β-hydroxy alkyl radicals with O₂ and NO (in the presence of NO_x) or RO₂ radicals (in the absence of NO_x) give mainly β-hydroxy alkoxy radicals. In the absence of NO_x self-reaction of the β-hydroxy alkyl peroxy radicals will also lead to formation of multifunctional group compounds while in the presence of NO_x, β-hydroxy alkyl peroxy radicals will almost completely react with NO to form β-hydroxy alkoxy radicals, which decompose to produce an alkyl formate and HCHO. The self reaction of the β-hydroxy alkyl peroxy radicals can explain the reduced yields of the formates and HCHO in the NO_x-free system. For the OH radical initiated oxidation of PVE, in the presence of NO_x, 77.0% C can be accounted for, compared to 63.4% C in the absence of NO_x. For the reaction of OH with BVE, in the presence of NO_x, 64.6% C can be accounted for, compared to 52.3% C in the absence of NO_x. The residual infrared product spectra suggest that nitrate or carbonyl nitrate products comprise the majority of the missing carbon in the NO_x-containing systems. However, under tropospheric conditions it is likely that hydroxyl carbonyls comprise the majority of the missing carbon in the reactions of PVE + OH and BVE + OH with the remainder being made up of multi-functional organic nitrates.

Two types of experiments were conducted for the product studies on the reactions of ozone with the alkyl vinyl ethers, i.e. i) in the presence of an OH radical scavenger, cyclohexane, and ii) in the presence of an OH radical tracer, 1,3,5-trimethyl-benzene (TMB). In the presence of the OH radical scavenger, the only product that could be

positively identified and quantified in each system was an alkyl formate. The formation yields for alkyl formates measured in both types of experiments were in good agreement (within the range of $75\pm 15\%$). Ozonolysis of the alkyl vinyl ethers also led to the formation of HCHO (within the range of $20\pm 10\%$), hydroperoxy methyl formate (HPMF, $\sim 12\%$), CO ($\sim 10\%$) and formic anhydride (FA, $\sim 2\%$). In the OH tracer type of experiment OH radical yields of $\sim 17\%$ have been estimated for the ozonolysis of the alkyl vinyl ethers.

The products identified in the ozonolysis of PVE and BVE presented above account for 81.9% and 70.2% of reacted carbon, respectively.

As for other carbon-carbon double bond containing compounds, the reactions of O_3 with alkyl vinyl ethers are initiated by addition of O_3 to the double bond to give energy rich primary ozonides. The decomposition of the ozonides leads to the formation of Criegee intermediates and end products, i.e. alkyl formates and HCHO. The branching ratios for the different channels of the decomposition of the ozonides depend on the structure of the individual vinyl ethers. The further reactions of the Criegee biradicals produce CO, HPMF, FA and OH radicals. Detailed reaction mechanisms describing the formation of the products are discussed in Chapter 4.

In the reactions of NO_3 radical initiated oxidation of alkyl vinyl ethers alkyl formates and HCHO were again observed as major products with molar formation yields of around 53% for PVE and around 45% for BVE.

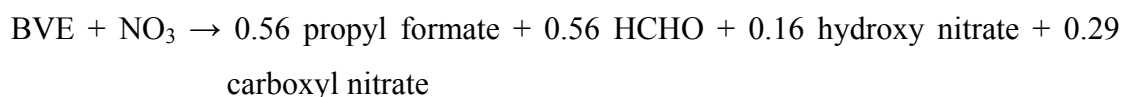
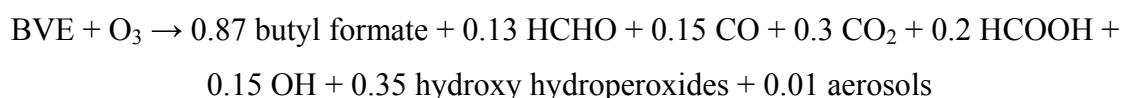
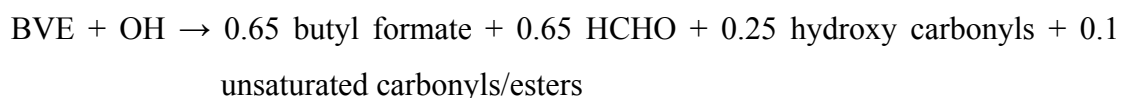
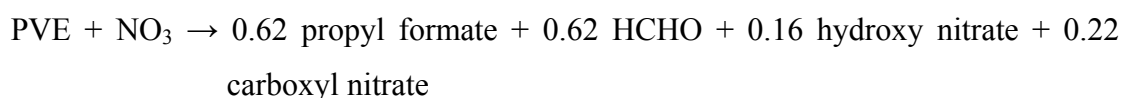
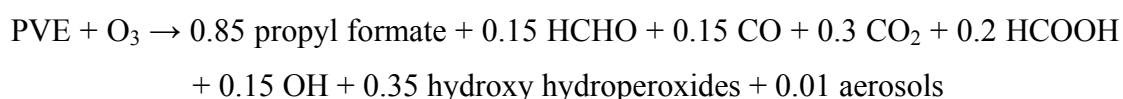
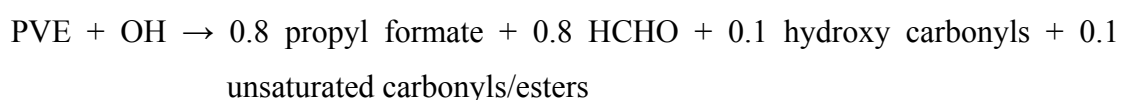
The gas-phase reactions of the NO_3 radical with alkyl vinyl ethers have been postulated to proceed via NO_3 radical addition to the double bond to form β -nitrooxy alkyl radicals. The subsequent reactions of the β -nitrooxy alkyl radicals are analogous to those of the β -hydroxy alkyl radicals formed from the corresponding OH radical reactions and lead to the formation of β -nitrooxy alkyl peroxy radicals. In the presence of NO_2 , β -nitrooxy alkyl peroxy radicals can react with NO_2 , to form thermally unstable peroxy nitrates, however, self-reactions and/or cross-reaction with peroxy radicals will also produce nitrooxy alkoxy radicals. There are several reaction channels open to nitrooxy alkoxy radicals: i) carbon-carbon bond scission to give the observed major products alkyl formates and HCHO; ii) reaction with NO_2 to form dinitrates; iii) reaction with O_2 to form the corresponding carbonyl nitrates.

From the formation yields of the alkyl formates and HCHO carbon balances of 53.2% and 44.3% are obtained for the reactions of NO_3 with PVE and BVE, respectively, and

total nitrate formation yields of about 56.0% and 57.1% have been estimated for the reactions of NO₃ with PVE and BVE, respectively.

Exploratory studies on secondary organic aerosol (SOA) formation in the reactions of ozone with PVE and BVE were performed in a 1080 l quartz glass reactor coupled with a scanning mobility particle sizer (SMPS) system at Wuppertal University. The observed aerosol profiles show typical behavior associated with homogeneous nucleation. In the presence of an excess amount of cyclohexane, SOA yields of 0.4% and 0.3-1.1% were obtained for PVE and BVE, respectively. The SOA formation mechanism and the role that the OH radical scavenger plays in the SOA formation remain unclear. There are indications that the SOA formation will be of negligible importance under atmospheric conditions.

Interest in the oxidation of alkyl vinyl ethers, i.e. PVE and BVE is likely to be mainly focused in urban air masses with significant NO_x, i.e. where the major emission sources will be. The reaction mechanisms developed in the present work are complex. Since CT-models generally require simple chemical mechanisms, therefore, based on the available product information (Chapter 4) and the conditions prevailing in the urban troposphere, the following highly simplified one-line mechanisms for use in chemical models of the OH radical, ozone and NO₃ radical initiated atmospheric oxidation of PVE and BVE are proposed:



Syntheses

I.1 Synthesis of methyl nitrite (CH₃ONO)

Methyl nitrite was prepared using the method described in the literature [126].

In a 2 l two-neck flask fitted with a magnetic stirrer and dropping funnel, 69 g (1 mol) of sodium nitrite (NaNO₂) and 50 ml methanol (CH₃OH) dissolved in 40 ml water. The flask was cooled with an ice bath.

A solution of 27 ml concentrated sulfuric acid in 50 ml water was added dropwise to the solution mentioned above. After being generated, the gaseous methyl nitrite was first dried by passing it through a glass tube containing calcium chloride (CaCl₂) and then collected in a glass cylinder placed in a cooling trap. The cooling bath is a combination of dry ice and ethanol (-68 °C). The pale yellow liquid methyl nitrite was stored in the glass cylinder at -78 °C in dry ice.

I.2 Synthesis of nitrous acid (HONO)

Nitrous acid was synthesized by the method of Cavalli *et al.* [71]

In a three-neck round-bottomed flask equipped with a magnetic stirrer, dropping funnel, thermometer and synthetic air inlet and outlet, 30 ml of a 30% sulfuric acid solution was placed. The synthetic air outlet was directly connected to the reaction chamber.

The nitrous acid was produced by adding a 1% sodium nitrite (NaNO₂) aqueous

solution dropwise into the stirred flask at 20 °C.



I.3 Synthesis of dinitrogen pentoxide (N₂O₅)

Dinitrogen pentoxide was synthesized by the method of Schott *et al.* [69].

1. NO₂ condensation to N₂O₄:

NO₂ was condensed from an NO₂ gas cylinder into a storage trap at -32 °C. Figure A.1 shows the experimental set-up used for the NO₂ condensation. NO₂ vapor was sucked out of the NO₂ gas cylinder slowly by a pump connected to the storage trap. Prior to condensation in the storage trap it was passed through a column of P₂O₅ coated glass beads.

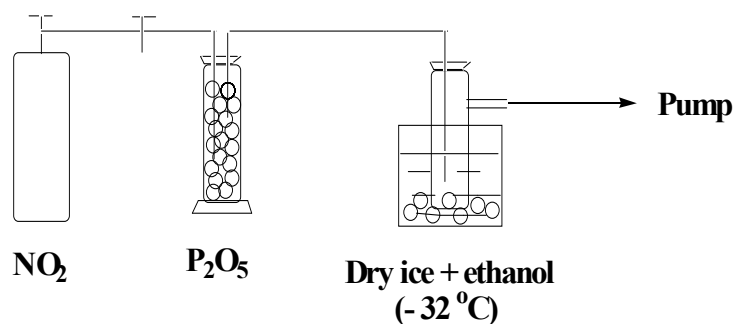


Figure A. 1 Schematic representation of the experimental set-up for the NO₂ condensation

2. Preparation of N₂O₅:

N₂O₅ was prepared from N₂O₄ by oxidation with O₃. Figure A.2 presents a schematic representation of the experimental set-up for the synthesis of N₂O₅.

The oxygen stream was divided into two. One stream passed through a column of P_2O_5 coated glass beads prior to entering the ozone generator. The other one passed over the solid N_2O_4 in a storage trap placed in a cooling bath at $-30\text{ }^\circ\text{C}$ and was then dried by a column of P_2O_5 coated glass beads. The flow rates were adjusted so that the stream was colorless after the two streams merged in the mixing column.

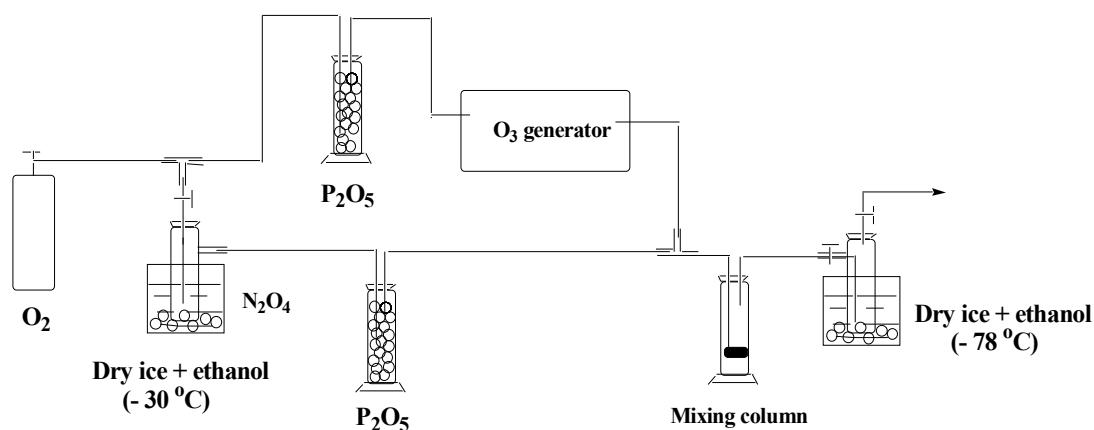


Figure A. 2 Schematic representation of the experimental set-up used in the synthesis of N_2O_5

The O_2 - O_3 - N_2O_5 gas mixture emerging from the mixing column passed through a collection trap at $-78\text{ }^\circ\text{C}$ and N_2O_5 was collected as a white solid on the walls of the collection trap.

The N_2O_5 was stored in solid form in dry ice at $-78\text{ }^\circ\text{C}$.

Appendix II

Gases and Chemicals Used

II.1 Gases

| Compounds | Origin | Purity (%) |
|---|------------------|----------------------------|
| Synthetic air O ₂ :N ₂ =20.5:79.5(%) | Messer-Griesheim | Hydrocarbon free 99.999 |
| O ₂ | Messer-Griesheim | 99.995 |
| CO | Messer-Griesheim | 99.997 |
| NO | Messer-Griesheim | 99.5 |
| NO ₂ | Messer-Griesheim | 98 |
| Isobutene | Messer-Griesheim | 99 |
| Ethene | Messer-Griesheim | 99.95 |
| Propene | Aldrich | 99 |
| Trans-2-butene | Messer-Griesheim | 99 |

II.2 Chemicals

| Compounds | State | Origin | Purity (%) |
|--------------------------------|--------|----------------|------------|
| Propyl vinyl ether | Liquid | Aldrich | 99 |
| Butyl vinyl ether | Liquid | Aldrich | 98 |
| Propyl formate | Liquid | Aldrich | 97 |
| Butyl formate | Liquid | Aldrich | 97 |
| Ethyleneglycol monovinyl ether | Liquid | Aldrich | 97 |
| Ethyleneglycol divinyl ether | Liquid | Aldrich | 97 |
| Diethyleneglycol divinyl ether | Liquid | Aldrich | 98 |
| Isoprene | Liquid | Aldrich | 99 |
| H ₂ O ₂ | Liquid | Peroxid-Chemie | 85 |
| Cyclohexane | Liquid | Aldrich | 99.9 |
| Cyclohexene | Liquid | Aldrich | 99 |
| 2,3-Dimethyl-1,3-butadiene | Liquid | Aldrich | 98 |
| 1,3-Cycloheptadiene | Liquid | Aldrich | 97 |
| 2-Methyl-1,3-dioxolane | Liquid | Aldrich | 97 |
| 1,3,5-Trimethylbenzene | Liquid | Aldrich | 99 |
| Methanol | Liquid | Fluka | 99.8 |
| 1-Propanol | Liquid | Merck | 99.7 (GC) |
| 1-Butanol | Liquid | Lancaster | 99 |
| Sodium formate | Solid | Fluka | 99.5 |

Gas-phase Infrared Absorption Cross Sections

III.1 Calibration method

The 405 l borosilicate glass chamber at the University of Wuppertal was used to determine the gas-phase FTIR absorption cross sections for several vinyl ethers and alkyl formates. The integral cross sections were determined using the procedure outlined by Etzkorn *et al.* [127] and Olariu [128]. Only a brief description of the method employed is given here.

Absorption cross sections are defined by Lambert-Beer's law:

$$\ln \left[\frac{I_0(\nu)}{I(\nu)} \right] = \sigma_e(\nu) \times c \times l = D(\nu) \quad (\text{XVII})$$

where $I_0(\nu)$ and $I(\nu)$ represent the measured light intensities at wavenumber ν with and without absorber present in the cell, $\sigma_e(\nu)$ denotes the absorption cross section at the wavenumber ν , c is the analyte concentration and l is the optical path length through the cell. The term $\ln(I_0(\nu)/I(\nu))$ is also known as the optical density $D(\nu)$ at the wavenumber ν . Integrated band intensities are defined as absorption cross sections integrated over a given wavenumber range, therefore the integration ranges used are reported with integrated band intensities.

Most compounds used in this work were liquids. The transfer of the liquid sample into the gas-phase was accomplished by injecting a known volume of the sample into a heated inlet connected with the evacuated chamber as described in the experimental section (Section 2.2.1). A valve controlling the bath gas was then opened to produce a strong gas flow. As a result the sample vaporizes into the reactor.

For solid and liquid samples with very low vapor pressures weighed amounts of the compounds were dissolved in HPLC grade dichloromethane. The concentrations of solution were chosen to result in total injected volumes between 100 and 1000 μl for the calibration.

For the calculation of the concentrations in the cell the uncertainty of the injected volume due to the unknown volume of the syringe needle has to be taken into account. The true concentration $c_{i,t}$ in the cell will be different from the concentration calculated from the injected volumes c_i by an offset α . By injecting different volumes for one compound this offset can be corrected.

Table III.1 gives the integrated absorption cross sections (base 10, in $\text{cm}^2 \text{ molecule}^{-1}$) for several vinyl ethers and alkyl formates determined in the present work.

Table III.1 Integrated absorption cross sections determined in this work (base 10)

| Compounds | Range / cm^{-1} | $\sigma_{10} / \text{cm}^2 \text{ molecule}^{-1}$ |
|--------------------|--------------------------|---|
| Propyl vinyl ether | 3180-3106 | $(7.74 \pm 0.21) \times 10^{-19}$ |
| | 1710-1560 | $(1.21 \pm 0.16) \times 10^{-17}$ |
| | 1250-1162 | $(1.39 \pm 0.12) \times 10^{-17}$ |
| Propyl formate | 1814-1680 | $(2.27 \pm 0.03) \times 10^{-17}$ |
| | 1251-1089 | $(3.16 \pm 0.04) \times 10^{-17}$ |
| Butyl vinyl ether | 3160-3106 | $(6.55 \pm 0.40) \times 10^{-19}$ |
| | 1720-1550 | $(1.07 \pm 0.10) \times 10^{-17}$ |
| | 1266-1158 | $(1.34 \pm 0.07) \times 10^{-17}$ |
| Butyl formate | 1845-1650 | $(2.10 \pm 0.07) \times 10^{-17}$ |
| | 1292-1039 | $(3.13 \pm 0.10) \times 10^{-17}$ |

References

1. Atkinson, R. Gas-phase tropospheric chemistry of organic compounds. *J. Phys. Chem. Ref. Data* **1994**, Monograph 2, 1-134.
2. Winer, A.M.; Arey, J.; Atkinson, R.; Aschmann, S.M.; Long, W.D.; Morrison, C.L.; Olszyk, D.M. Emission rates of organics from vegetation in California's central valley. *Atmos. Environ.*, **1992**, *26A*, 2647-2659.
3. Fung, I.; John, J.; Lerner, J.; Matthews, E.; Prather, M.; Steele, L.P.; Fraser, P.J. Three-dimensional model synthesis of the global methane cycle. *J. Geophys. Res.*, **1991**, *96*, 13033-13065.
4. Logan, J.A. Tropospheric ozone: Seasonal behavior, trends, and anthropogenic influence. *J. Geophys. Res.*, **1985**, *90*, 10463-10482.
5. Schwartz, S.E. Acid deposition: Unraveling a regional phenomenon. *Science*, **1989**, *243*, 753-763.
6. Pankow, J.F. Review and comparative analysis of the theories on partitioning between the gas and aerosol particulate phases in the atmosphere. *Atmos. Environ.*, **1987**, *21*, 2275-2283.
7. Bidleman, T.F. Atmospheric processes. *Environ. Sci. Technol.*, **1988**, *22*, 361-367.
8. Odum, J.R.; Hoffmann, T.; Bowman, F.; Collins, D.; Flagan, R.C.; Seinfeld, J.H. Gas/ particle partitioning and secondary organic aerosol yields. *Environ. Sci. Technol.*, **1996**, *30*, 2580-2585.
9. Odum, J.R.; Jungkamp, T.P.W.; Griffin, R.J.; Flagan, R.C.; Seinfeld, J.H. The atmospheric aerosol forming potential of whole gasoline vapor. *Science*, **1997**, *276*, 96-99.
10. Volz, A.; Kley, D. Evaluation of the montsouris series of ozone measurements made in the 19th century. *Nature*, **1988**, *332*, 240-242.
11. Derwent, R.G.; Jenkin, M.E.; Saunders, S.M.; Pilling, M.J. Photochemical ozone

- creation potentials for organic compounds in northwest Europe calculated with a master chemical mechanism. *Atmos. Environ.*, **1998**, *32*, 2429-2441.
12. Fenger, J. Urban air quality. *Atmos. Environ.*, **1999**, *33*, 4877-4900.
13. Singh, H.; Chen, Y.; Staudt, A.; Jacob, D.; Blake, D.; Heikes, B.; Snow, J. Evidence from the Pacific troposphere for large global sources of oxygenated organic compounds. *Nature*, **2001**, *410*, 1078-1081.
14. Lewis, A.C.; Carslaw, N.; Marriott, P.J.; Kinghorn, R.M.; Morrison, P.; Lee, A.L.; Bartle, K.D.; Pilling, M.J. A larger pool of ozone forming carbon compounds in urban atmospheres. *Nature*, **2000**, *405*, 778-781.
15. Atkinson R.; Arey, J. Atmospheric degradation of volatile organic compounds. *Chem. Rev.*, **2003**, *103*, 4605-4638.
16. Mellouki, A.; Le Bras, G.; Sidebottom, H. Kinetics and mechanisms of the oxidation of oxygenated organic compounds in the gas-phase. *Chem. Rev.*, **2003**, *103*, 5077-5096.
17. Kanakidou, M.; Seinfeld, J.H.; Pandis, S.N.; Barnes, I.; Dentener, F.J.; Facchini, M.C.; van Dingenen, R.; Ervens, B.; Nenes, A.; Nielsen, C.J.; Swietlicki, E.; Putaud, J.P.; Balkanski, Y.; Fuzzi, S.; Horth, J.; Moortgat, G.K.; Winterhalter, R.; Myhre, C.E.L.; Tsigaridis, K.; Vignati, E.; Stephanou E.G.; Wilson, J. Organic aerosol and global climate modeling: a review. *Atmos. Chem. Phys.*, **2005**, *5*, 1053-1123.
18. Aschmann, S. M.; Atkinson, R. Products of the gas-phase reactions of the OH radical with n-butyl methyl ether and 2-isopropoxyethanol: reactions of ROC(O) radicals. *Int. J. Chem. Kin.*, **1999**, *31*, 501-513.
19. Aschmann, S.M.; Arey, J.; Atkinson, R. Atmospheric chemistry of selected hydroxyl-carbonyls. *J. Phys. Chem. A* **2000**, *104*, 3998-4003.
20. Atkinson, R. Product studies of gas-phase reactions of organic compounds. *Pure Appl. Chem.*, **1998**, *70*, 1335-1343.
21. Atkinson, R. Gas-phase degradation of organic compounds in the troposphere. *Pure Appl. Chem.* **1998**, *70*, 1327-1334.
22. Becker, K.H.; Wiesen, P. Tropospheric photochemistry: recent work and unsolved problems. *Optics and Spectroscopy* **1997**, *83*, 529-533.
23. Atkinson, R. Atmospheric chemistry of VOCs and NO_x. *Atmos. Environ.*, **2000**, *34*, 2063-2101.
24. Aschmann, S.M.; Atkinson, R. Rate constants for the gas-phase reactions of

References

- selected dibasic esters with the OH radical. *Int. J. Chem. Kin.*, **1998**, *30*, 471-474.
25. Aschmann, S.M.; Atkinson, R. Kinetics of the gas-phase reactions of the OH radical with selected glycol ethers, glycols, and alcohols. *Int. J. Chem. Kin.*, **1998**, *30*, 533-540.
26. Aschmann, S.M.; Atkinson, R. Atmospheric chemistry of 1-methyl-2-pyrrolidone. *Atmos. Environ.*, **1999**, *33*, 591-599.
27. Atkinson, R.: Atmospheric oxidation. In Boethling, R.S.; Mackay, D. *Handbook of Property Estimation Methods for Chemicals-Environmental and Health Sciences*. Lewis Publishers, Boca Raton, **2000**.
28. Cavalli, F. Atmospheric oxidation of selected alcohols and esters. Ph.D. thesis, University of Wuppertal, **2000**.
29. Grosjean, E.; Grosjean, D. The reaction of unsaturated aliphatic oxygenates with ozone. *J. Atmos. Chem.*, **1999**, *32*, 205-232.
30. Hoffman, T.; Odum, J.R.; Bowman, F.; Collins, D.; Klockow, D.; Flagan, R.C.; Seinfeld, J.H. Formation of organic aerosol from the oxidation of biogenic hydrocarbons. *J. Atmos. Chem.*, **1997**, *26*, 189-222.
31. Cabañas, B.; Salgado, S.; Martin, P.; Baeza, M.T.; Martinez, E. Night-time atmospheric loss process for unsaturated aldehydes: reaction with NO₃ radicals. *J. Phys. Chem. A* **2001**, *105*, 4440-4445.
32. Aschmann, S.M.; Martin, P.; Tuazon, E.C.; Arey, J.; Atkinson, R. Kinetic and product studies of the reactions of selected glycol ethers with OH radicals. *Environ. Sci. Technol.*, **2001**, *35*, 4080-4088.
33. Johnson, D.; Andino, J.M. Laboratory studies of the OH-initiated photooxidation of ethyl-n-butyl ether and di-n-butyl ether. *Int. J. Chem. Kinet.*, **2001**, *33*, 328-341.
34. Noda, J.; Nyman, G.; Langer, S. Kinetics of the gas-phase reaction of some unsaturated alcohols with the nitrate radical. *J. phys. Chem. A* **2002**, *106*, 945-951.
35. O'Donnell, S.M.; Sidebottom, H.W.; Wenger, J.C.; Mellouki, A.; Le Bras, G. Kinetic studies on the reactions of hydroxyl radicals with a series of alkoxy esters. *J. Phys. Chem. A* **2004**, *108*, 7386-7392.
36. Holloway, A.-L.; Treacy, J.; Sidebottom, H.; Mellouki, A.; Daële, V.; Le Bras, G.; Barnes, I. Rate coefficients for the reactions of OH radicals with the keto/enol tautomers of 2,4-pentadione, allyl alcohol and methyl vinyl ketone using the enol and methyl nitrite as photolytic sources of OH. *J. Photochem. Photobio. A: Chemistry* **2005**, *176*, 183-190.

37. Forstner, H.J.L.; Flagan, R.C.; Seinfeld, J.H. Secondary organic aerosol from the photooxidation of aromatic hydrocarbons: molecular composition. *Environ. Sci. Technol.*, **1997**, *31*, 1345-1358.
38. Griffin, R.J.; Cocker III, D.R.; Seinfeld, J.H. Incremental aerosol reactivity: application to aromatic and biogenic hydrocarbons. *Environ. Sci. Technol.*, **1999**, *33*, 2403-2408.
39. Alvarado, A.; Tuazon, E.C.; Aschmann, S.M.; Arey, J.; Atkinson, R. Products and mechanisms of the gas-phase reactions of OH radicals and O₃ with 2-methyl-3-buten-2-ol. *Atmos. Environ.*, **1999**, *33*, 2893-2905.
40. Atkinson, R.; Baulch, D.L.; Cox, R.A.; Hampson, R.F., Jr.; Kerr, J.A.; Troe, J. Evaluated kinetic and photochemical data for atmospheric chemistry: supplement III. IUPAC subcommittee on gas kinetic data evaluation for atmospheric chemistry. *J. Phys. Chem. Ref. Data* **1989**, *18*, 881-1097.
41. Atkinson, R.; Baulch, D.L.; Cox, R.A.; Hampson, R.F., Jr.; Kerr, J.A.; Troe, J. Evaluated kinetic and photochemical data for atmospheric chemistry: supplement IV. IUPAC subcommittee on gas kinetic data evaluation for atmospheric chemistry. *J. Phys. Chem. Ref. Data* **1992**, *21*, 1125-1568.
42. Atkinson, R.; Baulch, D.L.; Cox, R.A.; Hampson, R.F., Jr.; Kerr, J.A.; Rossi, M.J.; Troe, J. Evaluated kinetic and photochemical data for atmospheric chemistry, organic species: supplement VII. IUPAC subcommittee on gas kinetic data evaluation for atmospheric chemistry. *J. Phys. Chem. Ref. Data* **1999**, *28*, 191-393.
43. Placet, M.; Mann, C.O.; Gilbert, R.O.; Niefer, M.J. Emissions of ozone precursors from stationary sources: a critical review. *Atmos. Environ.*, **2000**, *34*, 2183-2204.
44. Sawyer, R.F.; Harley, R.A.; Cadle, S.H.; Norbeck, J.M.; Slott, R.; Bravo, H.A. Mobile sources critical review: 1998 NARSTO assessment. *Atmos. Environ.*, **2000**, *34*, 2161-2181.
45. BASF. Home page. BASF: Ludwigshafen, Germany; <http://www.basf.de>.
46. M. Joly, Fédération des Industries de la Peinture, Encres et Colles, FIPEC, personal communication; S. Lemoine, European Solvents Industry Group, ESIG, personal communication (<http://www.esig.info/index.php>).
47. Perry, R.A.; Atkinson, R.; Pitts, Jr. J.N. Rate constants for the reaction of OH radicals with dimethyl ether and vinyl methyl ether over the temperature range 299–427K. *J. Chem. Phys.*, **1977**, *67*, 611-614.

References

48. Barnes, I.; Zhou, Sh.; Klotz, B. In *Final reports of the EU project MOST*; contract EVK2-CT-2001- 00114; European Union: Brussels, August **2005**.
49. Grosjean, D.; Williams II, E.L. Environmental persistence of organic compounds estimated from structure-reactivity and linear free-energy relationships for unsaturated aliphatics. *Atmos. Environ.*, **1992**, *26A*, 1395-1405.
50. Thiault, G.; Thévenet, R.; Mellouki, A.; Le Bras, G. OH and O₃-initiated oxidation of ethyl vinyl ether. *Phys. Chem. Chem. Phys.*, **2002**, *4*, 613-619.
51. Mellouki, A. Proceedings of the NATO ARW “Environmental Simulation Chambers – Application to Atmospheric Chemical Processes”, Zakopane, Poland 1-4 October 2004; NATO Science Series, IV. Earth and Environmental Sciences, Springer, Dordrecht, the Netherlands, **2006**, 163-170.
52. Klotz, B.; Barnes, I.; Imamura, T. Product study of the gas-phase reactions of O₃, OH and NO₃ radicals with methyl vinyl ether. *Phys. Chem. Chem. Phys.*, **2004**, *6*, 1725-1734.
53. Zhou, Sh.; Barnes, I.; Zhu, T.; Bejan, I.; Benter, Th. Kinetic study of the gas-phase reactions of OH and NO₃ radicals and O₃ with selected vinyl ethers. *J. Phys. Chem.*, **2006**, *110*, 7386-7392.
54. Zhou, Sh.; Barnes, I.; Zhu, T.; Klotz, B.; Albu, M.; Bejan, I.; Benter, Th. Product study of the OH, NO₃ and O₃ initiated atmospheric photooxidation of propyl vinyl ether. *Environ. Sci. Technol.*, **2006**, *40*, 5415-5421.
55. Al Mulla, I.A.S. Kinetic and mechanisms for the atmospheric degradation of unsaturated oxygen containing compounds. Ph.D. thesis, The National University of Ireland, **2006**.
56. Thiault, G.; Mellouki, A. Rate constants for the reaction of OH radicals with n-propyl, n-butyl, iso-butyl and tert-butyl vinyl ether. *Atmos. Environ.*, **2006**, *40*, 5566-5573.
57. Scarfogliero, M.; Picquet-Varrault, B.; Salce, J.; Durand-Jolibois, R.; Doussin, J.F. Kinetic and mechanistic study of the gas-phase reactions of a series of vinyl ethers with the nitrate radical. *J. Phys. Chem. A* **2006**, *110*, 11074-11081.
58. Grosjean, E.; Grosjean, D. The gas-phase reaction of unsaturated oxygenates with ozone: carbonyl products and comparison with the alkene-ozone reaction. *J. Atmos. Chem.*, **1997**, *27*, 271-289.
59. Grosjean, E.; Grosjean, D. Rate constants for the gas-phase reaction of ozone with unsaturated oxygenates. *Int. J. Chem. Kinet.*, **1998**, *30*, 21-29.

60. Pfrang C.; Tooze, C.; Nalty, A.; Canosa-Mas C.E.; Wayne R.P. Reactions of NO₃ with the man-made emissions 2-methylpent-2-ene, (Z)-3-methylpent-2-ene, ethyl vinyl ether, and the stress-induced plant emission ethyl vinyl ketone. *Atmos. Environ.*, **2006**, *40* 786-792.
61. Seinfeld, J.H.; Pandis, S.N. *Atmospheric chemistry and physics: From air pollution to climate change*, John Wiley & Sons Inc., New York, **1998**.
62. Seinfeld, J.H.; Pankow, J.F. Organic atmospheric particular material. *Annu. Rev. Phys. Chem.* **2003**, *54*, 121-140.
63. Pandis, S.N.; Harley, R.A.; Cass, G.R.; Seinfeld, J.H. Secondary organic aerosol formation and transport. *Atmos. Environ.*, **1992**, *26A*, 2269-2282.
64. Sadezky, A.; Chaimbault, P.; Mellouki, A.; Roempp, A.; Winterhalter, R.; Moortgat, G. K.; Le Bras, G. Formation of secondary organic aerosol and oligomers from the ozonolysis of enol ethers. *Atmos. Chem. Phys. Discuss.*, **2006**, *6*, 5629-5670.
65. Barnes, I.; Bastian, V.; Becker, K.H.; Fink, E.H.; Zabel, F. Reactivity studies of organic substances towards hydroxyl radicals under atmospheric conditions. *Atmos. Environ.*, **1982**, *16*, 545-550.
66. Barnes, I.; Becker, K.H.; Fink, E.H.; Reimer, A.; Zabel, F.; Niki, H. Rate constant and products of the reaction CS₂ + OH in the presence of O₂. *Int. J. Chem. Kinet.*, **1983**, *15*, 631-645.
67. Barnes, I.; Becker, K.H.; Mihalopoulos, N. An FTIR product study of photo-oxidation of dimethyl disulfide. *J. Atmos. Chem.*, **1994**, *18*, 267-289.
68. Fuchs, N.A. On the stationary charge distribution on aerosol particles in a bipolar ionic atmosphere. *Pure Appl. Geophys.*, **1963**, *56*, 185-193.
69. Schott, G.; Davidson, N. Shock waves in chemical kinetics: the decomposition of N₂O₅ at high temperatures. *J. Am. Chem. Soc.*, **1958**, *80*, 1841-1853.
70. Tuazon, E.C.; MacLeod, H.; Atkinson, R.; Carter, W.P.L. α -dicarbonyl yields from the NO_x-air photooxidations of a series of aromatic hydrocarbons in air. *Environ. Sci. Technol.*, **1985**, *20*, 383-387.
71. Cavalli, F.; Geiger, H.; Barnes, I.; Becker, K.H. FTIR kinetic, product, and modeling study of the OH-initiated oxidation of 1-butanol in air. *Environ. Sci. Technol.*, **2002**, *36*, 1263-1270.
72. Calvert, J.G.; Atkinson, R.; Kerr J.A.; Madronich, S., Moortgat G. K.; Wallington T. J.; Yarwood G. *The Mechanisms of Atmospheric Oxidation of the Alkenes*.

References

- Oxford University Press, Oxford, **2000**.
73. Saunders, S.M.; Baulch, D.L.; Cooke, K.M., Pilling, M.J.; Smurthwaite, P.I. Kinetics and mechanisms of the reactions of OH with some oxygenated compounds of importance in tropospheric chemistry. *Int. J. Chem. Kinet.*, **1994**, *26*, 113-130.
74. OVOC data base: <http://www.era-orleans.org/eradb>.
75. Atkinson, R., Gas-phase tropospheric chemistry of volatile organic compounds: 1. alkanes and alkenes. *J. Phys. Chem. Ref. Data* **1997**, *26*, 215-290.
76. Starkey, D.P.; Holbrook, K.A.; Oldershaw, G.A.; Walker, R.W. Kinetic of the reactions of hydroxyl radicals (OH) and of chlorine atoms (Cl) with methylethyl-ether over the temperature range 274-345K. *Int. J. Chem. Kinet.*, **1997**, *29*, 231-236.
77. Kwok, E.C.; Atkinson, R. Estimation of hydroxyl radical reaction rate constants for gas-phase organic compounds using a structure-reactivity relationship: an update. *Atmos. Environ.*, **1995**, *29*, 1685-1695.
78. Atkinson, R., Kinetics and mechanisms of the gas-phase reactions of the hydroxyl radical with organic compounds under atmospheric conditions. *Chem. Rev.*, **1985**, *85*, 69-201.
79. Atkinson, R.; Aschmann, S.M.; Pitts, J.N., Kinetics of the gas-phase reactions of OH radicals with a series of α,β -unsaturated carbonyls at 299 ± 2 K. *Int. J. Chem. Kinet.*, **1983**, *15*, 75-81.
80. Moriarty, J.; Sidebottom, H.; Wenger, J.; Mellouki, A.; Le Bras, G. Kinetic studies on the reactions of hydroxyl radicals with cyclic ethers and aliphatic diethers. *J. Phys. Chem. A* **2003**, *107*, 1499-1505.
81. Papagni, C.; Arey, J.; Atkinson, R. Rate constants for the gas-phase reactions of OH radicals with a series of unsaturated alcohols. *Int. J. Chem. Kinet.*, **2001**, *33*, 142-147.
82. Imamura, T.; Iida, Y.; Obi, K.; Nagatani, I.; Nakagawa, K.; Patroescu-Klotz, I.; Hatakeyama, S. Rate coefficients for the gas-phase reactions of OH radicals with methylbutanols at 298K. *Int. J. Chem. Kinet.*, **2004**, *36*, 379-385.
83. Orlando, J.J.; Tyndall, G.S.; Ceazan, N. Rate coefficients and product yields from reaction of OH with 1-penten-3-ol, (Z)-2-penten-1-ol, and allyl alcohol (2-propen-1-ol). *J. Phys. Chem. A* **2001**, *105*, 3564-3569.
84. Stemmler, K.; Mengon, W.; Kerr, J.A. OH radical initiated photooxidation of

- 2-ethoxy-ethanol under laboratory conditions related to troposphere: product studies and proposed mechanism. *Environ. Sci. Technol.*, **1996**, *30*, 3385-3391.
85. Atkinson, R.; Aschmann, S.M.; Winer, A.M.; Pitts, Jr.N.J. Rate constants for the gas-phase reactions of O₃ with a series of carbonyls at 296 K. *Int. J. Chem. Kinet.*, **1992**, *13*, 1133-1142.
86. Grosjean, D.; Grosjean, E.; Williams II, E.L. Rate constants for the gas-phase reactions of ozone with unsaturated alcohols, esters, and carbonyls. *Int. J. Chem. Kinet.*, **1993**, *25*, 783-794.
87. Kind, I; Berndt, T.; Bøge, O. Gas-phase rate constants for the reaction of NO₃ radicals with a series of cyclic alkenes, 2-ethyl-1-butene and 2,3-dimethyl-1,3-butadiene. *Chem. Phys. Lett.*, **1998**, *288*, 111-118.
88. Canosa-Mas, C.E., Carr S., King, M.D., Shallcross, D.E., Thompson, K.C., Wayne, R.P., A kinetic study of the reactions of NO₃ with methyl vinyl ketone, methacrolein, acrolein, methyl acrylate and methyl methacrylate. *Phys. Chem. Chem. Phys.*, **1999**, *1*, 4195-4202.
89. Oh, S., Andino, J.M., Effects of ammonium sulfate aerosols on the gas-phase reactions of the hydroxyl radical with organic compounds. *Atmos. Environ.*, **2000**, *34*, 2901-2908.
90. Oh, S., Andino, J.M. Kinetics of the gas-phase reactions of hydroxyl radicals with C1-C6 aliphatic alcohols in the presence of ammonium sulfate aerosols. *Int. J. Chem. Kinet.*, **2001**, *33*, 422-430.
91. Oh, S., Andino, J.M., Laboratory studies of the impact of aerosol composition on the heterogeneous oxidation of 1-propanol. *Atmos. Environ.*, **2002**, *36*, 149-156.
92. Sørensen, M., Hurley, M.D., Wallington, T.J., Dibble, T.S., Nielsen, O.J. Do aerosols act as catalysts in the OH radical initiated atmospheric oxidation of volatile organic compounds? *Atmos. Environ.*, **2002**, *36 A*, 5947-5952.
93. Wayne, R.P.; Barnes, I.; Biggs, P.; Burrows, J.P.; Canosa-Mas, C.E.; Hjorth, J.; Le Bras, G.; Moortgat, G.K.; Perner, D.; Poulet, G.; Restelli, G.; Sidebottom, H. The nitrate radical: physics, chemistry and the atmosphere. *Atmos. Environ.* **1991**, *25A*, 1-203.
94. Bale, C.S.E.; Canosa-Mas, C.E.; Flugge, M.L.; Wayne, R.P. An experimental study of the gas-phase reaction of the NO₃ radical with 1,4-pentadiene, Z-1,3-pentadiene and E-1,3-pentadiene. *Phys. Chem. Chem. Phys.*, **2002**, *4*, 5821-5826.

References

95. King, M.D.; Canosa-Mas, C.E.; Wayne, R.P. Frontier molecular orbital correlations for predicting rate constants between alkenes and the tropospheric oxidants NO₃, OH and O₃. *Phys. Chem. Chem. Phys.*, **1999**, *1*, 2231-2238.
96. Baumgartner, M.T.; Taccone, R.A.; Teruel, M.A.; Lane, S.I. Theoretical study of the relative reactivity of chloroethenes with atmospheric oxidants (OH, NO₃, O(³P), Cl(²P) and Br(²P)). *Phys. Chem. Chem. Phys.*, **2002**, *4*, 1028-1032.
97. Pfrang, C.; King, M.D.; Canosa-Mas, C.E.; Wayne, R.P. Correlations for gas-phase reactions of NO₃, OH and O₃ with alkenes: An update. *Atmos. Environ.*, **2006**, *40A*, 1170-1179.
98. Pfrang, C.; King, M.D.; Canosa-Mas, C.E.; Wayne, R.P. Structure–activity relations (SARs) for gas-phase reactions of NO₃, OH and O₃ with alkenes: An update. *Atmos. Environ.*, **2006**, *40*, 1180-1186.
99. Prinn, R.G.; Weiss, R.F.; Miller, B.R.; Huang, J.; Alyea, F.N.; Cunnold, D.M.; Fraser, P.J.; Hartley, D.E.; Simmonds, P.G. Atmospheric trends and lifetime of CH₃CCl₃ and global OH concerns. *Science*, **1995**, *269*, 187-192.
100. Shu, Y.; Atkinson, R. Atmospheric lifetimes and fates of a series of sesquiterpenes. *J. Geophys. Res.*, **1995**, *100*, 7275-7282.
101. Platt, U.; Heintz, F. Nitrate radicals in tropospheric chemistry. *Isr. J. Chem.*, **1994**, *34*, 289-300.
102. Calvert, J.G.; Atkinson, R.; Becker, K.H.; Kamens, R.M.; Seinfeld, J.H.; Wallington T.J.; Yarwood G. *The Mechanisms of Atmospheric Oxidation of Aromatic Hydrocarbons*. Oxford University Press, Oxford, **2002**.
103. Smith, D.F.; McIver, C.D.; Kleindienst, T.E. Primary product distribution from the reaction of OH with m-, p-xylene, 1,2,4- and 1,3,5-trimethylbenzene. *J. Atmos. Chem.*, **1999**, *34*, 339-364.
104. Hamilton, J.F.; Lewis, A.C.; Bloss, C.; Wagner, V.; Henderson, A.P.; Golding, B.T.; Wirtz, K.; Martin-Reviejo, M.; Pilling, M.J. Measurements of photo-oxidation products from the reaction of a series of alkyl-benzenes with hydroxyl radicals during EXACT using comprehensive gas chromatography. *Atmos. Chem. Phys.*, **2003**, *3*, 1999-2014.
105. Thamm, J.; Wolff, S.; Turner, W.V.; Gäb, S.; Thomas, W.; Zabel, F.; Fink, E.H.; Becker, K.H. Proof of the formation of hydroperoxymethyl formate in the ozonolysis of ethene: synthesis and FT-IR spectra of the authentic compound. *Chem. Phys. Lett.*, **1996**, *258*, 155-158.

106. Hasson, A.S.; Chung, M.Y.; Kuwata, K.T.; Converse, A.D.; Krohn, D.; Paulson, S.E. Reaction of Criegee intermediates with water vapor-an additional source of OH radicals in alkene ozonolysis? *J. Phys. Chem. A* **2003**, *107*, 6176-6182.
107. Paulson, E.S.; Chung, M.Y.; Hasson, A.S. OH radical formation from the gas-phase reaction of ozone with terminal alkenes and the relationship between structure and mechanism. *J. Phys. Chem. A* **1999**, *103*, 8125-8138.
108. Roberts, J.M. The atmospheric chemistry of organic nitrates. *Atmos. Environ.*, **1990**, *24A*, 243-287.
109. Barnes, I.; Bastian, V.; Becker K.H.; Zhu, T. Kinetics and products of the reactions of nitrate radical with monoalkenes, dialkenes, and monoterpenes. *J. Phys. Chem.*, **1990**, *94*, 2413-2419.
110. Carrington, R.A.G. The infrared spectra of some organic nitrates. *Spectrochim. Acta*, **1960**, *16*, 1279-1293.
111. Suto, M.; Manzanares, E.R.; Lee, L.C. Detection of sulfuric acid aerosols by ultraviolet scattering. *Environ. Sci. Technol.*, **1985**, *19*, 815-820.
112. Becker, K.H.; Bechara, J.; Brockmann, K.J. Studies on the formation of H₂O₂ in the ozonolysis of alkenes. *Atmos. Environ.*, **1993**, *27A*, 57-61.
113. Lightfoot, P.D.; Cox, R.A.; Crowley, J.N.; Destriau, M.; Hayman, G.D.; Jenkin, M.E.; Moortgat, G.K.; Zabel, F. Organic peroxy radicals: kinetics, spectroscopy and tropospheric chemistry. *Atmos. Environ.*, **1992**, *26 A*, 1805-1961.
114. IPCC. Climate Change: The scientific basis: contribution of working group I to the Third Assessment Report of the Intergovernmental Panel on Climate Change, Cambridge University Press, Cambridge, **2001**.
115. Docherty, K.S.; Ziemann, P.J. Effects of stabilized Criegee intermediate and OH radical scavengers on aerosol formation from reactions of β -pinene with O₃. *Aerosol Sci. Technol.*, **2003**, *37*, 877-891.
116. Ziemann, P.J. Formation of alkoxyhydroperoxy aldehydes and cyclic peroxyhemiacetals from reactions of cyclic alkenes with O₃ in the presence of alcohols. *J. Phys. Chem. A* **2003**, *107*, 2048-2060.
117. Keywood, M.D.; Kroll, J.H.; Varutbangkul, V.; Bahreini, R.; Flagan, R.C.; Seinfeld, J.H. Secondary organic aerosol formation from cyclohexene ozonolysis: effect of OH scavenger and the role of radical chemistry. *Environ. Sci. Technol.*, **2004**, *38*, 3343-3350.
118. Docherty, K.S.; Wu, W.; Lim, Y.B.; Ziemann, P.J. Contribution of organic

References

- peroxides to secondary aerosol formed from reactions of monoterpenes with O₃. *Environ. Sci. Technol.*, **2005**, *39*, 4049-4059.
119. Cocker, D.R.; Clegg, S.L.; Flagan, R.C., Seinfeld, J.H. The effect of water on gas-particle partitioning of secondary organic aerosol. Part I: alpha-pinene/ozone system. *Atmos. Environ.*, **2001**, *35*, 6049-6072.
120. Bonn, B.; Schuster, G.; Moortgat, G.K. Influence of water vapor on the process of new particle formation during monoterpene ozonolysis. *J. Phys. Chem. A* **2002**, *106*, 2869-2881.
121. Berndt, T.; Böge, O.; Stratmann, F. Gas-phase ozonolysis of alpha-pinene: gaseous products and particle formation. *Atmos. Environ.*, **2003**, *37*, 3933-3945.
122. Bonn, B.; Moortgat, G.K. New particle formation during alpha-and beta-pinene oxidation by O₃, OH and NO₃, and the influence of water vapor: particle size distribution studies. *Atmos. Chem. Phys.*, **2002**, *2*, 183-196.
123. Rohr, A.C.; Weschler, C.J.; Koutrakis, P.; Spengler, J.D. Generation and quantification of ultrafine particles through terpene/ozone reaction in a chamber setting. *Aerosol Sci. Technol.*, **2003**, *37*, 65-78.
124. Fick, J.; Pommer L.; Nilsson, C.; Andersson, B. Effect of OH radicals, relative humidity, and time on composition of the products formed in the ozonolysis of alpha-pinene. *Atmos. Environ.*, **2003**, *37*, 4087-4096.
125. Jonsson, A.M.; Hallquist, M.; Ljungstrom, E. Impact of humidity on the ozone initiated oxidation of limonene, Δ^3 -carene, and α -pinene. *Environ. Sci. Technol.*, **2006**, *40*, 188-194.
126. Taylor, W.D.; Allston, T.D.; Moscato, M.J.; Fazekas, G.B.; Kozlowski, R.; Takacs, G.A. Atmospheric photodissociation lifetimes for nitromethane, methyl nitrite, and methyl nitrate. *Int. J. Chem. Kinet.*, **1980**, *12*, 231-240.
127. Eitzkorn, T.; Klotz, B.; Sørensen, S.; Patroescu, I.V.; Barnes, I.; Becker, K.H.; Platt, U. Gas-phase absorption cross sections of 24 monocyclic aromatic hydrocarbon in the UV and IR spectral ranges. *Atmos. Environ.*, **1999**, *33*, 525-540.
128. Olariu, R.I. Atmospheric oxidation of selected hydrocarbons. Ph.D. thesis, University of Wuppertal, **2002**.